

Flow Matching: Markov Kernels, Stochastic Processes and Transport Plans

Christian Wald* Gabriele Steidl*

February 4, 2025

Abstract

Among generative neural models, flow matching techniques stand out for their simple applicability and good scaling properties. Here, velocity fields of curves connecting a simple latent and a target distribution are learned. Then the corresponding ordinary differential equation can be used to sample from a target distribution, starting in samples from the latent one. This paper reviews from a mathematical point of view different techniques to learn the velocity fields of absolutely continuous curves in the Wasserstein geometry. We show how the velocity fields can be characterized and learned via i) transport plans (couplings) between latent and target distributions, ii) Markov kernels and iii) stochastic processes, where the latter two include the coupling approach, but are in general broader.

Besides this main goal, we show how flow matching can be used for solving Bayesian inverse problems, where the definition of conditional Wasserstein distances plays a central role.

Finally, we briefly address continuous normalizing flows and score matching techniques, which approach the learning of velocity fields of curves from other directions.

*Institute of Mathematics, Technische Universität Berlin, Straße des 17. Juni 136, 10623 Berlin, Germany, {wald, steidl}@math.tu-berlin.de, <http://tu.berlin/imageanalysis>.

Contents

1	Introduction	3
2	Preliminaries and Notation	7
2.1	Special Metric Spaces	7
2.2	Push-Forward Operator	9
2.3	Disintegration and Markov Kernels	11
2.4	Couplings and Wasserstein Distance	13
3	Absolutely Continuous Curves in $(\mathcal{P}_2(\mathbb{R}^d), W_2)$	15
4	Curves Induced by Couplings	18
5	Curves via Markov kernels	26
5.1	General Construction	27
5.2	Curves induced by Couplings via Disintegration	30
6	Curves via Stochastic Processes	34
6.1	Conditional Expectation	34
6.2	Curve via Conditional Expectation	35
7	Flow Matching	38
8	Numerical Examples for Flow Matching	41
8.1	Flow Matching Algorithms	41
8.2	Numerical Examples	43
9	Flow Matching in Bayesian Inverse Problems	44
9.1	Conditional Wasserstein Distance	45
9.2	Almost Conditional Couplings	48

9.3	Bayesian Flow Matching	49
9.4	Numerical Examples of Bayesian Flow Matching	50
10	Continuous Normalizing Flows	51
10.1	Curves of Probability Measures from ODEs	52
10.2	Likelihood Loss for Continuous Normalizing Flow	54
10.3	Computing Gradients with the Adjoint Method	56
10.4	Numerical Examples of Continuous Normalizing Flows	58
11	A Glimpse at Score-Based Diffusion	58
	References	61
A	Proof of Theorem 3.1	64
B	Measurability of v_t in Lemma 5.7	65
C	Remark on Normalizing Flows	66

1 Introduction

Generative models with neural network approximations have shown impressive results in many applications, in particular in inverse problems and data assimilation. First developments in this direction were generative adversarial networks by Goodfellow et al. [16] in 2014 and variational autoencoders by Kingma and Welling [24] in 2013. In this paper, we are interested in recent flow matching techniques pioneered by Liu et al. [28, 29] in 2022/23 from the point of view of stochastic processes, and by Lipman et al. [27] in 2023 via conditional probability paths. Flow matching is closely related to continuous normalizing flows (CNFs), also called neural ordinary differential equations by Chen et al. [9] in 2018, and to score-based diffusion models introduced by Sohl-Dickstein et al. [36] and Ermon and Song [38] in 2015 and 2019, respectively. The later ones can be considered as an instance of CNFs, but add the perspective of stochastic differential equations. To provide a more complete picture, we will briefly consider these approaches in Sections 10 and 11. Flow matching techniques stand out for their simple applicability and good scaling properties. They can be easily

incorporated into other optimization techniques like plug-and-play approaches [30] and can be generalized for solving Bayesian inverse problems as we will see in Section 9.

We will approach the topic of flow matching from a mathematical point of view, where we intend to make the paper to a certain degree self-contained. However, for the practical implementation of flow matching, we assume that the reader is familiar with training neural networks once a tractable loss function is given.

The basic task of generative modeling consists in generating new samples from a probability distribution P_{data} , where we have only access to a set of samples, e.g. from the distribution of face images. This is a quite classical task in stochastics, since it is in general hard to sample from a high-dimensional distribution even if its density is known. Few examples, where it is easy to sample from in multiple dimensions, are the Gaussian distribution and their relatives. In this paper, we focus on the standard Gaussian distribution as so-called "latent" distribution P_{latent} . Then, the idea is to approximate a "nice" curve $t \mapsto \mu_t$, mapping a time $t \in [0, 1]$ to a probability measure μ_t , where

$$\mu_0 = P_{\text{latent}} \quad \text{and} \quad \mu_1 = P_{\text{data}}.$$

Our curves of interest are absolutely continuous curves in the Wasserstein space, which we introduce in Section 3. Due to the special metric

of the Wasserstein space, such a curve possesses a vector field $v : [0, 1] \times \mathbb{R}^d \rightarrow \mathbb{R}^d$ such that the curve-velocity pair (μ_t, v_t) fulfills the continuity equation

$$\partial_t \mu_t + \nabla_x \cdot (\mu_t v_t) = 0.$$

For the associated vector field v_t , under mild additional conditions, there exists a solution $\phi : [0, 1] \times \mathbb{R}^d \rightarrow \mathbb{R}^d$ of the ordinary differential equation (ODE)

$$\partial_t \phi(t, x) = v_t(\phi(t, x)), \quad \phi(0, x) = x,$$

and the curve μ_t is just the push-forward of the latent distribution by this solution

$$\mu_t = \phi(t, \cdot) \# \mu_0 := \mu_0 \circ \phi^{-1}(t, \cdot).$$

Thus, if the vector field v_t is known, it remains to solve the ODE by some standard solver starting at $t = 0$ with a sample of the latent distribution to produce a desired data sample at time $t = 1$. An illustration of the flow of samples from the one-dimensional standard Gaussian distribution to a Gaussian mixture is given in Figure 1. For a higher-dimensional example, see Figure 8.

Before learning the velocity fields via a neural network approximation, we have to determine appropriate curve-velocity pairs (μ_t, v_t) fulfilling in particular the continuity equation. In Sections 4 - 6, we provide three approaches. We will see that the

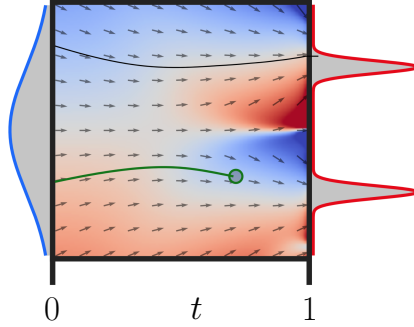


Figure 1: Illustration of a curve from the standard Gaussian distribution to a Gaussian mixture in one dimension. The plot shows $t \mapsto \phi(t, x^i)$, $i = 1, 2$ for two different samples x^i (black, green), the vectors $(1, \partial_t \phi)$ and the red-blue color-coded velocity field $\partial_t \phi$. Courtesy: Blogpost [5]

first one follows as a special case both from the second and third one. Ultimately, we develop the second approach with Markov kernels to explain the setting of Lipman et al. in [27] also for measures without densities.

1. **Curves induced by couplings:** Given a probability measure α on $\mathbb{R}^d \times \mathbb{R}^d$ with marginals μ_0 and μ_1 , also called "coupling" of μ_0 and μ_1 , the curve-velocity pair induced by α is given by the push-forwards

$$\mu_t := e_{t,\#} \alpha \quad \text{and} \quad v_t \mu_t := e_{t,\#} [(y - x) \alpha]$$

with

$$e_t(x, y) := (1 - t)x + ty, \quad t \in [0, 1].$$

Here $v_t \mu_t = e_{t,\#} [(y - x) \alpha]$ is a vector valued measures, where you may note that for $\gamma \in \mathcal{P}_2(\mathbb{R}^n)$, $f \in L^1(\mathbb{R}^n, \gamma)$ the vector valued measure $f \gamma$ is defined by

$$\int_{\mathbb{R}^n} \varphi(x) df \gamma(x) = \int_{\mathbb{R}^n} \varphi(x) f(x) d\gamma(x)$$

for every bounded measurable function $\varphi : \mathbb{R}^n \rightarrow \mathbb{R}$. Most common couplings are independent couplings $\alpha = \mu_0 \times \mu_1$ and so-called "optimal" transport couplings with respect to the Wasserstein distance. The optimal couplings stand out by the fact that the induced curves are geodesics in the Wasserstein space, which in particular are minimal length curves connecting μ_0 and μ_1 . In an alternative formulation, we may start with random variables with joint law $\alpha = P_{X_0, X_1}$ so that $\mu_0 = P_{X_0}$ and $\mu_1 = P_{X_1}$. Then the induced curve by α becomes $\mu_t = P_{X_t}$, where

$$X_t := e_t(X_0, X_1) = (1 - t)X_0 + tX_1.$$

2. **Curves via Markov kernels:** We start with a family of Markov kernels $(\mathcal{K}_t)_{t \in [0,1]}$ with the property that "conditioned to $y \in \mathbb{R}^d$ ", the curve $t \mapsto \mathcal{K}_t(y, \cdot)$ is absolutely continuous with associated vector field v_t^y . Then we define a time-dependent sequence of measures on $\mathbb{R}^d \times \mathbb{R}^d$ by glueing the Markov kernel with μ_1 as second marginal, i.e.

$$\alpha_t := \mathcal{K}_t(y, \cdot) \times_y \mu_1.$$

Denoting by ν_t its first marginal and using the disintegration $\alpha_t = \alpha_t^x \times_x \nu_t$, we will show that the curve $t \mapsto \nu_t$ is also absolutely continuous with associated velocity field

$$v_t(x) := \int_{\mathbb{R}^d} v_t^y d\alpha_t^x(y).$$

Note that the curve ν_t does not necessarily fulfill $\nu_1 = \mu_1$ or admit a ν_0 that is easy to sample from. But for reasonable choices it is possible to obtain that ν_0 is a standard Gaussian distribution and $\nu_1 \cong \mu_1$. An tractable pair (ν_t, v_t) which cannot be deduced from a curve-velocity pair induced by a coupling between μ_0 and μ_1 is given in Example 5.4.

However, for the following special setting, we obtain our induced curves from couplings α of μ_0 and μ_1 : Let $\alpha = \alpha^y \times_y \mu_1$ be the disintegration with respect to the second marginal. Then, $\alpha_t := (e_t, \pi^2)_\# \alpha$ fits into the above setting with

$$\mathcal{K}_t(y, \cdot) = e_{t,\#}(\alpha^y \times \delta_y) \quad \text{and} \quad v_t^y = \frac{y - x}{1 - t}, \quad t \in (0, 1)$$

and α_t has the first marginal $\nu_t = e_{t,\#} \alpha$ which is exactly μ_t from item 1.

3. **Curves via stochastic processes:** Starting with a time differentiable stochastic process $(X_t)_{t \in [0,1]}$, Liu et al. [28, 29] determined (μ_t, v_t) using the conditional expectation

$$\mu_t := P_{X_t} \quad \text{and} \quad v_t(x) := \mathbb{E}[\partial_t X_t | X_t = x].$$

For the special process $X_t := (1 - t)X_0 + tX_1$, $t \in [0, 1]$, this results again in a curve-velocity pair induced by the coupling from the joint distribution $\alpha = P_{X_0, X_1}$.

Section 7 deals with the actual flow matching, i.e., how we can learn the above vector fields. Actually, we will see that the vector field v of the curve-velocity pair (ν_t, v_t) in the Markov kernel approach appears as minimizer of a functional

$$v = \operatorname{argmin}_u \int_0^1 \int_{\mathbb{R}^d \times \mathbb{R}^d} \|u_t(x) - v_t^y(x)\|^2 d\alpha_t(x, y) dt$$

which suggests to use the loss function

$$\text{FM}_{\alpha_t}(\theta) := \int_0^1 \int_{\mathbb{R}^d \times \mathbb{R}^d} \|u_t^\theta(x) - v_t^y(x)\|^2 d\alpha_t(x, y) dt$$

for determining the parameters θ of a neural network that approximates v . In the original paper [27], the notation "conditional flow matching" (CFM) was used instead of FM which refers to a "conditional flow path". We prefer FM, since we will later deal with Bayesian inverse problems, where the notation of being "conditional" is occupied in a different way. For the numerical simulation, we have i) to sample from $\alpha_t = \mathcal{K}_t(y, \cdot) \times_y \mu_1$ and ii) to compute $v_t^y(x)$. Samples $y_i, i = 1, \dots, n$ from the data distribution μ_1 are usually available and it should be easy to sample from the distributions $\mathcal{K}_t(y_i, \cdot), i = 1, \dots, n$. In the special case, where $(\nu_t, v_t) = (\mu_t, v_t)$ is induced by a coupling α , we have a simple formula for v_t^y for which the loss function becomes

$$\text{FM}_\alpha(\theta) = \int_0^1 \int_{\mathbb{R}^d \times \mathbb{R}^d} \|u_t^\theta(e_t(x, y)) - (y - x)\|^2 d\alpha(x, y) dt. \quad (\text{FM})$$

Similarly, for the approach via a stochastic process, we get

$$v = \underset{u}{\operatorname{argmin}} \int_0^1 \mathbb{E} [\|\partial_t X_t - u_t(X_t)\|^2] dt.$$

Again, for the special stochastic process $X_t = (1 - t)X_0 + tX_1$ leading to a curve-velocity pair induced by the plan $\alpha = P_{X_0, X_1}$ this results in (FM). For the independent coupling $\alpha = \mu_0 \times \mu_1$ and the "optimal" one, this can be minimized numerically.

Let us start with the necessary notation agreements in the next section.

2 Preliminaries and Notation

Throughout this paper, we equip \mathbb{R}^d with the σ -algebra of Borel sets $\mathcal{B}(\mathbb{R}^d)$, and by "measurable" sets/functions we always refer to "Borel measurable". Speaking about absolutely continuous measures on \mathbb{R}^d , we mean absolutely continuous with respect to the Lebesgue measure \mathcal{L} on \mathbb{R}^d . By \mathcal{L}_A we denote the Lebesgue measure restricted to the measurable set $A \subset \mathbb{R}^d$. By $e_i, i = 1, \dots, d$ we denote the canonical basis elements of \mathbb{R}^d .

2.1 Special Metric Spaces

Let $C_b(\mathbb{R}^d)$ be the Banach space of bounded, continuous, real-valued functions with norm

$$\|\varphi\|_\infty := \sup_{x \in \mathbb{R}^d} |\varphi(x)|,$$

$C_0(\mathbb{R}^d)$ its closed subspace of continuous functions vanishing at infinity, and $C_c(\mathbb{R}^d)$ the space of continuous functions with compact support. Further, $C^l(\mathbb{R}^d), l \geq 1$, denotes the space of l times continuously differentiable functions and $C^\infty(\mathbb{R}^d)$ the

space of infinity often differentiable functions likewise combined with the above compact support property $C_c^\infty(\mathbb{R}^d)$. Instead of \mathbb{R}^d , functions may be also defined on time intervals $I \subset \mathbb{R}$ or direct products $I \times \mathbb{R}^d$ with the corresponding adaptation of the notation. We will also consider the vector-valued functions mapping into \mathbb{R}^m and use the notation $C^l(\mathbb{R}^d, \mathbb{R}^m)$ here.

By $\mathcal{M}(\mathbb{R}^d)$, we denote the Banach space of finite Borel measures on \mathbb{R}^d equipped with the *total variation norm*

$$\|\mu\|_{\text{TV}} := \sup \left\{ \sum_{k=1}^{\infty} |\mu(B_k)| : \bigcup_{k=1}^{\infty} B_k = \mathbb{R}^d \right\}$$

for any pairwise disjoint Borel sets B_k , $k \in \mathbb{N}$. It is the dual space of $C_0(\mathbb{R}^d)$, in particular, every measure $\mu \in \mathcal{M}(\mathbb{R}^d)$ defines a continuous, linear functional on $C_0(\mathbb{R}^d)$ via

$$\varphi \mapsto \langle \mu, \varphi \rangle = \int_{\mathbb{R}^d} \varphi(x) \, d\mu(x)$$

and

$$\|\mu\|_{\mathcal{M}(\mathbb{R}^d)} = \sup_{\|\varphi\|_{C_0(\mathbb{R}^d)} \leq 1} |\langle \mu, \varphi \rangle|.$$

A sequence $(\mu_n)_n \subset \mathcal{M}(\mathbb{R}^d)$ *converges weak-** to a measure $\mu \in \mathcal{M}(\mathbb{R}^d)$, if

$$\int_{\mathbb{R}^d} \varphi \, d\mu_n = \int_{\mathbb{R}^d} \varphi \, d\mu \quad \text{for all } \varphi \in C_0(\mathbb{R}^d).$$

We are mainly interested in the subset of probability measures

$$\mathcal{P}(\mathbb{R}^d) := \{\mu \in \mathcal{M}(\mathbb{R}^d) : \mu \geq 0, \mu(\mathbb{R}^d) = 1\}.$$

Unfortunately, a sequence of probability measures $(\mu_n)_n$ may not converge in the weak-*** sense to a probability measure. For example, $\mu_n := \delta_n$, $n \in \mathbb{N}$, converges weak-*** towards $\mu \equiv 0$ which is not a probability measure. Therefore, the concept of narrow convergence¹ was introduced: a sequence $(\mu_n)_n \subset \mathcal{M}(\mathbb{R}^d)$ *converges narrowly* to a measure $\mu \in \mathcal{M}(\mathbb{R}^d)$, written $\mu_n \rightharpoonup \mu$ as $n \rightarrow \infty$, if

$$\int_{\mathbb{R}^d} \varphi \, d\mu_n = \int_{\mathbb{R}^d} \varphi \, d\mu \quad \text{for all } \varphi \in C_b(\mathbb{R}^d).$$

If $\mu_n \in \mathcal{P}(\mathbb{R}^d)$ with $\mu_n \rightharpoonup \mu$ as $n \rightarrow \infty$, then also $\mu \in \mathcal{P}(\mathbb{R}^d)$. However, note that $\mathcal{M}(\mathbb{R}^d)$ is not the dual space of $C_b(\mathbb{R}^d)$, which is indeed the space $\text{rba}(\mathbb{R}^d)$ of finitely additive set functions. For more information, see [32, Section 4.4].

¹In measure theory, narrow convergence of measures is also called weak convergence. We do not use the later notation to avoid confusion with the notation of weak convergence in functional analysis.

Remark 2.1 (Test functions). The interpretation of $\mathcal{M}(\mathbb{R}^d)$ as the dual of $C_0(\mathbb{R}^d)$ implies that $\mu = \nu$ in $\mathcal{M}(\mathbb{R}^d)$ if and only if

$$\int_{\mathbb{R}^d} \varphi \, d\mu = \int \varphi \, d\nu \text{ for all } \varphi \in C_0(\mathbb{R}^d).$$

Since $C_c^\infty(\mathbb{R}^d)$ is dense in $C_0(\mathbb{R}^d)$ with respect to the $\|\cdot\|_\infty$ norm, we could also just test against all $\varphi \in C_c^\infty(\mathbb{R}^d)$. \diamond

For $\mu \in \mathcal{P}(\mathbb{R}^d)$, let $L^p(\mathbb{R}^m, \mu)$, $p \in [1, \infty)$, denote the Banach space of (equivalence classes of) μ -measurable functions $f : \mathbb{R}^d \rightarrow \mathbb{R}^m$ with

$$\|f\|_{L^p(\mathbb{R}^m, \mu)} := \left(\int_{\mathbb{R}^d} \|f\|^p \, d\mu \right)^{\frac{1}{p}} < \infty,$$

where $\|\cdot\|$ is the Euclidean norm on \mathbb{R}^m . In case of the Lebesgue measure $\mu = \mathcal{L}$, we will skip the μ in the notation. Furthermore, we write L^1 for $L^1(\mathbb{R}, \mathcal{L})$.

2.2 Push-Forward Operator

The *push-forward measure* of $\mu \in \mathcal{M}(\mathbb{R}^d)$ by a measurable map $T : \mathbb{R}^d \rightarrow \mathbb{R}^n$ is defined by

$$T_{\#}\mu = \mu \circ T^{-1}$$

with the preimage $T^{-1}(B)$ of $B \in \mathcal{B}(\mathbb{R}^n)$.

Then, a function $f : \mathbb{R}^d \rightarrow \mathbb{R}$ is integrable with respect to $T_{\#}\mu$ if $f \circ T$ is integrable with respect to μ and

$$\int_{\mathbb{R}^d} f(y) \, dT_{\#}\mu(y) = \int_{T^{-1}(\mathbb{R}^d)} f(T(x)) \, d\mu(x).$$

If $T : \mathbb{R}^d \rightarrow \mathbb{R}^d$ is a C^1 diffeomorphism and μ is absolutely continuous with density p_μ , then we have by the *transformation theorem*, also known as *change-of-variable formula* for all measurable, bounded functions f that

$$\int_{\mathbb{R}^d} f(y) \, dT_{\#}\mu(y) = \int_{\mathbb{R}^d} f(T(x)) p_\mu(x) \, dx = \int_{\mathbb{R}^d} f(y) p_\mu(T^{-1}(y)) |\det(\nabla T^{-1}(y))| \, dy,$$

where ∇T denotes the Jacobian of T . In particular, $T_{\#}\mu$ has the density

$$p_{T_{\#}\mu}(y) = p(T^{-1}(y)) |\det(\nabla T^{-1}(y))| = p(T^{-1}(y)) / |\det(\nabla T(y))|. \quad (1)$$

Recall that the convolution of measures $\mu, \nu \in \mathcal{P}(\mathbb{R}^d)$ is defined to be the measure $\mu * \nu \in \mathcal{P}(\mathbb{R}^d)$ which fulfills

$$\int_{\mathbb{R}^d} \varphi(x) \, d(\mu * \nu)(x) = \int_{\mathbb{R}^d \times \mathbb{R}^d} \varphi(x + y) \, d\mu(x) d\nu(y)$$

for all $\varphi \in C_b(\mathbb{R}^d)$. If μ, ν have densities $p_\mu, p_\nu \in L^1$, then $\mu * \nu$ has the density $p_{\mu*\nu} \in L^1$ given by

$$p_{\mu*\nu} = \int_{\mathbb{R}^d} p_\mu(x) p_\nu(\cdot - x) dx.$$

Measures can be characterized via laws of random variables.

Remark 2.2 (Random variables). Let $(\Omega, \Sigma, \mathbb{P})$ be a probability space. Recall that a random variable $X : \Omega \rightarrow \mathbb{R}^d$ is a measurable map $X : \Omega \rightarrow \mathbb{R}^d$ and the push-forward measure

$$P_X := X_{\#}\mathbb{P} = \mathbb{P} \circ X^{-1}$$

is known as law of X . Note that different random variables can have the same law. For every measure $\mu \in \mathcal{P}_2(\mathbb{R}^d)$ there exists a random variable with $P_X = \mu$. If $X_0, X_1 : \Omega \rightarrow \mathbb{R}^d$ are independent random variables, then

- i) $(X_0, X_1) : \Omega \rightarrow \mathbb{R}^d \times \mathbb{R}^d$ has law $P_{X_0, X_1} = P_{X_0} \times P_{X_1}$, and
- ii) $Z := a_0 X_0 + a_1 X_1 : \Omega \rightarrow \mathbb{R}^d$, $a_0, a_1 \neq 0$ has law $P_Z = a_{0,\#} P_{X_0} * a_{1,\#} P_{X_1}$, where we abbreviated $a_i \text{Id}$ by a_i in the last formula. If P_{X_i} has a density p_{X_i} , then $a_{i,\#} P_{X_i}$ has the density $p_{X_i}(a_i^{-1}\cdot)$, $i = 0, 1$, and Z has the density

$$p_Z = \int_{\mathbb{R}^d} p_{X_0}(a_0^{-1}x) p_{X_1}(a_1^{-1}(\cdot - x)) dx. \quad \diamond$$

For comparing measures, in particular $T_{\#}P_{\text{latent}}$ and P_{data} , divergences between measures can be used. A divergence has the main property that it achieves a minimum exactly if both measures coincide. One of the most frequently used divergence is the Kullback-Leibler one.

Remark 2.3 (Kullback-Leibler divergence). The *Kullback-Leibler (KL) divergence* $\text{KL} : \mathcal{P}(\mathbb{R}^d) \times \mathcal{P}(\mathbb{R}^d) \rightarrow [0, +\infty]$ of two measures $\mu, \nu \in \mathcal{P}(\mathbb{R}^d)$ with existing Radon-Nikodym derivative $\frac{d\mu}{d\nu}$ of μ with respect to ν is defined by

$$\text{KL}(\mu, \nu) := \int_{\mathbb{R}^d} \log \left(\frac{d\mu}{d\nu} \right) d\mu.$$

If the Radon-Nikodym derivative does not exist, we set $\text{KL}(\mu, \nu) := +\infty$. If μ, ν have densities p_μ, p_ν , where $p_\nu(x) = 0$ implies $p_\mu(x) = 0$, then

$$\begin{aligned} \text{KL}(\mu, \nu) &:= \int_{\mathbb{R}^d} \log \left(\frac{p_\mu}{p_\nu} \right) p_\mu dx \\ &= \mathbb{E}_{x \sim p_\mu} [\log p_\mu] - \mathbb{E}_{x \sim p_\mu} [\log p_\nu]. \end{aligned}$$

The Kullback-Leibler divergence is a so-called Bregman distance related to the Shannon entropy. It is not a distance, since it is neither symmetric nor fulfills a triangular

inequality. However, it holds $\text{KL}(\mu, \nu) \geq 0$ for all $\mu, \nu \in \mathcal{P}(\mathbb{R}^d)$ with equality if and only if the measures $\nu = \mu$ coincide.

If the latent distribution P_{latent} has a density p_{latent} , and $T : \mathbb{R}^d \rightarrow \mathbb{R}^d$ is a C^1 diffeomorphism, then by (1) also $T_{\#}P_{\text{latent}}$ has a density which we denote by $T_{\#}p_{\text{latent}}$. Thus, if the data distribution admits a density p_{data} , then we get

$$\text{KL}(P_{\text{data}}, T_{\#}P_{\text{latent}}) = \underbrace{\mathbb{E}_{x \sim p_{\text{data}}}[\log p_{\text{data}}]}_{\text{constant}} - \mathbb{E}_{x \sim p_{\text{data}}}[\log T_{\#}p_{\text{latent}}].$$

◇

2.3 Disintegration and Markov Kernels

In this paper, we consider projections $\pi^i : \mathbb{R}^d \times \mathbb{R}^d \rightarrow \mathbb{R}^d$, $i = 1, 2$, defined by

$$\pi^1(x, y) := x, \quad \pi^2(x, y) := y.$$

Then, for a measure $\alpha \in \mathcal{P}(\mathbb{R}^d \times \mathbb{R}^d)$, we have that $\pi_{\#}^1\alpha$ and $\pi_{\#}^2\alpha$ are the left and right marginals of α , respectively.

For a measure $\alpha \in \mathcal{P}(\mathbb{R}^d \times \mathbb{R}^d)$ with marginal $\pi_{\#}^1\alpha = \mu$, there exists a μ -a.e. uniquely defined family of probability measures $\{\alpha^x\}_x$, called *disintegration of α with respect to π^1* , such that the map $x \mapsto \alpha^x(B)$ is measurable for every $B \in \mathcal{B}(\mathbb{R}^d)$, and

$$\alpha = \alpha^x \times_x \mu$$

meaning that

$$\int_{\mathbb{R}^d \times \mathbb{R}^d} f(x, y) d\alpha(x, y) = \int_{\mathbb{R}^d} \int_{\mathbb{R}^d} f(x, y) d\alpha^x(y) d\mu(x)$$

for every measurable, bounded function $f : \mathbb{R}^d \times \mathbb{R}^d \rightarrow \mathbb{R}$. For an illustration, see Figure 2. Similarly, we define for a measure $\alpha \in \mathcal{P}(\mathbb{R}^d \times \mathbb{R}^d)$ with marginal $\pi_{\#}^2\alpha = \nu$ the *disintegration of α with respect to π^2* as

$$\alpha = \alpha^y \times_y \nu.$$

The notation of disintegration is directly related to Markov kernels. A *Markov kernel* is a map $\mathcal{K} : \mathbb{R}^d \times \mathcal{B}(\mathbb{R}^d) \rightarrow \mathbb{R}$ such that

- i) $\mathcal{K}(x, \cdot)$ is a probability measure on \mathbb{R}^d for every $x \in \mathbb{R}^d$, and
- ii) $\mathcal{K}(\cdot, B)$ is a Borel measurable map for every $B \in \mathcal{B}(\mathbb{R}^d)$.

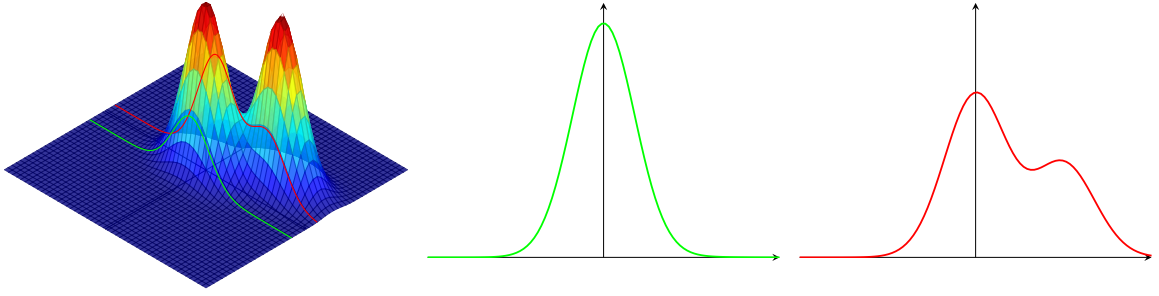


Figure 2: Disintegration of the measure $\alpha \in \mathcal{P}(\mathbb{R} \times \mathbb{R})$ (left). Measures $\alpha^{-0.3} \in \mathcal{P}(\mathbb{R})$ (middle, green) and $\alpha^{0.2} \in \mathcal{P}(\mathbb{R})$ (right, red).

Hence, given a probability measure $\mu \in \mathcal{P}(\mathbb{R}^d)$, we can define a new measure $\alpha := \alpha^x \times_x \mu \in \mathcal{P}(\mathbb{R}^d \times \mathbb{R}^d)$ by

$$\int_{\mathbb{R}^d \times \mathbb{R}^d} f(x, y) d\alpha(x, y) := \int_{\mathbb{R}^d} \int_{\mathbb{R}^d} f(x, y) d\mathcal{K}(x, \cdot)(y) d\mu(x)$$

for all measurable, bounded functions f . Identifying $\alpha^x(B)$ with $\mathcal{K}(x, B)$, we see that conversely, $\{\alpha^x\}_x$ is the disintegration of α with respect to π^1 .

Remark 2.4 (Random variables). Let $X_0, X_1 : \Omega \rightarrow \mathbb{R}^d$ be random variables with joint distribution P_{X_0, X_1} . Then the conditional distribution $\{P_{X_1|X_0=x}\}_x$ provides the disintegration of P_{X_0, X_1} , i.e.

$$\int_{\mathbb{R}^d \times \mathbb{R}^d} f(x, y) dP_{X_0, X_1}(x, y) = \int_{\mathbb{R}^d} \int_{\mathbb{R}^d} f(x, y) dP_{X_1|X_0=x}(y) dP_{X_0}(x).$$

In other words, $\mathcal{K} = P_{X_1|X_0}$ is a Markov kernel. If P_{X_0, X_1} admits a density p_{X_0, X_1} and P_{X_0} a density $p_{X_0} > 0$, then $P_{X_1|X_0=x}$ has the density $p_{X_1|X_0=x} = p_{X_0, X_1}(x, \cdot) / p_{X_0}(x)$. \diamond

Example 2.5. For $\mathcal{X} := \{x_i \in \mathbb{R}^d : i = 1, \dots, n\}$ and $\mathcal{Y} := \{y_j \in \mathbb{R}^d, j = 1, \dots, m\}$, the discrete probability measure

$$\alpha := \sum_{i,j=1}^{n,m} \alpha_{i,j} \delta_{(x_i, y_j)},$$

has first and second marginals

$$\begin{aligned} \mu &= \pi_{\#}^1 \alpha = \sum_{i=1}^n \left(\sum_{j=1}^m \alpha_{i,j} \right) \delta_{x_i} = \sum_{i=1}^n \mu_i \delta_{x_i}, \\ \nu &= \pi_{\#}^2 \alpha = \sum_{j=1}^m \left(\sum_{i=1}^n \alpha_{i,j} \right) \delta_{y_j} = \sum_{j=1}^m \nu_j \delta_{y_j}, \end{aligned}$$

see Figure 3. The disintegration of α with respect to π^1 is given by the family of measures

$$\alpha^{x_i} = \mathcal{K}(x_i, \cdot) = \sum_{j=1}^m \frac{\alpha_{i,j}}{\mu_i} \delta_{y_j} = \sum_{j=1}^m k_{i,j} \delta_{y_j},$$

$$\alpha^{x_i}(B) = \mathcal{K}(x_i, B) = \sum_{y_j \in B} k_{i,j}$$

for all $B \in \mathcal{B}(\mathbb{R}^d)$. The Markov kernel fulfills

$$\sum_{j=1}^m k_{i,j} = 1, \quad \sum_{i=1}^n k_{i,j} \mu_i = \nu_j.$$

In other words, with the vector $\mathbf{1}_m$ consisting of m entries one, and $\boldsymbol{\mu} := (\mu_i)_{i=1}^n$, $\boldsymbol{\nu} := (\nu_j)_{j=1}^m$, as well as $\mathbf{K} := (k_{i,j})_{i,j=1}^{n,m}$, we have

$$\mathbf{K} \mathbf{1}_n = \mathbf{1}_m, \quad \mathbf{K}^\top \boldsymbol{\mu} = \boldsymbol{\nu}$$

meaning that \mathbf{K}^\top is a stochastic matrix and a "transfer matrix" from μ to ν . \diamond

	ν_1	\dots	ν_j	\dots	ν_m		ν_1/μ		ν_j/μ		ν_m/μ
μ_1	$\alpha_{1,1}$	\dots	$\alpha_{1,j}$	\dots	$\alpha_{1,m}$	1	$\frac{\alpha_{1,1}}{\mu_1}$	\dots	$\frac{\alpha_{1,j}}{\mu_1}$	\dots	$\frac{\alpha_{1,m}}{\mu_1}$
\vdots			\vdots		\vdots	\vdots			\vdots		\vdots
μ_i	$\alpha_{i,1}$	\dots	$\alpha_{i,j}$	\dots	$\alpha_{i,m}$	1	$\frac{\alpha_{i,1}}{\mu_i}$	\dots	$\frac{\alpha_{i,j}}{\mu_i}$	\dots	$\frac{\alpha_{i,m}}{\mu_i}$
\vdots			\vdots		\vdots	\vdots			\vdots		\vdots
μ_n	$\alpha_{n,1}$	\dots	$\alpha_{n,j}$	\dots	$\alpha_{n,m}$	1	$\frac{\alpha_{n,1}}{\mu_n}$	\dots	$\frac{\alpha_{n,j}}{\mu_n}$	\dots	$\frac{\alpha_{n,m}}{\mu_n}$

Figure 3: Plan/Coupling of two discrete measures μ and ν (left) and Markov kernel/disintegration (right) with row and column sums.

2.4 Couplings and Wasserstein Distance

Let

$$\mathcal{P}_2(\mathbb{R}^d) := \{\mu \in \mathcal{P}(\mathbb{R}^d) : \int_{\mathbb{R}^d} \|x\|^2 d\mu < \infty\}$$

be the probability measures with finite second moments. For $\mu, \nu \in \mathcal{P}_2(\mathbb{R}^d)$, we define the set of *plans* or *couplings* with marginals μ and ν by

$$\Gamma(\mu, \nu) := \left\{ \alpha \in \mathcal{P}(\mathbb{R}^d \times \mathbb{R}^d) : \pi_{\#}^1 \alpha = \mu, \pi_{\#}^2 \alpha = \nu \right\}.$$

The set $\Gamma(\mu, \nu)$ is a compact subset of $\mathcal{P}_2(\mathbb{R}^d \times \mathbb{R}^d)$ with respect to the narrow topology. The *Wasserstein(-2) distance* is defined by

$$W_2(\mu, \nu) := \min_{\alpha \in \Gamma(\mu, \nu)} \|x - y\|_{L^2(\mathbb{R}^d \times \mathbb{R}^d, \alpha)} = \min_{\alpha \in \Gamma(\mu, \nu)} \left(\int_{\mathbb{R}^d \times \mathbb{R}^d} \|x - y\|^2 d\alpha(x, y) \right)^{\frac{1}{2}}. \quad (2)$$

Indeed, the above minimum is attained, see, e.g. [34, Theorem 1.7], and the *set of optimal plans* is denoted by $\Gamma_o(\mu, \nu)$. The space $(\mathcal{P}_2(\mathbb{R}^d), W_2)$ is a complete metric space. Speaking about $\mathcal{P}_2(\mathbb{R}^d)$, we will always equip it with the W_2 metric. Then we have for a sequence $(\mu_n)_n$ of measures in $\mathcal{P}_2(\mathbb{R}^d)$ that

$$\mu_n \rightarrow \mu \quad \text{if and only if} \quad \mu_n \rightharpoonup \mu \quad \text{and} \quad \lim_{n \rightarrow \infty} \int_{\mathbb{R}^d} \|x\|^2 d\mu_n = \int_{\mathbb{R}^d} \|x\|^2 d\mu.$$

In general, the minimizer in (2) is not unique. However, if μ is absolutely continuous, then uniqueness is ensured by the following theorem.

Theorem 2.6 (Brenier). *Let $\mu \in \mathcal{P}_2(\mathbb{R}^d)$ be absolutely continuous and $\nu \in \mathcal{P}_2(\mathbb{R}^d)$. Then there is a unique plan $\alpha \in \Gamma_o(\mu, \nu)$, which is induced by a unique measurable optimal transport map, also called Monge map, $T: \mathbb{R}^d \rightarrow \mathbb{R}^d$, i.e.,*

$$\alpha = (\text{Id}, T)_{\#}\mu$$

and

$$W_2^2(\mu, \nu) = \min_{T: \mathbb{R}^d \rightarrow \mathbb{R}^d} \int_{\mathbb{R}^d} \|x - T(x)\|_2^2 d\mu(x) \quad \text{subject to} \quad T_{\#}\mu = \nu.$$

Further, $T = \nabla\psi$, where $\psi: \mathbb{R}^d \rightarrow (-\infty, +\infty]$ is convex, lower semi-continuous (lsc) and μ -a.e. differentiable. Conversely, if ψ is convex, lsc and μ -a.e. differentiable with $\nabla\psi \in L_2(\mu, \mathbb{R}^d)$, then $T := \nabla\psi$ is an optimal map from μ to $\nu := T_{\#}\mu \in \mathcal{P}_2(\mathbb{R}^d)$.

The transport map between Gaussian distributions can be given analytically.

Example 2.7. For two Gaussians $\mu = \mathcal{N}(m_\mu, \Sigma_\mu)$ and $\nu = \mathcal{N}(m_\nu, \Sigma_\nu)$, where $\mathcal{N}(m, \Sigma)$ has the density

$$p(x) := (2\pi)^{-\frac{d}{2}} (\det \Sigma)^{-\frac{1}{2}} e^{-\frac{1}{2}(x-m)^T \Sigma^{-1}(x-m)},$$

the transport map is given by

$$T(x) = m_\nu + A(x - m_\mu), \quad A := \Sigma_\mu^{-\frac{1}{2}} \left(\Sigma_\mu^{\frac{1}{2}} \Sigma_\nu \Sigma_\mu^{\frac{1}{2}} \right) \Sigma_\mu^{-\frac{1}{2}}, \quad (3)$$

see e.g. [31, Remark 2.31]. ◇

3 Absolutely Continuous Curves in $(\mathcal{P}_2(\mathbb{R}^d), W_2)$

In the rest of this paper, let $I := [a, b]$, $a < b$. The main player in this paper are curves

$$\mu_t : I \rightarrow \mathcal{P}_2(\mathbb{R}^d), \quad t \mapsto \mu_t.$$

Unfortunately, there is an ambiguity here which is usual in the literature, namely that the curve itself as well as the value of the curve at time $t \in I$ is denoted by μ_t . Usually it becomes clear from the context what is meant. We are only interested in *narrowly continuous curves*, meaning that for $t \rightarrow t'$ we have $\mu_t \rightarrow \mu_{t'}$. Indeed, to make the definition of integrals

$$\int_I \int_{\mathbb{R}^d} f(t, x) d\mu_t dt$$

meaningful for any measurable, bounded function f , we have to consider $\mu_t : I \times \mathcal{B}(\mathbb{R}^d) \rightarrow \mathbb{R}$ as a Markov kernel, which is possible by the following theorem whose proof is given in Appendix A.

Theorem 3.1. *Let $\mu_t : I \rightarrow \mathcal{P}_2(\mathbb{R}^d)$ be a narrowly continuous curve. Then, for every Borel set $B \subseteq \mathbb{R}^d$, we have that $t \mapsto \mu_t(B)$ is measurable, i.e., $\mu_t : I \times \mathcal{B}(\mathbb{R}^d) \rightarrow \mathbb{R}$ is a Markov kernel.*

Recall that in a complete metric space (X, d) , a curve $\gamma : I \rightarrow X$ is called *absolutely continuous*, if there exists as $m \in L^1([a, b])$ such that

$$d(\gamma(s), \gamma(t)) \leq \int_s^t m(r) dr \quad \text{for all } a \leq s \leq t \leq b. \quad (4)$$

Here $L^1([a, b])$ denotes the space of (equivalence classes of) absolutely integrable real-valued function defined on an interval I . The *metric derivative* of γ (if it exists) is defined by

$$|\gamma'| := \lim_{h \rightarrow 0} \frac{d(\gamma(t), \gamma(t+h))}{|h|}.$$

For our special space $\mathcal{P}_2(\mathbb{R}^d)$ with $d = W_2$, absolute continuity of a curve can be characterized by a continuity equation. To this end, let $\mu_t : I \rightarrow \mathcal{P}_2(\mathbb{R}^d)$ be a narrowly continuous curve and $v : I \times \mathbb{R}^d \rightarrow \mathbb{R}^d$ be a measurable vector field. For $v(t, \cdot) : \mathbb{R}^d \rightarrow \mathbb{R}^d$ we alternatively write v_t . We say that the curve-velocity pair (μ_t, v_t) satisfies the *continuity equation*

$$\partial_t \mu_t + \nabla_x \cdot (\mu_t v_t) = 0 \quad (\text{CE})$$

in the sense of distributions, if

$$\int_I \int_{\mathbb{R}^d} \partial_t \varphi + \langle \nabla_x \varphi, v_t \rangle d\mu_t dt = 0$$

for all $\varphi \in C_c^\infty((a, b) \times \mathbb{R}^d)$. Here ∇_x is the gradient with respect to x for $\varphi = \varphi(t, x)$.

Remark 3.2. The term "in the sense of distributions" for the (CE) has the following meaning: Consider the measure $\mu = \mu_t \times_t dt$. Then $\partial_t \mu$ is the distribution

$$\partial_t \mu(\varphi) = -\mu(\partial_t \varphi) = -\int_I \int_{\mathbb{R}^d} \partial_t \varphi \, d\mu, \quad \varphi \in C_c^\infty((a, b) \times \mathbb{R}^d).$$

Further $\mu v(\varphi) = \mu(v\varphi)$ and

$$\begin{aligned} \operatorname{div}(\mu v)(\varphi) &= \sum_{i=1}^d \partial_i(\mu v_i)(\varphi) = -\sum_{i=1}^d (\mu v_i)(\partial_i \varphi) = -\sum_{i=1}^d \mu(v_i \partial_i \varphi) \\ &= -\mu(\langle \nabla_x \varphi, v \rangle) = -\int_I \int_{\mathbb{R}^d} \langle \nabla_x \varphi, v \rangle \, d\mu. \end{aligned}$$

Thus, the continuity equation can be seen as an equation of distributions. \diamond

Now we have the following fundamental theorem.

Theorem 3.3. [2, Theorem 8.3.1] *Let $\mu_t : I \rightarrow \mathcal{P}_2(\mathbb{R}^d)$ be a narrowly continuous curve. Then μ_t is absolutely continuous if and only if there exists a Borel measurable vector field $v : I \times \mathbb{R}^d \rightarrow \mathbb{R}^d$ such that the following two conditions are fulfilled:*

- i) $\|v_t\|_{L^2(\mathbb{R}^d, \mu_t)} \in L^1(I)$,
- ii) (μ_t, v_t) fulfills (CE).

In this case, the metric derivative $|\mu'_t|$ exists and we have $|\mu'_t| \leq \|v_t\|_{L^2(\mathbb{R}^d, \mu_t)}$ for a.e. $t \in I$.

We call a measurable vector field $v : I \times \mathbb{R}^d \rightarrow \mathbb{R}^d$ associated to an absolutely continuous curve $\mu_t : I \rightarrow \mathcal{P}_2(\mathbb{R}^d)$, if (μ_t, v_t) fulfill (CE) and $\|v_t\|_{L^2(\mathbb{R}^d, \mu_t)} \in L^1(I)$.

Indeed, an absolutely continuous curve may admit different associated velocity fields. For an illustration, see Example 4.9 and Figure 5. By the following remark, a unique associated vector field is characterized by having minimal $L^2(\mathbb{R}^d, \mu_t)$ -norm for a.e. $t \in I$, or equivalently, by being in the tangent space of μ_t .

Remark 3.4 (Minimal velocity fields of absolutely continuous curves). Let v_t, \tilde{v}_t be associated vector fields of an absolutely continuous curve μ_t with minimal norm $\|v_t\|_{L^2(\mathbb{R}^d, \mu_t)} = \|\tilde{v}_t\|_{L^2(\mathbb{R}^d, \mu_t)} =: z_t$ for a.e. $t \in I$ among all associated vector fields of μ_t . By the linear structure of (CE), also $\frac{v_t + \tilde{v}_t}{2}$ is associated to μ_t . Assume that $v_t \neq \tilde{v}_t$. By the strict convexity of $L^2(\mathbb{R}^d, \mu_t)$, it follows the contradiction $\|\frac{v_t + \tilde{v}_t}{2}\|_{L^2(\mathbb{R}^d, \mu_t)} < z_t$. Hence, we have the uniqueness $v_t = \tilde{v}_t$.

For an equivalent description, consider the *regular tangent space* $\mathcal{T}_\mu = T_\mu \mathcal{P}_2(\mathbb{R}^d)$ at $\mu \in \mathcal{P}_2(\mathbb{R}^d)$ which is defined by

$$\begin{aligned} \mathcal{T}_\mu &:= \overline{\{\nabla \phi : \phi \in C_c^\infty(\mathbb{R}^d)\}}^{L^2(\mathbb{R}^d, \mu)} \\ &= \overline{\{\lambda(T - \operatorname{Id}) : (\operatorname{Id}, T)_{\#} \mu \in \Gamma_o(\mu, T_{\#} \mu), \lambda > 0\}}^{L^2(\mathbb{R}^d, \mu)}, \end{aligned} \tag{5}$$

see [2, § 8]. The second description can be interpreted as locally moving mass in an "optimal way". Note that \mathcal{T}_μ is an infinite-dimensional subspace of $L^2(\mathbb{R}^d, \mu)$ if μ is absolutely continuous, and it is just \mathbb{R}^d if $\mu = \delta_x$, $x \in \mathbb{R}^d$. There is another description of \mathcal{T}_μ , namely, for a vector field $v \in L^2(\mathbb{R}^d, \mu)$, we have

$$\begin{aligned} v \in \mathcal{T}_\mu &\iff \int_{\mathbb{R}^d} \langle w, v \rangle d\mu = 0 \text{ for all } w \in L^2(\mathbb{R}^d, \mu) \text{ with } \nabla \cdot (w\mu) = 0, \\ &\iff \|v + w\|_{L^2(\mathbb{R}^d, \mu)} \geq \|v\|_{L^2(\mathbb{R}^d, \mu)} \text{ for all } w \in L^2(\mathbb{R}^d, \mu) \text{ with } \nabla \cdot (w\mu) = 0, \end{aligned} \quad (6)$$

where the last equation is meant again in the distributional sense $\int_{\mathbb{R}^d} \langle w, \nabla \varphi \rangle d\mu = 0$ for all $\varphi \in C_c^\infty(\mathbb{R}^d)$, see [2, Lemma 8.4.2].

Now let $v_t \in \mathcal{T}_{\mu_t}$ be a vector field associated to μ_t . For any other vector field \tilde{v}_t associated to μ_t , it holds $\nabla \cdot ((v_t - \tilde{v}_t)\mu) = 0$, and hence by (6), $\|\tilde{v}_t\|_{L^2(\mathbb{R}^d, \mu)} \geq \|v_t\|_{L^2(\mathbb{R}^d, \mu)}$, meaning that v_t has minimal $L^2(\mathbb{R}^d, \mu_t)$ -norm. On the other hand, let v_t be associated to μ_t having minimal norm. By [2, Theorem 8.3.1], there *exists* a vector field $\tilde{v}_t \in \mathcal{T}_{\mu_t}$ being associated to μ_t and having minimal norm. By the uniqueness shown above, it follows $v_t = \tilde{v}_t \in \mathcal{T}_{\mu_t}$.

Therefore, we have proven that the associated velocity field v_t of an absolutely continuous curve μ_t is unique if we require that it has minimal $L^2(\mathbb{R}^d, \mu_t)$ -norm, or equivalently, lies in the tangent space \mathcal{T}_{μ_t} . \diamond

The following theorem connects absolutely continuous curves with flow ODEs.

Theorem 3.5. [2, Theorem 8.1.8] *Let $\mu_t : I \rightarrow \mathcal{P}_2(\mathbb{R}^d)$ be an absolutely continuous curve with associated vector field v_t such that for every compact Borel set $B \subset \mathbb{R}^d$ it holds*

$$\int_I \left(\sup_{x \in B} \|v_t(x)\| + \text{Lip}(v_t, B) \right) dt < \infty.$$

Then there exists a solution $\phi : I \times \mathbb{R}^d \rightarrow \mathbb{R}^d$ of the ODE

$$\partial_t \phi(t, x) = v_t(\phi(t, x)), \quad \phi(0, x) = x \quad (7)$$

and $\phi(t, \cdot) \# \mu_0 = \mu_t$.

Theorem 3.5 indicates why absolutely continuous curves can be used as a tool for sampling. A common practice considers such curves starting in $\mu_0 := \mathcal{N}(0, 1)$ towards a target measure $\mu_1 = P_{\text{data}}$ and try to approximate the vector field v_t by a neural network v_t^θ for trainable parameters θ . To sample from μ_1 , we then can just sample from $\mu_0 = \mathcal{N}(0, 1)$ and solve the ODE (7) for these samples.

Remark 3.6. Also the other direction in Theorem 3.5 is true under some conditions. To see this, assume that ϕ is measurable and satisfies (7) for some locally bounded

vector field v_t . For $\varphi \in C_c^\infty((a, b) \times \mathbb{R}^d)$, we can compute

$$\begin{aligned}
0 &= \varphi(b, \phi(b, x)) - \varphi(a, \phi(a, x)) = \int_{\mathbb{R}^d} \varphi(b, \phi(b, x)) - \varphi(a, \phi(a, x)) d\mu_0 \\
&= \int_{\mathbb{R}^d} \int_a^b \frac{d}{dt} (\varphi(t, \phi(t, x))) dt d\mu_0 \\
&= \int_{\mathbb{R}^d} \int_a^b \langle \nabla_x \varphi(t, \phi(t, x)), v_t(t, \phi(t, x)) \rangle + (\partial_t \varphi)(t, \phi(t, x)) dt d\mu_0 \\
&= \int_a^b \int_{\mathbb{R}^d} \langle \nabla_x \varphi, v_t \rangle + \partial_t \varphi d[\phi(t, \cdot)_\# \mu_0] dt
\end{aligned}$$

and thus $\mu_t := \phi(t, \cdot)_\# \mu_0$ satisfies the continuity equation (in a weak sense). \diamond

In the following Sections 4 - 6 we show different methods for the construction of curve-velocity pairs fulfilling the conditions of Theorem 3.3, i.e. providing absolutely continuous curves in the Wasserstein geometry. Having (7) in mind, this will lead to a sampling procedure.

4 Curves Induced by Couplings

We start with curves induced by couplings $\alpha \in \Gamma(\mu_0, \mu_1)$. There are three important kinds of couplings:

- optimal couplings $\alpha \in \Gamma_o(\mu_0, \mu_1)$, since they correspond to geodesics in $\mathcal{P}_2(\mathbb{R}^d)$.
- couplings arising from maps, since their induced curves and vector fields are particularly simple, as we will see later.
- product couplings $\mu_0 \times \mu_1$, since we can easily sample from them by sampling from μ_0 and μ_1 and no extra computation is needed.

Using couplings it is also easy to see, that the space $\mathcal{P}_2(\mathbb{R}^d)$ is *path connected*, i.e., any two measures can be connected by a continuous curve (with respect to W_2). Even more, $\mathcal{P}_2(\mathbb{R}^d)$ is a *geodesic space*, meaning that any two measures can be connected by a geodesic. Recall that a curve $\mu_t : [0, 1] \rightarrow \mathcal{P}_2(\mathbb{R}^d)$ is called a (constant speed) *geodesic* if

$$W_2(\mu_s, \mu_t) = (t - s)W_2(\mu_0, \mu_1) \quad \text{for all } 0 \leq s \leq t \leq 1.$$

Let $e_t : \mathbb{R}^d \times \mathbb{R}^d \rightarrow \mathbb{R}^d$ be defined by

$$e_t(x, y) := (1 - t)x + ty, \quad t \in [0, 1].$$

Let $\mu_0, \mu_1 \in \mathcal{P}_2(\mathbb{R}^d)$ and $\alpha \in \Gamma(\mu_0, \mu_1)$. We call a *curve* $\mu_t : [0, 1] \rightarrow \mathcal{P}_2(\mathbb{R}^d)$ *induced by the coupling or plan* α , if

$$\mu_t := e_{t,\#}\alpha, \quad (8)$$

i.e., by definition of the push-forward measure,

$$\int_{\mathbb{R}^d} f \, d\mu_t = \int_{\mathbb{R}^d \times \mathbb{R}^d} f(e_t(x, y)) \, d\alpha = \int_{\mathbb{R}^d \times \mathbb{R}^d} f((1-t)x + ty) \, d\alpha$$

for every measurable, bounded function $f : \mathbb{R}^d \rightarrow \mathbb{R}$.

Remark 4.1 (Couplings induced by maps). For couplings induced by maps, i.e., $\alpha = (\text{Id}, T)\# \mu_0$, the induced curves admit a simple form, namely

$$\mu_t = (T_t)\# \mu_0 \quad \text{with} \quad T_t(x) = (1-t)x + tT(x). \quad (9)$$

In general, also optimal plans $\alpha \in \Gamma_o(\mu_0, \mu_1)$ may not be induced by a Monge map. However, if α is optimal and $\mu_t = e_{t,\#}\alpha$, then, for $s \in (0, 1)$, there exists an optimal map T^s such that $\Gamma_o(\mu_s, \mu_1) = \{(\text{Id}, T^s)\# \mu_t\}$, see [2, Lemma 7.2.1]. Moreover, by [2, Theorem 7.2.2], the curve induced by T^s coincides, up to time parametrizations, with μ_t for $t \in [s, 1]$, $s > 0$. Figure 4a shows a curve from an optimal plan which does not arise from a map and Figure 4b a curve induced by a plan with Monge map. However, in each case, the plan $\Gamma_o(\mu_s, \mu_1)$ is induced by a map for $s \in (0, 1)$.

This behavior is not necessarily the case for non-optimal plans even if they are induced by a map. As an example, see Figure 4c, where the paths of two particles cross at a certain time $s \in (0, 1)$, and $\Gamma_o(\mu_s, \mu_1)$ cannot be obtained from a map. \diamond



(a) μ_t for an optimal plan without map. (b) μ_t for an optimal plan with Monge map T . (c) μ_t for a non-optimal plan with map T .

Figure 4: Curve induced by $\alpha = (\text{Id}, T)\# \mu_0$ from $\mu_0 = \delta_{x_0}$, resp. $\mu_0 = \frac{1}{2}(\delta_{x_0} + \delta_{x_1})$ to $\mu_1 = \frac{1}{2}(\delta_{y_0} + \delta_{y_1})$. In (c), at the crossing time s of the path, there does not exist a map T_s that induces an element in $\Gamma_o(\mu_s, \mu_1)$. Red arrows: vector fields computed via 23

Remark 4.2 (Random variables). Curves induced by plans can also be interpreted via random variables: Let $X_0, X_1 : \Omega \rightarrow \mathbb{R}^d$ be random variables with laws $P_{X_0} = \mu_0$ resp. $P_{X_1} = \mu_1$. Then $\alpha = P_{X_0, X_1} \in \Gamma(\mu_0, \mu_1)$ and the induced curve in (8) reads as

$$\mu_t = P_{X_t}, \quad \text{where} \quad X_t := (1-t)X_0 + tX_1.$$

In particular, if X_0 and X_1 are independent, then $P_{X_0, X_1} = \mu_0 \times \mu_1$ and

$$\mu_t = P_{X_t} = ((1-t)\#P_{X_0}) * (t\#P_{X_1}).$$

Conversely, for $\alpha \in \Gamma(\mu_0, \mu_1)$, there is a random variable $Z : \Omega \rightarrow \mathbb{R}^d \times \mathbb{R}^d$ with law $P_Z = \alpha$, we can choose $X_0 := \pi^1 \circ Z$, $X_1 = \pi^2 \circ Z$ and obtain $\mu_0 = P_{X_0}$, $\mu_1 = P_{X_1}$ and $P_{X_0, X_1} = \alpha$. \diamond

First of all, curves induced by plans are narrowly continuous, as the following lemma shows.

Lemma 4.3. *Let $\mu_0, \mu_1 \in \mathcal{P}_2(\mathbb{R}^d)$ and $\alpha \in \Gamma(\mu_0, \mu_1)$. Then $\mu_t := e_{t,\#}\alpha$ is narrowly continuous.*

Proof. Let $f \in C_b(\mathbb{R}^d)$. Then $f \circ e_t \in C_b(\mathbb{R}^d \times \mathbb{R}^d)$ is measurable and bounded by $|(f \circ e_t)(x, y)| \leq \|f\|_\infty$ for all $(x, y) \in \mathbb{R}^d \times \mathbb{R}^d$ and $f \circ e_{t'} \rightarrow f \circ e_t$ pointwise for $t' \rightarrow t$. Thus, by the dominated convergence theorem, we have

$$\begin{aligned} \lim_{t' \rightarrow t} \int_{\mathbb{R}^d} f \, d\mu_{t'} &= \lim_{t' \rightarrow t} \int_{\mathbb{R}^d} f \circ e_{t'} \, d\alpha = \int_{\mathbb{R}^d} \lim_{t' \rightarrow t} f \circ e_{t'} \, d\alpha \\ &= \int_{\mathbb{R}^d} f \circ e_t \, d\alpha = \int_{\mathbb{R}^d} f \, d\mu_t \end{aligned}$$

and hence the claim. \square

Moreover, curves induced by optimal plans are geodesics, see [2, Chapter 7.2].

Proposition 4.4. *Let $\mu_0, \mu_1 \in \mathcal{P}_2(\mathbb{R}^d)$ and $\alpha \in \Gamma_o(\mu_0, \mu_1)$. Then $\mu_t := e_{t,\#}\alpha$ is a geodesic between μ_0 and μ_1 and every geodesic connecting μ_0 and μ_1 is of this form.*

Next, we want to show that a curve induced by a plan is also absolutely continuous. For this, we have to find a velocity field fulfilling i) and ii) in Theorem 3.3 so that (μ_t, v_t) satisfy (CE). To this end, we associate to a plan α the velocity field $v : [0, 1] \times \mathbb{R}^d \rightarrow \mathbb{R}^d$ as follows: Consider $\underline{\alpha} := \mathcal{L}_{[0,1]} \times \alpha$ and

$$e : [0, 1] \times \mathbb{R}^d \times \mathbb{R}^d \rightarrow [0, 1] \times \mathbb{R}^d, \quad (t, x, y) \mapsto (t, e_t(x, y)).$$

Then, by [1, Section 17], there exists a *unique vector field* $v \in L^2(e_{\#}\underline{\alpha}, \mathbb{R}^d)$ such that

$$v(e_{\#}\underline{\alpha}) = e_{\#}[(y - x)\underline{\alpha}]. \quad (10)$$

Since every $e_{\#}\underline{\alpha}$ -measurable function has a Borel measurable representative, see [6, Proposition 2.1.11], we can choose v Borel measurable. We call a measurable *vector field* $v : [0, 1] \times \mathbb{R}^d \rightarrow \mathbb{R}^d$ *induced by a plan* α , if it fulfills (10).

Lemma 4.5. *Let $\mu_t = e_{t,\#}\alpha$ be the curve induced by the plan α . Then (10) is equivalent to*

$$v_t\mu_t = e_{t,\#}[(y-x)\alpha] \quad \text{for a.e. } t \in [0, 1]. \quad (11)$$

Proof. For $f \in C_b([0, 1] \times \mathbb{R}^d)$, the left-hand side of (10) means

$$\begin{aligned} \int_0^1 \int_{\mathbb{R}^d} f v \, de_{t,\#}\underline{\alpha} &= \int_0^1 \int_{\mathbb{R}^d \times \mathbb{R}^d} f(t, e_t(x, y)) v(t, e_t(x, y)) \, d\underline{\alpha} \\ &= \int_0^1 \int_{\mathbb{R}^d} f v \, d(e_{t,\#}\alpha) dt \\ &= \int_0^1 \int_{\mathbb{R}^d} f(t, x) v(t, x) \, d\mu_t dt \end{aligned}$$

and the right-hand side

$$\begin{aligned} \int_0^1 \int_{\mathbb{R}^d} f \, de_{t,\#}[(y-x)\underline{\alpha}] &= \int_0^1 \int_{\mathbb{R}^d \times \mathbb{R}^d} f(t, e_t(x, y)) (y-x) \, d\underline{\alpha} \\ &= \int_0^1 \int_{\mathbb{R}^d} f \, de_{t,\#}[(y-x)\alpha] dt. \end{aligned}$$

Thus, (11) implies (10).

Conversely, assume that (10) holds true. Then we have

$$\int_0^1 \int_{\mathbb{R}^d} f(t, x) v(t, x) \, d\mu_t dt = \int_0^1 \int_{\mathbb{R}^d} f \, de_{t,\#}[(y-x)\alpha] dt.$$

Let $\{g_n\}_{n \in \mathbb{N}} \subset C_b(\mathbb{R}^d)$ be a dense subset. Then we obtain for any $h \in C_b([0, 1])$ and all $n \in \mathbb{N}$ that

$$\int_0^1 h \left(\int_{\mathbb{R}^d} g_n v_t \, d\mu_t - \int_{\mathbb{R}^d} g_n \, de_{t,\#}[(y-x)\alpha] \right) dt = 0$$

and consequently

$$\int_{\mathbb{R}^d} g_n v_t \, d\mu_t = \int_{\mathbb{R}^d} g_n \, de_{t,\#}[(y-x)\alpha] \quad \text{a.e. } t \in [0, 1]. \quad (12)$$

Since the number of test functions g_n is countable, there exists a zero set $\mathcal{I} \subset [0, 1]$ such that (12) holds true on $[0, 1] \setminus \mathcal{I}$ for all $n \in \mathbb{N}$. Since $\{g_n\}_{n \in \mathbb{N}}$ is dense in $C_b(\mathbb{R}^d)$ we obtain that $v_t\mu_t = e_{t,\#}[(y-x)\alpha]$ for a.e. $t \in [0, 1]$. More precisely, the last equation is an equation of vector-valued finite signed measures and thus it is enough to test equality at a dense subset of $C_b(\mathbb{R}^d)$. \square

Using the above lemmas, we obtain that curve-velocity pairs induced by couplings have the following favorable properties.

Theorem 4.6. *Let $\mu_0, \mu_1 \in \mathcal{P}_2(\mathbb{R}^d)$ and $\alpha \in \Gamma(\mu_0, \mu_1)$. Let (μ_t, v_t) be a curve-velocity pair induced by α , i.e.*

$$\mu_t = e_{t,\#}\alpha, \quad \text{and} \quad v_t \mu_t = e_{t,\#}[(y-x)\alpha] \quad \text{for a.e. } t \in [0, 1]. \quad (13)$$

Then the following holds true:

i) (μ_t, v_t) satisfy (CE) and

$$\|v_t\|_{L^2(\mathbb{R}^d, \mu_t)} \leq \|y-x\|_{L^2(\mathbb{R}^d \times \mathbb{R}^d, \alpha)} \quad \text{for a.e. } t \in [0, 1].$$

In particular, we have $\|v_t\|_{L^2(\mathbb{R}^d, \mu_t)} \in L^1(I)$ and μ_t is an absolutely continuous curve.

ii) *If $\alpha \in \Gamma_o(\mu_0, \mu_1)$, then $W_2(\mu_t, \mu_{t+h}) = hW_2(\mu_0, \mu_1)$ and*

$$|\mu'_t| = W_2(\mu_0, \mu_1) = \|v_t\|_{L^2(\mathbb{R}^d, \mu_t)} \quad \text{for a.e. } t \in [0, 1]. \quad (14)$$

Proof. Assertion i) follows as in [1, Theorem 17.2, Lemma 17.3], see also [7, proof of Proposition 6].

For Assertion ii), let α be an optimal plan. Since μ_t is a geodesic, we obtain $W_2(\mu_t, \mu_{t+h}) = hW_2(\mu_0, \mu_1)$, which immediately implies the first equality (14). By i) and since α is optimal, we know that $\|v_t\|_{L^2(\mathbb{R}^d, \mu_t)} \leq W_2(\mu_0, \mu_1)$ for a.e. $t \in [0, 1]$. Finally, by Theorem 3.3, we have $\|v_t\|_{L^2(\mathbb{R}^d, \mu_t)} \geq |\mu'_t| = W_2(\mu_0, \mu_1)$ for a.e. $t \in [0, 1]$. \square

By the above theorem, we immediately see that the Wasserstein distance between two measures can be described by the velocity field of any geodesic connecting them (curve energy).

Corollary 4.7 (Benamou-Brenier). *The Wasserstein distance is given by*

$$W_2(\mu, \nu) = \min_{(\mu_t, v_t)} \left(\int_0^1 \|v_t\|_{L^2(\mathbb{R}^d, \mu_t)}^2 dt \right)^{\frac{1}{2}}$$

where the minimum is taken over all pairs (μ_t, v_t) , where v_t is a measurable vector field, μ_t a narrowly continuous curve with $\mu_0 = \mu, \mu_1 = \nu$ and (μ_t, v_t) satisfy (CE).

By the following corollary, curve-velocity pairs induced by optimal plans have the favorable property of minimal vector fields. This ensures "short" curves in the related ODE.

Corollary 4.8. *Let $\mu_0, \mu_1 \in \mathcal{P}_2(\mathbb{R}^d)$ and $\alpha \in \Gamma_o(\mu_0, \mu_1)$. Let (μ_t, v_t) be curve-velocity pair induced by α . Then, $v_t \in \mathcal{T}_{\mu_t}$ for a.e. $t \in [0, 1]$.*

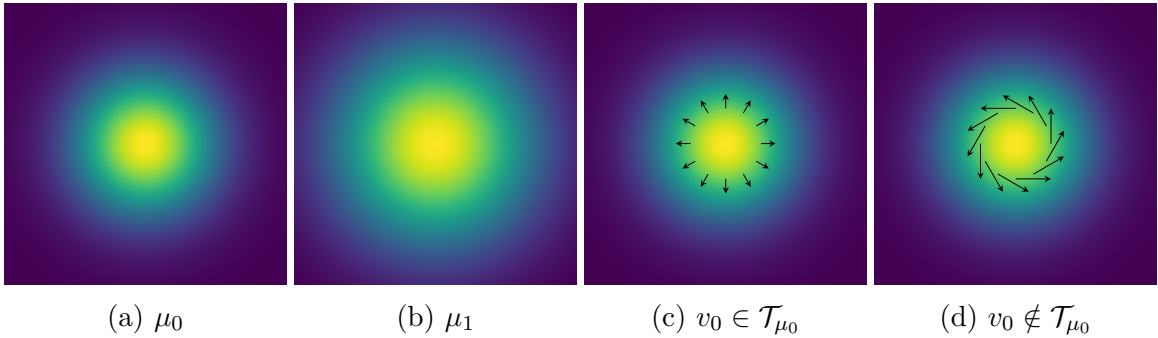


Figure 5: Illustration to Example 4.9. Both vector fields generate the same curves μ_t but in (d) mass is rotated unnecessarily, which makes the trajectories of single particles longer than for the vector field in (c).

Proof. By Theorem 4.6ii) we know that $\|v_t\|_{\mathcal{L}^2(\mathbb{R}^d, \mu_t)} = |\mu_t'|$ for a.e. $t \in [0, 1]$. Thus [2, Proposition 8.4.5] implies $v_t \in \mathcal{T}_{\mu_t}$ for a.e. $t \in [0, 1]$. \square

If α is not only optimal, but also induced by a Monge map $T : \mathbb{R}^d \rightarrow \mathbb{R}^d$, it is often the case that the trajectories are straight, in the sense that the solution of $\partial_t \phi_t(x) = v_t(\phi_t(x))$, $\phi_0(x) = x$, is T_t . This is in particular the case, if μ_0, μ_1 are empirical measures with the same number of points. For a proof and further cases, e.g. if both measures admit densities with a certain regularity, see [7, Proposition 16].

The above minimality property, i.e. laying in the tangent space, is quite special for optimal plans. Indeed, by the following example, this is not the case for arbitrary induced velocity fields, see also [28, Example 3.5].

Example 4.9. We consider a radial density $p_0(x) := f(\|x\|^2)$ for some $f \in C^\infty(\mathbb{R})$ with corresponding measure $\mu_0 := p_0 dx$, and the linear maps $T_t : \mathbb{R}^2 \rightarrow \mathbb{R}^2$, $t \in [0, 1]$ defined by

$$T_t(x) := \begin{pmatrix} 1 & -t \\ t & 1 \end{pmatrix} x = x + tw(x), \quad w(x) := \begin{pmatrix} 0 & -1 \\ 1 & 0 \end{pmatrix} x,$$

which fulfill

$$T_t^{-1}(x) = \frac{1}{1+t^2} \begin{pmatrix} 1 & t \\ -t & 1 \end{pmatrix} x = \frac{1}{1+t^2} (x - tw(x)), \quad \det(\nabla T_t(x)) = \frac{1}{1+t^2}.$$

We are interested in the plan induced by $T = T_1$, i.e.,

$$\alpha := (\text{Id}, T)_\# \mu_0 \in \Gamma(\mu_0, T_\# \mu_0).$$

We will show that the induced vector field $v_t \mu_t = e_{t,\#}((y-x)\alpha)$ is not minimal. By the change of variable formula (1), the induced curve

$$\mu_t := e_{t,\#} \alpha = T_{t,\#} \mu_0,$$

has the density

$$p_t(x) = \frac{(\rho \circ T_t^{-1})(x)}{\det(\nabla T_t(x))} = (1+t^2)f\left(\frac{1}{1+t^2}\|x\|^2\right)$$

which is radial again. In particular, the gradient $\nabla p_t(x)$ is a multiple of x and therefore we get by definition of w that $\langle \nabla p_t(x), w(x) \rangle = 0$. Further, we have $\nabla \cdot w = 0$ and consequently

$$\nabla \cdot (p_t w) = \langle \nabla p_t, w \rangle + p_t \nabla \cdot w = 0$$

Hence, by (6), we know that every $u_t \in \mathcal{T}_{\mu_t}$ must satisfy $\int_{\mathbb{R}^d} \langle w, u_t \rangle d\mu_t = 0$ for a.e. $t \in [0, 1]$. Unfortunately, the induced velocity field fulfills $\int_{\mathbb{R}^d} \langle w, v_t \rangle d\mu_t > 0$ for an non zero subset of $[0, 1]$ by the following reasons:

$$\begin{aligned} \int_{\mathbb{R}^d} \langle w, v_t \rangle d\mu_t &= \int_{\mathbb{R}^d \times \mathbb{R}^d} \langle w(e_t(x, y)), y - x \rangle d\alpha \\ &= \int_{\mathbb{R}^d \times \mathbb{R}^d} \langle w(e_t(x, y)), y - x \rangle d[(\text{Id}, T)_\# \mu_0] \\ &= \int_{\mathbb{R}^d} \langle w((1-t)x + tT(x)), T(x) - x \rangle d\mu_0 \\ &= \int_{\mathbb{R}^d} \langle w(x + tw(x)), w(x) \rangle d\mu_0. \end{aligned}$$

The last expression is continuous in t and equal to $\|w\|_{L^2(\mathbb{R}^2, \rho)}^2$ for $t = 0$. Since $\|w\|_{L^2(\mathbb{R}^2, \rho)}^2 > 0$, there exists an open non empty interval, such that $\int_{\mathbb{R}^d} \langle w, v_t \rangle d\mu_t > 0$. Thus, we have $v_t \notin \mathcal{T}_{\mu_t}$. \diamond

Example 4.10. Let $\mu_0 = \frac{1}{2}\delta_{x_0} + \frac{1}{2}\delta_{x_1}$, $\mu_1 = \frac{1}{3}\delta_{y_0} + \frac{2}{3}\delta_{y_1}$ and $\alpha = \mu_0 \times \mu_1$. Then

$$\begin{aligned} \mu_t &= \frac{1}{6}\delta_{e_t(x_0, y_0)} + \frac{1}{3}\delta_{e_t(x_0, y_1)} + \frac{1}{6}\delta_{e_t(x_1, y_0)} + \frac{1}{3}\delta_{e_t(x_1, y_1)} \\ \alpha_t &= \frac{1}{6}\delta_{e_t(x_0, y_0), y_0} + \frac{1}{3}\delta_{e_t(x_0, y_1), y_1} + \frac{1}{6}\delta_{e_t(x_1, y_0), y_0} + \frac{1}{3}\delta_{e_t(x_1, y_1), y_1}. \end{aligned}$$

Assume furthermore that for some $s \in (0, 1)$ we have that $e_s(x_0, y_1) = e_s(x_1, y_0) =: \hat{x}_s$, but $e_s(x_0, y_0) \neq \hat{x}_s \neq e_s(x_1, y_1)$, see Figure 6. We then have that

$$\begin{aligned} \mu_s &= \frac{1}{6}\delta_{e_s(x_0, y_0)} + \frac{1}{2}\delta_{\hat{x}_s} + \frac{1}{3}\delta_{e_s(x_1, y_1)} \\ \alpha_s &= \frac{1}{6}\delta_{e_s(x_0, y_0), y_0} + \frac{1}{3}\delta_{\hat{x}_s, y_1} + \frac{1}{6}\delta_{\hat{x}_s, y_0} + \frac{1}{3}\delta_{e_s(x_1, y_1), y_1}, \end{aligned}$$

which implies $\alpha_s^{\hat{x}_s} = \frac{1}{3}\delta_{y_0} + \frac{2}{3}\delta_{y_1}$. Hence using Proposition 5.7 we obtain

$$v_s(\hat{x}_s) = \frac{1}{3} \frac{y_0 - \hat{x}_s}{1-s} + \frac{2}{3} \frac{y_1 - \hat{x}_s}{1-s}.$$

Note that since at μ_s the mass in \hat{x}_s has to be split, μ_t cannot be described by a pushforward of a solution of an ODE and thus the assumptions of Theorem 3.5 cannot be fulfilled. \diamond

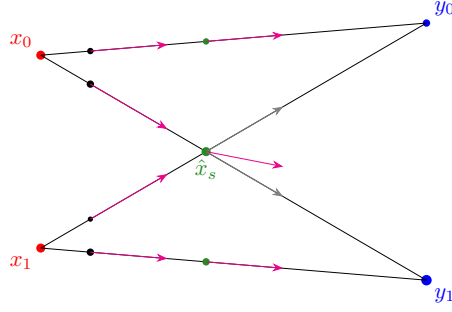


Figure 6: Curve and vector field associated to $\alpha = \mu_0 \times \mu_1$, where $\mu_0 = \frac{1}{2}\delta_{x_0} + \frac{1}{2}\delta_{x_1}$ and $\mu_1 = \frac{1}{3}\delta_{y_0} + \frac{2}{3}\delta_{y_1}$. Vectors are scaled by 0.2 for better visibility.

We have already seen that vector fields v_t associated to optimal plans are minimal ones, meaning that $v_t \in \mathcal{T}_{\mu_t}$. This is in general not true for an independent coupling $\alpha = \mu_0 \times \mu_1$ with an arbitrary μ_0 , see Figure 6. Fortunately, the independent coupling with a Gaussian marginal μ_0 has this minimality property as the following example shows, see also [28, Section 5.1].

Proposition 4.11. *Let $\mu_0 \sim \mathcal{N}(0, I_d)$, $\mu_1 \in \mathcal{P}_2(\mathbb{R}^d)$ and $\alpha = \mu_0 \times \mu_1$. Let $\mu_t := e_{t,\#}\alpha$ be the induced curve and v_t the induced velocity field v_t in (11). Then μ_t admits the strictly positive density*

$$p_t(x) := (1-t)^{-d} (2\pi)^{-\frac{d}{2}} \int_{\mathbb{R}^d} e^{-\frac{\|x-ty\|^2}{2(1-t)^2}} d\mu_1(y), \quad t \in [0, 1), \quad (15)$$

and

$$v_t = \nabla f_t \quad \text{with} \quad f_t := \frac{1-t}{t} \log p_t + \frac{1}{2t} \|\cdot\|^2, \quad t \in (0, 1), \quad (16)$$

Further, it holds $v_t \in \mathcal{T}_{\mu_t}$.

The expression $\nabla \log p_t$ will reappear as so-called "score" in Section 11.

Proof. 1. Relation (15) follows by directly computing for $g \in C_c^\infty(\mathbb{R}^d)$,

$$\begin{aligned} \int_{\mathbb{R}^d} g d\mu_t &= \int_{\mathbb{R}^d \times \mathbb{R}^d} g(e_t(x, y)) d\alpha(x, y) \\ &= \frac{1}{(2\pi)^{\frac{d}{2}}} \int_{\mathbb{R}^d \times \mathbb{R}^d} g((1-t)x + ty) e^{-\frac{\|x\|^2}{2}} dx d\mu_1(y) \end{aligned}$$

and substituting x by $\frac{z-ty}{1-t}$ then

$$\int_{\mathbb{R}^d} g d\mu_t = \frac{1}{(1-t)^d (2\pi)^{\frac{d}{2}}} \int_{\mathbb{R}^d} g(z) e^{-\frac{\|z-ty\|^2}{2(1-t)^2}} d\mu_1(y) dz.$$

2. Concerning relation (16), we verify

$$\begin{aligned}
\int_{\mathbb{R}^d} g \nabla f_t \, d\mu_t &= \frac{1-t}{t} \int_{\mathbb{R}^d} g(x) \frac{\nabla p_t(x)}{p_t(x)} p_t(x) \, dx + \frac{1}{t} \int_{\mathbb{R}^d} g(x) x p_t(x) \, dx \\
&= \frac{1}{t(1-t)^{d+1} (2\pi)^{\frac{d}{2}}} \int_{\mathbb{R}^d \times \mathbb{R}^d} g(x) (ty - x) e^{-\frac{\|x-ty\|^2}{2(1-t)^2}} \, d\mu_1(y) \, dx \\
&\quad + \frac{1}{t(1-t)^d (2\pi)^{\frac{d}{2}}} \int_{\mathbb{R}^d \times \mathbb{R}^d} g(x) x e^{-\frac{\|x-ty\|^2}{2(1-t)^2}} \, d\mu_1(y) \, dx \\
&= \frac{1}{(1-t)^{d+1} (2\pi)^{\frac{d}{2}}} \int_{\mathbb{R}^d \times \mathbb{R}^d} g(x) (y - x) e^{-\frac{\|x-ty\|^2}{2(1-t)^2}} \, d\mu_1(y) \, dx.
\end{aligned}$$

On the other hand, we have for the induced velocity field that

$$\begin{aligned}
\int_{\mathbb{R}^d} g v_t \, d\mu_t &= \int_{\mathbb{R}^d} g \, de_{t,\#}(y-x)\alpha = \frac{1}{(2\pi)^{\frac{d}{2}}} \int g(e_t(x,y))(y-x) e^{-\frac{\|x\|^2}{2}} \, d\mu_1(y) \, dx \\
&= \frac{1}{(1-t)^{d+1} (2\pi)^{\frac{d}{2}}} \int_{\mathbb{R}^d \times \mathbb{R}^d} g(z) (y-z) e^{-\frac{\|z-ty\|^2}{2(1-t)^2}} \, d\mu_1(y) \, dz,
\end{aligned}$$

which yields the assertion. Note that, in particular $\nabla f_t \in L^2(\mathbb{R}^d, \mu_t)$.

3. It remains to prove the minimality property of v_t . Since $\mu_t \in \mathcal{P}_2(\mathbb{R}^d)$, we have $\nabla \|x\|^2 \in \mathcal{T}_{\mu_t}$. Thus, we are left to show that $\nabla \log p_t \in \mathcal{T}_{\mu_t}$.

First, we have $p_t \in C^\infty(\mathbb{R}^d)$, $t \in [0, 1)$ and since $p_t > 0$ also $\log p_t \in C^\infty(\mathbb{R}^d)$. Since $\nabla \|x\|^2, \nabla f_t \in L^2(\mathbb{R}^d, \mu_t)$, we conclude that also $\nabla \log p_t \in L^2(\mathbb{R}^d, \mu_t)$. Furthermore, it is easy to see that $\lim_{r \rightarrow \infty} \max\{\log p_t(x) : \|x\| \geq r\} \rightarrow -\infty$. Consequently, we obtain for functions $h_n \in C_c^\infty(\mathbb{R})$ that $\phi_n := h_n \circ \log p_t \in C_c^\infty(\mathbb{R}^d)$. Now consider especially functions with $h_n(s) = s$ for $-n \leq s \leq \|\log p_t\|_\infty$ and $|h_n'| \leq 1$. Then we obtain with $C_n := \{x \in \mathbb{R}^d : \log p_t(x) \geq -n\}$ that $\phi_n(x) = \log p_t(x)$ for $x \in C_n$ and thus

$$\begin{aligned}
\int_{\mathbb{R}^d} \|\nabla \phi_n - \nabla \log p_t\|^2 \, d\mu_t &= \int_{\mathbb{R}^d \setminus C_n} \|\nabla \phi_n - \nabla \log p_t\|^2 \, d\mu_t \\
&\leq 4 \int_{\mathbb{R}^d \setminus C_n} \|\nabla \log p_t\|^2 \, d\mu_t.
\end{aligned}$$

Since $\nabla \log p_t \in L^2(\mathbb{R}^d, \mu_t)$, the latter converges to zero. Hence, by (5), this yields $\nabla \log p_t \in \mathcal{T}_{\mu_t}$. \square

5 Curves via Markov kernels

Unfortunately, the approach of Lipman et al. [27], see Example 5.4, is not covered by the previous section. Indeed, we need a more general viewpoint via Markov kernels which is given in the following Subsection 5.1. We will see in Subsection 5.2 that curve-velocity pairs induced by couplings fit into this general setting.

5.1 General Construction

The main observation is the following theorem, which describes how to construct a curve velocity pair (ν_t, v_t) when we are given a family of Markov kernels $\mathcal{K}_t(y, \cdot)$ and a measure μ_1 . Note that in this construction it is not necessarily the case that ν_0 is tractable and $\nu_1 = \mu_1$. But we will see later that for suitable chosen $\mathcal{K}_t(y, \cdot)$, we can achieve $\nu_0 = \mathcal{N}(0, 1)$ and $\nu_1 \cong \mu_1$.

Theorem 5.1. *Let $(\mathcal{K}_t)_{t \in [0,1]}$ be a family of Markov kernels $\mathcal{K}_t : \mathbb{R}^d \times \mathcal{B}(\mathbb{R}^d) \rightarrow \mathbb{R}$. For a given measure $\mu_1 \in \mathcal{P}_2(\mathbb{R}^d)$, we consider*

$$\alpha_t := \mathcal{K}_t(y, \cdot) \times_y \mu_1$$

and introduce the measure

$$\nu_t := \pi_{\sharp}^1 \alpha_t \quad \text{so that} \quad \alpha_t = \alpha_t^x \times_x \nu_t.$$

Assume that $\mathcal{K}_t(y, \cdot)$ is an absolutely continuous curve in $\mathcal{P}_2(\mathbb{R}^d)$ for μ_1 -a.e. $y \in \mathbb{R}^d$ with a vector field v_t^y such that $(\mathcal{K}_t(y, \cdot), v_t^y)$ fulfills (CE) for a.e. y . Further, let $(t, x, y) \mapsto v_t^y$ be measurable and $\|v_t^y\|_{L^2(\mathbb{R}^d \times \mathbb{R}^d, \alpha_t)} \in L^1([0, 1])$. Then α_t and ν_t are narrowly continuous. The curve ν_t is absolutely continuous and (ν_t, v_t) satisfies (CE), where

$$v_t(x) := \int_{\mathbb{R}^d} v_t^y d\alpha_t^x(y). \quad (17)$$

Proof. 1. For $f \in C_b(\mathbb{R}^d \times \mathbb{R}^d)$ with $\|f\|_\infty \leq C$ we have $|\int_{\mathbb{R}^d} f d\mathcal{K}_t(y, \cdot)| \leq C$. Thus, using the dominated convergence theorem and the fact that $\mathcal{K}_t(y, \cdot)$ is absolutely continuous for μ_1 -a.e. $y \in \mathbb{R}^d$, we conclude

$$\begin{aligned} \lim_{t \rightarrow t'} \int_{\mathbb{R}^d \times \mathbb{R}^d} f d\alpha_t &= \int_{\mathbb{R}^d} \lim_{t \rightarrow t'} \int_{\mathbb{R}^d} f d\mathcal{K}_t(y, \cdot) d\mu_1(y) = \int_{\mathbb{R}^d} \int_{\mathbb{R}^d} f d\mathcal{K}_{t'}(y, \cdot) d\mu_1(y) \\ &= \int_{\mathbb{R}^d \times \mathbb{R}^d} f d\alpha_{t'} \quad \text{for all } f \in C_b(\mathbb{R}^d \times \mathbb{R}^d), \end{aligned}$$

so that α_t is narrowly continuous and the same holds true for $\nu_t = \pi_{\sharp}^1 \alpha_t$.

2. For any $\varphi \in C_c^\infty([0, 1] \times \mathbb{R}^d)$, we obtain

$$\begin{aligned}
& \int_0^1 \int_{\mathbb{R}^d} \left\langle \nabla_x \varphi(t, x), \int_{\mathbb{R}^d} v_t^y(x) d\alpha_t^x(y) \right\rangle d\nu_t(x) dt \\
&= \int_0^1 \int_{\mathbb{R}^d \times \mathbb{R}^d} \langle \nabla_x \varphi(t, x), v_t^y(x) \rangle d\alpha_t(x, y) dt \\
&= \int_0^1 \int_{\mathbb{R}^d} \int_{\mathbb{R}^d} \langle \nabla_x \varphi(t, x), v_t^y(x) \rangle d\mathcal{K}_t(y, \cdot)(x) d\mu_1(y) dt \\
&= \int_{\mathbb{R}^d} \int_0^1 \int_{\mathbb{R}^d} \langle \nabla_x \varphi(t, x), v_t^y(x) \rangle d\mathcal{K}_t(y, \cdot)(x) dt d\mu_1(y) \\
&= \int_{\mathbb{R}^d} \int_0^1 \int_{\mathbb{R}^d} \partial_t \varphi(t, x) d\mathcal{K}_t(y, \cdot)(x) dt d\mu_1(y) \\
&= \int_0^1 \int_{\mathbb{R}^d \times \mathbb{R}^d} \partial_t \varphi(t, x) d\alpha_t dt = \int_0^1 \int_{\mathbb{R}^d \times \mathbb{R}^d} \partial_t \varphi(t, x) d(\pi_{\sharp}^1 \alpha_t) dt \\
&= \int_0^1 \int_{\mathbb{R}^d} \partial_t \varphi(t, x) d\nu_t(x) dt,
\end{aligned}$$

so that (ν_t, v_t) fulfills (CE).

3. Finally, we conclude

$$\begin{aligned}
\int_0^1 \|v_t\|_{L^2(\mathbb{R}^d, \nu_t)} dt &= \int_0^1 \left(\int_{\mathbb{R}^d} \|v_t\|^2 d\nu_t \right)^{\frac{1}{2}} dt \leq \int_0^1 \left(\int_{\mathbb{R}^d} \int_{\mathbb{R}^d} \|v_t^y(x)\|^2 d\alpha_t^x(y) d\nu_t(x) \right)^{\frac{1}{2}} dt \\
&= \int_0^1 \left(\int_{\mathbb{R}^d \times \mathbb{R}^d} \|v_t^y(x)\|^2 d\alpha_t \right)^{\frac{1}{2}} dt < \infty,
\end{aligned}$$

which finishes the proof, where the measurability of v is left to the reader. \square

Remark 5.2. In general, every curve $\mu_t \in \mathcal{P}_2(\mathbb{R}^d)$ can be written as in Theorem 5.1. Namely, $\mathcal{K}_t(y, \cdot) := \mu_t(\cdot)$ is a Markov kernel and for $\alpha_t := \mathcal{K}_t(y, \cdot) \times_y \mu_1$ it holds that $\nu_t := \pi_{\sharp}^1 \alpha_t = \mu_t$. Of course, we don't win anything using this construction since $v_t^y = v_t$ and thus we do not obtain a more tractable vector field. \diamond

Remark 5.3 (Relation to Lipman et al. [27]). The authors in [27] argue only with densities. Then the notation of the so-called "conditional probability path" translates as

$$\mathcal{K}_t(y, \cdot) \longleftrightarrow p_t(x|y).$$

Further, we have

$$\alpha_t = \mathcal{K}_t(y, \cdot) \times_y \mu_1 \longleftrightarrow p_t(x, y), \quad \alpha_t^x \longleftrightarrow p_t(y|x), \quad \pi_{\sharp}^2 \alpha_t = \mu_1 \longleftrightarrow q(y)$$

and

$$\int_{\mathbb{R}^d} \varphi d\nu_t(x) = \int_{\mathbb{R}^d \times \mathbb{R}^d} \varphi(x) d\mathcal{K}_t(y, \cdot) d\mu_1(y) \longleftrightarrow p_t(x) = \int_{\mathbb{R}^d} p_t(y|x) q(y) dy$$

so that $\nu_t \longleftrightarrow p_t$. By the Bayesian law, we know that $p_t(y|x) = \frac{p_t(x|y)}{p_t(x)}q(y)$, so that we finally obtain the correspondence

$$v_t(x) = \int_{\mathbb{R}^d} v_t^y(x) d\alpha_t^x(y) \longleftrightarrow v_t = \int_{\mathbb{R}^d} v_t(x|y) \frac{p_t(x|y)}{p_t(x)} q(y) dy. \quad \diamond$$

We recap the example in [27, Example II] with our approach.

Example 5.4. For fixed $r \in (0, 1)$, we consider the family of Markov kernels

$$\mathcal{K}_t(y, \cdot) := \mathcal{N}(ty, (1 - rt)^2 I_d), \quad t \in [0, 1].$$

By (3), there is an optimal transport map $T : \mathbb{R}^d \rightarrow \mathbb{R}^d$ between the Gaussians $\mathcal{K}_0(y, \cdot) = \mathcal{N}(0, I_d) =: \mu_0$ and $\mathcal{K}_1(y, \cdot) = \mathcal{N}(y, (1 - r)^2 I_d)$ given by

$$T(x) = y + (1 - r)x$$

with corresponding plan $\gamma = (\text{Id}, T)_{\#}\mu_0$ and

$$T_t(x) = e_{t, \#}(x, T(x)) = (1 - tr)x + ty, \quad T_t^{-1}(z) = \frac{z - ty}{1 - tr}.$$

Let $\mu_1 \in \mathcal{P}_2(\mathbb{R}^d)$. Further, it can be easily verified that

$$\mathcal{K}_t(y, \cdot) = e_{t, \#}((\text{Id}, T)_{\#}\mu_0) = (T_t)_{\#}\mu_0.$$

By Corollary 5.10, we obtain that $(\mathcal{K}_t(y, \cdot), v_t^y$ with the velocity field

$$v_t^y(x) = T(T_t^{-1}(x)) - T_t^{-1}(x) = \frac{y - rx}{1 - tr},$$

fulfills (CE). Now, let $\mu_1 \in \mathcal{P}_2(\mathbb{R}^d)$ and consider the family of plans

$$\alpha_t := \mathcal{K}_t(y, \cdot) \times_y \mu_1 \quad \text{and} \quad \nu_t := \pi_{\#}^1 \alpha_t.$$

It is easy to check that $\nu_0 = \mathcal{N}(0, I_d)$. Then we know by Proposition 5.1 that the curve ν_t is absolutely continuous and fulfills (CE) with the velocity field v_t in (17). However, if we want to sample from the target density μ_1 , this can only be done approximately by following the path of ν_t , since

$$\nu_1 = \pi_{\#}^1 \left[\mathcal{N}(y, (1 - r)^2 I_d) \times_y \mu_1(y) \right] = \mathcal{N}(0, (1 - r)^2 I_d) * \mu_1 \neq \mu_1.$$

By [2, Lemma 7.1.10] we have that $W_2(\nu_1, \mu_1) \leq (1 - r) \sqrt{\int \|x\|^2 d\mu_1}$ and thus ν_1 converges to μ_1 in $\mathcal{P}_2(\mathbb{R}^d)$ as $r \rightarrow 1$. The authors of [27] then learn the velocity field v_t of ν_t as explained in Example 7.2. \diamond

A curve that can be described by Markov kernels, but is not induced by any coupling is given in the following example.

Example 5.5. Let μ_t be a curve induced by $\alpha \in \Gamma(\mu_0, \mu_1)$. Then, by Proposition 4.6 and Corollary 4.7 of Benamou-Brenier, we obtain

$$W_2(\mu_t, \mu_{t+h})^2 \leq h^2 \|x - y\|_{L^2(\mathbb{R}^d \times \mathbb{R}^d, \alpha)}^2 \leq h^2 \left(\|x\|_{L^2(\mathbb{R}^d, \mu_0)} + \|x\|_{L^2(\mathbb{R}^d, \mu_1)} \right)^2,$$

which is a bound independent of the plan. Thus, if μ_t is not constant, we can find a monotone function $f \in C^\infty([0, 1])$ with $f(0) = 0, f(1) = 1$, such that $\gamma_t := \mu_{f(t)}$ cannot be induced by a plan by simply speeding up μ_t such that the above inequality for $W_2(\gamma_t, \gamma_{t+h})^2$ is not satisfied. However, we can construct it via a Markov kernel. Consider $\bar{\alpha}_t = \alpha_{f(t)}$, where as usual $\alpha_t = (e_t, \pi^2)_\# \alpha$ and $\alpha_t^y \times_y \mu_1 = \alpha_t$. Then $\bar{\alpha}_t^y := \alpha_{f(t)}^y$ is absolutely continuous. Furthermore, for $\bar{v}_t^y := f'(t)v_{f(t)}^y$ we obtain that $(\bar{\alpha}_t^y, \bar{v}_t^y)$ fulfills the continuity equation. The curve $\bar{\mu}_t$ associated to the Markov kernel $\bar{\alpha}_t^y$ and μ_1 is γ_t , which cannot be induced by a plan. \diamond

5.2 Curves induced by Couplings via Disintegration

Next, let us see how curve-velocity pairs induced by couplings $\alpha \in \Gamma(\mu_0, \mu_1)$ fit into the general setting of the previous subsection. Let $(e_t, \pi^2) : \mathbb{R}^d \times \mathbb{R}^d \rightarrow \mathbb{R}^d \times \mathbb{R}^d$ be given by $(x, y) \mapsto (e_t(x, y), y)$ and define a family of couplings

$$\alpha_t := (e_t, \pi^2)_\# \alpha, \quad t \in [0, 1]. \quad (18)$$

Then α_t has the marginals

$$\pi_{\#}^1 \alpha_t = e_{t, \#} \alpha = \mu_t \quad \text{and} \quad \pi_{\#}^2 \alpha_t = \mu_1,$$

and corresponding disintegrations

$$\alpha_t = \alpha_t^x \times_x \mu_t \quad \text{and} \quad \alpha_t = \alpha_t^y \times_y \mu_1 = \mathcal{K}_t(y, \cdot) \times_y \mu_1. \quad (19)$$

By the following proposition, α_t^y is a curve induced by the independent coupling of α^y and δ_y .

Proposition 5.6. *The disintegration α_t^y in (19) fulfills*

$$\alpha_t^y = e_{t, \#}(\alpha^y \times \delta_y) \quad \text{for } \mu_1 - \text{a.e. } y \quad (20)$$

and

$$v_t^y(x) := \frac{y - x}{1 - t}, \quad t \in (0, 1) \quad (21)$$

is an induced velocity field of $\alpha^y \times \delta_y$. In particular, α_t^y is absolutely continuous for μ_1 -a.e. $y \in \mathbb{R}^d$, $v_t^y \in \mathcal{T}_{\alpha_t^y}$ and (α_t^y, v_t^y) fulfills (CE).

Proof. For any measurable, bounded function $f : \mathbb{R}^d \rightarrow \mathbb{R}^d$, we obtain

$$\begin{aligned} \int_{\mathbb{R}^d \times \mathbb{R}^d} f(x, y) d\alpha_t &= \int_{\mathbb{R}^d \times \mathbb{R}^d} f(e_t(x, y), y) d\alpha = \int_{\mathbb{R}^d \times \mathbb{R}^d} f(e_t(x, y), y) d\alpha^y(x) d\mu_1(y) \\ &= \int_{\mathbb{R}^d \times \mathbb{R}^d} f(e_t(x, z), y) d(\alpha^y \times \delta_y)(x, z) d\mu_1(y) \\ &= \int_{\mathbb{R}^d \times \mathbb{R}^d} f(x, y) de_{t, \#}[\alpha^y \times \delta_y](x) d\mu_1(y), \end{aligned}$$

which implies (20). Furthermore, we get for v_t^y in (21) that

$$\begin{aligned} \int_{\mathbb{R}^d} f(x) v_t^y(x) d\alpha_t^y &= \int_{\mathbb{R}^d} f(x) \frac{y-x}{1-t} de_{t, \#}(\alpha^y \times_y \delta_y) = \int_{\mathbb{R}^d} f(e_t(x, y))(y-x) d\alpha^y(x) \\ &= \int_{\mathbb{R}^d \times \mathbb{R}^d} f(e_t(x, z))(z-x) d(\alpha^y \times \delta_y) \\ &= \int_{\mathbb{R}^d \times \mathbb{R}^d} f de_{t, \#}[(z-x)(\alpha^y \times \delta_y)]. \end{aligned}$$

Hence, by (11), the velocity field v_t^y is associated to $\alpha^y \times \delta_y$. Since $\Gamma(\alpha^y, \delta_y) = \Gamma_0(\alpha^y, \delta_y) = \{\alpha^y \times \delta_y\}$, we obtain by Theorem 4.6 that α_t^y is absolutely continuous. By Corollary 4.8, we know that $v_t^y \in \mathcal{T}_{\alpha_t^y}$. \square

By the next proposition, we can rewrite the α -induced velocity field in (11) using the disintegration α_t^x .

Proposition 5.7. *For $\mu_0, \mu_1 \in \mathcal{P}_2(\mathbb{R}^d)$, let $\alpha \in \Gamma(\mu_0, \mu_1)$ and $\mu_t := e_{t, \#}\alpha$. Then $v_t : \mathbb{R}^d \rightarrow \mathbb{R}^d$ defined by*

$$v_t(x) := \int_{\mathbb{R}^d} \frac{y-x}{1-t} d\alpha_t^x(y), \quad t \in (0, 1). \quad (22)$$

is the induced velocity field by α .

Proof. The assertion follows by straightforward computation:

$$\begin{aligned} \int_{\mathbb{R}^d} f(x) v_t(x) d\mu_t &= \int_{\mathbb{R}^d} \int_{\mathbb{R}^d} f(x) \frac{y-x}{1-t} d\alpha_t^x(y) d\mu_t(x) \\ &= \int_{\mathbb{R}^d \times \mathbb{R}^d} f(x) \frac{y-x}{1-t} d\alpha_t(x, y) \\ &= \int_{\mathbb{R}^d} f((1-t)x + ty)(y-x) d\alpha(x, y) \\ &= \int_{\mathbb{R}^d \times \mathbb{R}^d} f de_{t, \#}[(y-x)\alpha]. \end{aligned}$$

\square

Note that it is not a priori clear, that there are representatives of v_t such that v_t seen as a function $[0, 1] \times \mathbb{R}^d \rightarrow \mathbb{R}^d$ is measurable. We show in Proposition B.1 why this is the case.

We summarize the last two propositions in the following theorem.

Theorem 5.8. *Let $\mu_0, \mu_1 \in \mathcal{P}_2(\mathbb{R}^d)$ and $\alpha \in \Gamma(\mu_0, \mu_1)$. Then the pair*

$$\mathcal{K}_t(y, \cdot) = e_{t, \#}(\alpha^y \times_y \delta_y), \quad v_t^y = \frac{y - x}{1 - t}$$

fulfills the conditions of Theorem 5.1 and in this case

$$\mu_t := e_{t, \#}\alpha = \nu_t := \pi_{\#}^1(\mathcal{K}_t(y, \cdot) \times_y \mu_1), \quad v_t(x) = \int_{\mathbb{R}^d} v_t^y d\alpha_t^x(y)$$

is a curve-velocity pair induced by α .

Here is the relation to random variables.

Remark 5.9 (Random variables). Consider two random variables X_0, X_1 with law $\mu_0, \mu_1 \in \mathcal{P}_2(\mathbb{R}^d)$, $X_t = (1 - t)X_0 + tX_1$ and $\alpha = P_{X_0, X_1}$. Then $\alpha_t = P_{X_t, X_1}$ and $\alpha_t^x = P_{X_1|X_t=x}$, where $P_{X_1|X_t=x}$ is defined via $P_{X_t, X_1} = P_{X_1|X_t=x} \times_x P_{X_t}$. Thus (22) reads as

$$v_t(x) = \int_{\mathbb{R}^d} \frac{y - x}{1 - t} dP_{X_1|X_t=x}(y).$$

◇

If the coupling $\alpha \in \Gamma(\mu_0, \mu_1)$ comes from a map T , we can characterize the induced velocity field using the map as in the following corollary.

Corollary 5.10. *Let $\mu_0, \mu_1 \in \mathcal{P}_2(\mathbb{R}^d)$ and let $T : \mathbb{R}^d \rightarrow \mathbb{R}^d$ be an invertible measurable map such that $T_{\#}\mu_0 = \mu_1$. Consider the coupling $\alpha := (\text{Id}, T)_{\#}\mu_0$ and the curve (9) induced by α . Assume that $T_t(x) := (1 - t)x + tT(x)$ is invertible for $t \in [0, 1]$. Then it holds that $\alpha_t = (T_t, T)_{\#}\mu_0$ with disintegrations*

$$\alpha_t^x = \delta_{T(T_t^{-1}(x))} \quad \text{and} \quad \alpha_t^y = \delta_{T_t(T^{-1}(y))}$$

and the α -velocity field in (22) reads as $v_t(x) = T(T_t^{-1}(x)) - T_t^{-1}(x)$. In other words, we have a linear velocity field $v_t(T_t(x)) = T(x) - x$.

Proof. Then we see that

$$\begin{aligned} \int_{\mathbb{R}^d \times \mathbb{R}^d} f(x, y) d\alpha_t &= \int_{\mathbb{R}^d \times \mathbb{R}^d} f(e_t(x, y), y) d\alpha \\ &= \int_{\mathbb{R}^d} f(e_t((x, T(x)), T(x)) d\mu_0 \\ &= \int_{\mathbb{R}^d} f(T_t(x), T(x)) d\mu_0, \end{aligned} \tag{23}$$

which yields $\alpha_t = (T_t, T)_\# \mu_0$ and by (19) also $\mu_t = (T_t)_\# \mu_0$. Further, this implies

$$\begin{aligned} \int_{\mathbb{R}^d \times \mathbb{R}^d} f(x, y) \, d\alpha_t &= \int_{\mathbb{R}^d} f\left(T_t(x), T\left(T_t^{-1}T_t(x)\right)\right) \, d\mu_0 \\ &= \int_{\mathbb{R}^d \times \mathbb{R}^d} f\left(e_t(x, y), T\left(T_t^{-1}(e_t(x, y))\right)\right) \, d\alpha \\ &= \int_{\mathbb{R}^d \times \mathbb{R}^d} f\left(x, T\left(T_t^{-1}(x)\right)\right) \, d\alpha_t \\ &= \int_{\mathbb{R}^d} f\left(x, T\left(T_t^{-1}(x)\right)\right) \, d\pi_\#^1 \alpha_t, \end{aligned}$$

so that $\alpha_t^x = \delta_{T(T_t^{-1}(x))}$. On the other hand, we obtain by (23) that

$$\begin{aligned} \int_{\mathbb{R}^d \times \mathbb{R}^d} f(x, y) \, d\alpha_t &= \int_{\mathbb{R}^d} f((1-t)y + tT(y), T(y)) \, d\mu_0 \\ &= \int_{\mathbb{R}^d} f((1-t)T^{-1}(T(y)) + tT(y), T(y)) \, d\mu_0 \\ &= \int_{\mathbb{R}^d \times \mathbb{R}^d} f((1-t)T^{-1}(y) + ty, y) \, d\alpha \\ &= \int_{\mathbb{R}^d \times \mathbb{R}^d} f((1-t)T^{-1}(y) + ty, y) \, d\alpha_t \\ &= \int_{\mathbb{R}^d \times \mathbb{R}^d} f((1-t)T^{-1}(y) + ty, y) \, d\pi_\#^2 \alpha_t, \end{aligned}$$

meaning that $\alpha_t^y = \delta_{T_t(T^{-1}(y))}$. Finally, we get by (22) that

$$v_t(x) = \int_{\mathbb{R}^d} \frac{y-x}{1-t} \, d\delta_{T_t^{-1}(x)} = \frac{T(T_t^{-1}(x)) - x}{1-t} = T(T_t^{-1}(x)) - T_t^{-1}(x).$$

□

Example 5.11. In Example 5.4, we have seen that the curve ν_t is unfortunately not induced by the coupling $\mathcal{N}(0, I_d) \times \mu_1$. This would be only the case for $r = 0$. But then $\mathcal{K}_1(y, \cdot) = \delta_y$ has no longer a density. However, also for $r \in (0, 1)$, the curve ν_t is induced by another plan, namely

$$\tilde{\alpha} := \tilde{e}_\#(\mathcal{N}(0, I_d) \times \mu_1) \quad \text{with} \quad \tilde{e}(x, y) := (x, (1-r)x + y),$$

since

$$\begin{aligned} \int_{\mathbb{R}^d} f(x) \, d\nu_t(x) &= \int_{\mathbb{R}^d} f(x) \, d\pi_\#^1(\mathcal{K}_t(y, \cdot) \times_y \mu_1(y)) \\ &= \int_{\mathbb{R}^d \times \mathbb{R}^d} f(x) \, d\mathcal{N}(ty, (1-rt)^2) d\mu_1(y) \\ &= \int_{\mathbb{R}^d \times \mathbb{R}^d} f((1-rt)x + ty) \, d\mathcal{N}(0, 1)(y) d\mu_1(y) \\ &= \int_{\mathbb{R}^d} f(x) \, d(e_t \circ \tilde{e})_\#(\mathcal{N}(0, 1) \times \mu_1)(x), \end{aligned}$$

i.e., $\nu_t = e_{t,\sharp}(\tilde{\alpha})$. By Example 7.2 the vector field induced by $\tilde{\alpha}$ coincides with the vector field constructed in (17).

However, considering the family $\tilde{\alpha}_t = (e_t, \pi^2)_{\sharp}\tilde{\alpha}$, we have that $\pi_{\sharp}^2\tilde{\alpha}_t = \mathcal{N}(0, (1-r)^2 \text{Id}) * \mu_1$, which is not the construction of $\pi_{\sharp}^2\alpha_t = \mu_1$ from Example 5.4. In particular, the family of Markov kernels inducing a curve is not unique. \diamond

6 Curves via Stochastic Processes

This section resembles the results from the papers of Liu et al. [28, 29] with our notation. As already mentioned in the introduction, these authors use a stochastic process $(X_t)_t$ to determine an absolutely continuous curve μ_t and an associated vector field v_t based on the conditional expectation

$$\mu_t := P_{X_t} \quad \text{and} \quad v_t(x) := \mathbb{E}[\partial_t X_t | X_t = x],$$

see Theorem 6.3. For the special process $X_t := (1-t)X_0 + tX_1$, this will again result in a curve-velocity pair induced by a coupling, namely $\alpha = P_{X_0, X_1}$, see Corollary 6.4. We start by recalling the notation of conditional expectation in Subsection 6.1 and use this in Subsection 6.2 to deduce appropriate curve-velocity pairs.

6.1 Conditional Expectation

Throughout this section, let $(\Omega, \Sigma, \mathbb{P})$ be a probability space and $X, Y : \Omega \rightarrow \mathbb{R}^d$ be square integrable random variables, i.e., $\int_{\Omega} \|X\|^2 d\mathbb{P} < \infty$. Furthermore, let

$$\sigma(Y) := \{Y^{-1}(A) : A \in B(\mathbb{R}^d)\}$$

be the Σ -algebra generated by Y . The *conditional expectation* $\mathbb{E}[X|Y] : \Omega \rightarrow \mathbb{R}^d$ is a square integrable random variable on $(\Omega, \sigma(Y), \mathbb{P})$ characterized by

$$\mathbb{E}_{\mathbb{P}}[f \mathbb{E}[X|Y]] = \mathbb{E}_{\mathbb{P}}[fX]$$

for all $\sigma(Y)$ -measurable, bounded functions $f : \Omega \rightarrow \mathbb{R}$.

Conditional expectations $\mathbb{E}[X|Y]$ of random vectors can also be interpreted as Borel measurable functions $\psi : \mathbb{R}^d \rightarrow \mathbb{R}^d$ via the Doob–Dynkin Lemma, see [22, Lemma 1.14].

Proposition 6.1 (Doob–Dynkin Lemma). *Let $(\Omega, \Sigma, \mathbb{P})$ be a measure space and let C and D be metric spaces endowed with the Borel Σ -algebra. Let $f : \Omega \rightarrow C$, $g : \Omega \rightarrow D$ be measurable functions. Then the following are equivalent:*

i) f is $\sigma(g)$ -measurable.

ii) There exists Borel measurable function $\psi : D \rightarrow C$ such that $f = \psi \circ g$.

If $C = \mathbb{R}^d$, $D = \mathbb{R}^m$ and $f \in L^2(\Omega, \mathbb{R}^d, \mathbb{P})$, then we have $\psi \in L^2(\mathbb{R}^m, \mathbb{R}^d, g_{\#}\mathbb{P})$.

By the Doob-Dynkin Lemma, there exists a function $\psi \in L^2(\mathbb{R}^d, Y_{\#}\mathbb{P})$ such that

$$\mathbb{E}[X|Y] = \psi \circ Y.$$

We also write $\mathbb{E}[X|Y = y]$ for $\psi(y)$. Strictly speaking, this notation only makes sense for $y \in Y(\Omega)$, but every measurable subset of $Y(\Omega)^C$ is a $Y_{\#}\mathbb{P}$ zero set. By definition it holds that $\mathbb{E}[X|Y = \cdot] \circ Y = \mathbb{E}[X|Y]$.

We can express $\mathbb{E}[X|Y = y]$ also by disintegration of measures.

Proposition 6.2. Consider the disintegration

$$\alpha := P_{X,Y} = \alpha^y \times_y P_Y.$$

Then it holds $\mathbb{E}[X|Y] = \psi \circ Y$ with

$$\psi(y) := \int_{\mathbb{R}^d} x \, d\alpha^y(x). \quad (24)$$

Proof. We check that $\mathbb{E}_{\mathbb{P}}[f\psi \circ Y] = \mathbb{E}_{\mathbb{P}}[fX]$ for every $\sigma(Y)$ -measurable bounded function $f : \Omega \rightarrow \mathbb{R}$. By the Doob-Dynkin Lemma there exists a Borel measurable function $g : \mathbb{R}^d \rightarrow \mathbb{R}^d$ such that $f = g \circ Y$. Thus we can compute, changing the integral order by Fubini,

$$\begin{aligned} \mathbb{E}_{\mathbb{P}}[f\psi \circ Y] &= \int_{\Omega} (g \circ Y)(\omega) \int_{\mathbb{R}^d} x \, d\alpha^{Y(\omega)}(x) \, d\mathbb{P}(\omega) \\ &= \int_{\mathbb{R}^d \times \mathbb{R}^d} g(y)x \, d\alpha^y(x) \, d(Y_{\#}\mathbb{P})(y) \\ &= \int_{\mathbb{R}^d \times \mathbb{R}^d} g(y)x \, d\alpha^y(x) \, dP_Y(y) = \int_{\mathbb{R}^d \times \mathbb{R}^d} g(y)x \, dP_{X,Y}(x, y) \\ &= \int_{\Omega} f(\omega)X(\omega) \, d\mathbb{P}(\omega) = \mathbb{E}_{\mathbb{P}}[fX]. \end{aligned}$$

□

6.2 Curve via Conditional Expectation

A family of random variables $X_t : \Omega \rightarrow \mathbb{R}^d$, $t \in [0, 1]$, is called a *stochastic process*. We say that X_t is *continuously differentiable in $t_0 \in [0, 1]$* , if, for a.e. $\omega \in \Omega$, the

map $t \mapsto X_t(\omega)$ is continuously differentiable in t_0 , where we mean the continuous extension to the boundary if $t_0 \in \{0, 1\}$. We denote the derivative with respect to t by $\partial_t X_t$.

In [29, Theorem 3.3] it was proven that for well-behaved stochastic processes $(X_t)_t$ the conditional expectation can be used to obtain a vector field v_t such that $(X_{t,\#}\mathbb{P}, v_t)$ fulfills the continuity equation. For convenience, we include the proof.

Theorem 6.3. *Let $X_t \in L^2(\Omega, \mathbb{R}^d, \mathbb{P})$ be continuously differentiable in every $t \in [0, 1]$. Let*

$$\mu_t := X_{t,\#}\mathbb{P} = P_{X_t}, \quad \text{and} \quad v_t := \mathbb{E}[\partial_t X_t | X_t = \cdot]. \quad (25)$$

Assume that μ_t is a narrowly continuous curve, $v_t \in L^2(\mathbb{R}^d, \mu_t)$ for $t \in [0, 1]$ and $\|v_t\|_{L^2(\mathbb{R}^d, \mu_t)} \in L^1([0, 1])$. Then μ_t is an absolutely continuous curve in $\mathcal{P}_2(\mathbb{R}^d)$ and (μ_t, v_t) fulfills the continuity equation.

Proof. For $X_t \in L^2(\Omega, \mathbb{R}^d, \mathbb{P})$, we know that $\mu_t = X_{t,\#}\mathbb{P} \in \mathcal{P}_2(\mathbb{R}^d)$. Since μ_t is narrowly continuous and $\|v_t\|_{L^2(\mu_t, \mathbb{R}^d)} \in L^1([0, 1])$, it suffices by Theorem 3.3 to show that (μ_t, v_t) satisfy the continuity equation (CE). For $\varphi \in C_c^\infty((0, 1) \times \mathbb{R}^d)$, we have

$$\frac{d}{dt}(\varphi_t \circ X_t) = (\partial_t \varphi_t) \circ X_t + \langle \nabla_x \varphi_t \circ X_t, \partial_t X_t \rangle,$$

so that

$$\begin{aligned} 0 &= \int_{\Omega} (\varphi_1 \circ X_1 - \varphi_0 \circ X_0) d\mathbb{P} = \int_{\Omega} \int_0^1 \frac{d}{dt}(\varphi_t \circ X_t) dt d\mathbb{P} \\ &= \int_0^1 \int_{\Omega} (\partial_t \varphi_t) \circ X_t + \langle \nabla_x \varphi_t \circ X_t, \partial_t X_t \rangle d\mathbb{P} dt \\ &= \int_0^1 \int_{\mathbb{R}^d} \partial_t \varphi_t d\mu_t dt + \int_0^1 \mathbb{E}[\langle \nabla_x \varphi_t \circ X_t, \partial_t X_t \rangle] dt \\ &= \int_0^1 \int_{\mathbb{R}^d} \partial_t \varphi_t d\mu_t dt + \int_0^1 \mathbb{E}[\langle \nabla_x \varphi_t \circ X_t, \mathbb{E}[\partial_t X_t | X_t] \rangle] dt \\ &= \int_0^1 \int_{\mathbb{R}^d} \partial_t \varphi_t d\mu_t dt + \int_0^1 \mathbb{E}[\langle \nabla_x \varphi_t \circ X_t, \mathbb{E}[\partial_t X_t | X_t = x] \circ X_t \rangle] dt \\ &= \int_0^1 \int_{\mathbb{R}^d} \partial_t \varphi_t d\mu_t dt + \int_0^1 \int_{\mathbb{R}^d} \langle \nabla_x \varphi_t, \mathbb{E}[\partial_t X_t | X_t = x] \rangle d\mu_t dt. \end{aligned}$$

It remains to verify the measurability of v which can be done similarly as in the proof of Proposition 4.5. Set $X : [0, 1] \times \Omega \rightarrow [0, 1] \times \mathbb{R}^d$ with $(t, \omega) \mapsto (t, X_t(\omega))$. Then X is measurable, since it can be written as limit of measurable functions by approximating it in t by step functions. Similarly, we have that $d_t X : [0, 1] \times \Omega \rightarrow \mathbb{R}^d$ given by $(t, \omega) \mapsto \partial_t X_t(\omega)$ is measurable. Thus, we can define a measurable function $v : [0, 1] \times \mathbb{R}^d \rightarrow \mathbb{R}^d$ by $(t, x) \mapsto \mathbb{E}[d_t X | X = (t, x)]$. Then it holds $v(t, \cdot) = \mathbb{E}[\partial_t X_t | X_t = \cdot]$ for a.e. $t \in [0, 1]$ by the following reason: let $\{g_n\}_{n \in \mathbb{N}} \subset C_b(\mathbb{R}^d)$ be a dense subset

and $h \in C_b([0, 1])$. Then we have

$$\mathbb{E}_{(t,\omega) \sim \mathcal{L}_{[0,1]} \times \mathbb{P}}[(h g_n) \circ X] (v \circ X) = \int_0^1 h(t) \mathbb{E}[(g_n \circ X_t) (v(t, \cdot) \circ X_t)] dt$$

and

$$\mathbb{E}_{(t,\omega) \sim \mathcal{L}_{[0,1]} \times \mathbb{P}}[(h g_n) \circ X] d_t X = \int_0^1 h(t) \mathbb{E}[(g_n \circ X_t) \partial_t X_t] dt$$

and the left hand sides are equal by definition of v . This means that

$$\mathbb{E}[(g_n \circ X_t) (v(t, \cdot) \circ X_t)] = \mathbb{E}[(g_n \circ X_t) \partial_t X_t]$$

for a.e. $t \in [0, 1]$ and all $n \in \mathbb{N}$. Since $\{g_n\}_{n \in \mathbb{N}}$ is dense in $C_b(\mathbb{R}^d)$ and $C_b(\mathbb{R}^d)$ is dense in $L^2(\mathbb{R}^d, X_{t, \#} \mathbb{P})$, which contains the bounded measurable functions, we can conclude that $v(t, \cdot) = \mathbb{E}[\partial_t X_t | X_t = \cdot]$ for a.e. $t \in [0, 1]$. \square

The following special case of Theorem 4.6 gives a relation to curve-velocity pairs induced by couplings.

Corollary 6.4. *For the special stochastic process $X_t = (1-t)X_0 + tX_1$, $t \in [0, 1]$ and the plan $\alpha = P_{X_0, X_1}$, the curve-velocity field (25) coincides with those induced by α in (13).*

Proof. Let (μ_t, v_t) be given by (25). By (24), we can rewrite

$$v_t(x) = \mathbb{E}[\partial_t X_t | X_t = x] = \int_{\mathbb{R}^d} z dP_{\partial_t X_t | X_t = x}.$$

Since $X_t = (1-t)X_0 + tX_1$, $t \in [0, 1]$, we obtain $\partial_t X_t = X_1 - X_0$ and further, for any $f \in C_b(\mathbb{R}^d)$, that

$$\begin{aligned} \int_{\mathbb{R}^d} f v_t d\mu_t &= \int_{\mathbb{R}^d} f(x) \int_{\mathbb{R}^d} z dP_{\partial_t X_t | X_t = x} dP_{X_t} = \int_{\mathbb{R}^d \times \mathbb{R}^d} f(x) z dP_{\partial_t X_t, X_t} \\ &= \int_{\mathbb{R}^d \times \mathbb{R}^d} f(x) z dP_{X_1 - X_0, X_t} = \int_{\mathbb{R}^d \times \mathbb{R}^d} f(e_t(x, y))(y - x) dP_{X_0, X_1} \\ &= \int_{\mathbb{R}^d} f de_{t, \#}((y - x)\alpha). \end{aligned}$$

\square

Remark 6.5. Let $X_t = (1-t)X_0 + tX_1$ for independent random variables X_0, X_1 , where $X_0 \sim \mathcal{N}(0, I_d)$. Then in [43, Appendix A1] it is shown that the formula for the vector field associated with μ_t ,

$$v_t = \frac{1-t}{t} \nabla_x \log p_t(x) + \frac{x}{t}, \quad t \in (0, 1)$$

from Proposition 4.11 can also be derived via the velocity field from Theorem 6.3 and Tweedie's formula. Recall that Tweedie's formula [12, Lemma 3.2] for X_t reads as

$$\nabla_x \log p_t(x) = \frac{t\mathbb{E}[X_1|X_t = x] - x}{(1-t)^2},$$

and thus $\mathbb{E}[X_1|X_t = x] = \frac{(1-t)^2}{t} \nabla_x \log p_t(x) + \frac{x}{t}$. Using $X_0 = \frac{X_t - tX_1}{1-t}$ for $t \in (0, 1)$ we obtain

$$\begin{aligned} v_t(x) &= \mathbb{E}[\partial_t X_t | X_t = x] = \mathbb{E}[X_1 - X_0 | X_t = x] \\ &= \mathbb{E}\left[\frac{X_1}{1-t} - \frac{X_t}{1-t} \middle| X_t = x\right] \\ &= \frac{1-t}{t} \nabla_x \log p_t(x) + \frac{x}{t(1-t)} - \frac{x}{1-t} \\ &= \frac{1-t}{t} \nabla_x \log p_t(x) + \frac{x}{t}, \end{aligned}$$

where we used Tweedie's formula and the fact that $\mathbb{E}[X_t|X_t] = X_t$. \diamond

7 Flow Matching

In this section, we will see how we can approximate velocity fields of certain absolutely continuous curves $\mu_t : [0, 1] \rightarrow \mathcal{P}(\mathbb{R}^d)$ by neural networks. If the velocity field is known and the starting measure μ_0 is such that we can easily sample from, like the standard Gaussian one, then we can use the ODE (7) to produce samples from μ_t .

We consider the velocity fields v_t associated to the absolutely continuous curves ν_t from Proposition 5.1. By the next proposition, these velocity fields can be obtained as minimizers of a certain loss function.

Proposition 7.1. *Let $\mu_1 \in \mathcal{P}_2(\mathbb{R}^d)$, and let $\mathcal{K}_t(y, \cdot) : [0, 1] \rightarrow \mathcal{P}_2(\mathbb{R}^d)$ be absolutely continuous curves with associated velocity fields v_t^y for μ_1 -a.e. $y \in \mathbb{R}^d$. Further, assume that $(t, x, y) \mapsto v_t^y$ is measurable and $\|v_t^y\|_{L^2(\mathbb{R}^d \times \mathbb{R}^d, \alpha_t)} \in L^1([0, 1])$. For $\alpha_t := \mathcal{K}_t(y, \cdot) \times_y \mu_1$, we consider the absolutely continuous curve $\nu_t := \pi_{\sharp}^1 \alpha_t$. Then its associated velocity field $v : [0, 1] \times \mathbb{R}^d \rightarrow \mathbb{R}^d$ defined by (17) fulfills*

$$v = \underset{u \in L^2(\mathbb{R}^d, \nu_t \times_t \mathcal{L}_{(0,1)})}{\operatorname{argmin}} \mathbb{E}_{(t,x,y) \sim \alpha_t \times_t \mathcal{L}_{(0,1)}} \left[\|u_t(x) - v_t^y(x)\|^2 \right].$$

Proof. Starting with

$$\|u_t(x) - v_t^y(x)\|^2 = \|u_t(x)\|^2 - 2\langle u_t(x), v_t^y(x) \rangle + \|v_t^y(x)\|^2,$$

we deal with each part individually. It holds

$$\begin{aligned}\mathbb{E}_{(t,x,y)\sim\alpha_t\times_t\mathcal{L}_{(0,1)}}\left[\|u_t(x)\|^2\right] &= \mathbb{E}_{t\sim\mathcal{L}_{(0,1)}}\mathbb{E}_{y\sim\nu_t}\left[\mathbb{E}_{y\sim\alpha_t^x}\left[\|u_t(x)\|^2\right]\right] \\ &= \mathbb{E}_{(t,x)\sim\nu_t\times_t\mathcal{L}_{(0,1)}}\left[\|u_t(x)\|^2\right].\end{aligned}$$

For the second term, we obtain with Fubini's theorem

$$\begin{aligned}\mathbb{E}_{(t,x,y)\sim\alpha_t\times_t\mathcal{L}_{(0,1)}}\left[\langle u_t(x), v_t^y(x) \rangle\right] &= \mathbb{E}_{(t,x)\sim\nu_t\times_t\mathcal{L}_{(0,1)}}\left[\int_{\mathbb{R}^d}\langle u_t(x), v_t^y(x) \rangle d\alpha_t^x(y)\right] \\ &= \mathbb{E}_{(t,x)\sim\nu_t\times_t\mathcal{L}_{(0,1)}}\left[\langle u_t(x), \int_{\mathbb{R}^d} v_t^y(x) d\alpha_t^x(y) \rangle\right] \\ &= \mathbb{E}_{(t,x)\sim\nu_t\times_t\mathcal{L}_{(0,1)}}\left[\langle u_t(x), v_t^y(x) \rangle\right].\end{aligned}$$

Putting everything together, we get

$$\begin{aligned}\mathbb{E}_{(t,x,y)\sim\alpha_t\times_t\mathcal{L}_{(0,1)}}\left[\|u_t(x) - v_t^y(x)\|^2\right] &= \mathbb{E}_{(t,x)\sim\nu_t\times_t\mathcal{L}_{(0,1)}}\left[\|u_t(x) - v_t(x)\|^2\right] \\ &\quad - \mathbb{E}_{(t,x)\sim\nu_t\times_t\mathcal{L}_{(0,1)}}\left[\|v_t(x)\|^2\right] + \mathbb{E}_{(t,x,y)\sim\alpha_t\times_t\mathcal{L}_{(0,1)}}\left[\|v_t^y(x)\|^2\right].\end{aligned}$$

Since the last two terms do not depend on u and the minimizer of the first term is v , we obtain the assertion. \square

In order to learn v , the proposition suggests to use the loss

$$\text{FM}_{\alpha_t}(\theta) := \mathbb{E}_{(t,x,y)\sim\alpha_t\times_t\mathcal{L}_{(0,1)}}\left[\|u_t^\theta(x) - v_t^y(x)\|^2\right]. \quad (26)$$

The name "FM" comes from "flow matching". In the original paper [27], the notation "conditional flow matching" was used which refers to a "conditional flow path", see Remark 5.3. In practice, we work with the empirical expectation. To this end, we will need to be able to sample from $\alpha_t = \mathcal{K}_t(y, \cdot) \times_y \mu_1$ and to compute $v_t^y(x)$. A typical scenario is that samples y_i , $i = 1, \dots, n$ from the data distribution μ_1 are available and that it is easy to sample from the Markov kernel $\mathcal{K}_t(y_i, \cdot)$, $i = 1, \dots, n$.

Example 7.2. A setting, where FM_{α_t} is tractable is Example 5.4. Here $\mu_0 = \mathcal{N}(0, I_d)$ and

$$\mathcal{K}_t(y, \cdot) = \mathcal{N}(ty, (1 - rt)^2 I_d) \quad \text{and} \quad v_t^y = \frac{y - rx}{1 - tr},$$

and we obtain

$$\begin{aligned}\text{FM}_{\alpha_t}(\theta) &= \mathbb{E}_{(t,x,y)\sim\alpha_t\times_t\mathcal{L}_{(0,1)}}\left[\|u_t^\theta(x) - v_t^y(x)\|^2\right] \\ &= \mathbb{E}_{t\sim[0,1]}\mathbb{E}_{y\sim\mu_1}\mathbb{E}_{x\sim\mathcal{N}(ty, (1-rt)^2 I_d)}\left[\|u_t^\theta(x) - \frac{y - rx}{1 - tr}\|^2\right] \\ &= \mathbb{E}_{t\sim[0,1]}\mathbb{E}_{y\sim\mu_1}\mathbb{E}_{x\sim\mathcal{N}(0, I_d)}\left[\|u_t((1 - tr)x + ty) - (y - rx)\|^2\right] \\ &= \mathbb{E}_{t\sim[0,1], (x,y)\sim\mu_0\times\mu_1}\left[\|u_t((1 - tr)x + ty) - (y - rx)\|^2\right].\end{aligned}$$

For α_t coming from a coupling $\alpha \in \Gamma(\mu_0, \mu_1)$ as in (18) with disintegration kernel $\mathcal{K}_t(y, \cdot)$, the associated velocity field v_t^y has the simple form (21). In this important case, the loss function (26) can be simplified.

Proposition 7.3. *Let $\alpha \in \Gamma(\mu_0, \mu_1)$ and $\mu_t = e_{t, \#} \alpha$. Then the velocity field $v : [0, 1] \times \mathbb{R}^d \rightarrow \mathbb{R}^d$ induced by α fulfills*

$$v = \operatorname{argmin}_{u \in L^2(\mathbb{R}^d, \mu_t \times_t \mathcal{L}_{(0,1)})} \mathbb{E}_{(t,x,y) \sim \mathcal{L}_{(0,1)} \times \alpha} \left[\|u_t(e_t(x, y)) - (y - x)\|^2 \right].$$

Proof. By Proposition 5.6, we know that $\mathcal{K}_t(y, \cdot)$ given via

$$\alpha_t := (e_t, \pi^2)_{\#} \alpha = \mathcal{K}_t(y, \cdot) \times_y \mu_1$$

is an absolutely continuous curve for μ_1 -a.e. $y \in \mathbb{R}^d$ with associated simple velocity field $v_t^y(x) := \frac{y-x}{1-t}$, $t \in [0, 1)$. Further, $\mu_t = \nu_t := \pi_{\#}^1 \alpha_t$ and the velocity field induced by α in (22) coincides with those in (17). Thus, by Proposition 7.1, we can calculate

$$\begin{aligned} v &= \operatorname{argmin}_{u \in L^2(\mathbb{R}^d, \mu_t \times_t \mathcal{L}_{(0,1)})} \mathbb{E}_{(t,x,y) \sim \alpha_t \times_t \mathcal{L}_{(0,1)}} \left[\|u_t(x) - v_t^y(x)\|^2 \right] \\ &= \operatorname{argmin}_{u \in L^2(\mathbb{R}^d, \mu_t \times_t \mathcal{L}_{(0,1)})} \mathbb{E}_{(t,x,y) \sim \alpha_t \times_t \mathcal{L}_{(0,1)}} \left[\left\| u_t(x) - \frac{y-x}{1-t} \right\|^2 \right] \\ &= \operatorname{argmin}_{u \in L^2(\mathbb{R}^d, \mu_t \times_t \mathcal{L}_{(0,1)})} \mathbb{E}_{(t,x,y) \sim \alpha \times \mathcal{L}_{(0,1)}} \left[\|u_t(e_t(x, y)) - (y - x)\|^2 \right]. \end{aligned}$$

□

Thus, for curves and velocity fields induced by plans $\alpha \in \Gamma(\mu_0, \mu_1)$ we can use the simplified flow matching objective

$$\text{FM}_{\alpha}(\theta) = \mathbb{E}_{t \sim [0,1], (x,y) \sim \alpha} \left[\|u_t^{\theta}(e_t(x, y)) - (y - x)\|^2 \right]. \quad (27)$$

Computing the empirical expectation requires only samples from the coupling $\alpha \in \Gamma(\mu_0, \mu_1)$. Two canonical choices of couplings, which we can usually sample from, are

- the independent coupling $\alpha = \mu_0 \times \mu_1$, which requires only samples of both μ_0 and μ_1 , and
- an optimal coupling $\alpha \in \Gamma_o(\mu_0, \mu_1)$, which is usually approximated by applying an optimal transport solver on empirical measures approximating μ_i , $i = 0, 1$.

Finally, for a curve arising from a stochastic process also the description of the velocity field by conditional expectation in (25),

$$v_t := \mathbb{E}[\partial_t X_t | X_t = \cdot]$$

can be interpreted as a minimization problem. Namely, it is well-known, see, e.g., [6, 10.1.5 (5)], that

$$\mathbb{E}[X|Y = \cdot] = \operatorname{argmin}_{f \in L^2(\mathbb{R}^d, Y_{\#}\mathbb{P})} \mathbb{E}_{\mathbb{P}}[\|X - f(Y)\|^2].$$

Thus, we obtain

$$v = \operatorname{argmin}_{u \in L^2(\mathbb{R}^d, \mu_t \times \mathcal{L}_{(0,1)})} \mathbb{E}_{\mathcal{L}_{(0,1)} \times \mathbb{P}}[\|\partial_t X_t - u_t(X_t)\|^2].$$

For the special stochastic process $X_t = (1-t)X_0 + tX_1$ in Corollary 6.4, leading to curves induced by plans, this becomes

$$\begin{aligned} v &= \operatorname{argmin}_{u \in L^2(\mathbb{R}^d, \mu_t \times \mathcal{L}_{(0,1)})} \mathbb{E}_{\mathcal{L}_{(0,1)} \times \mathbb{P}}[\|X_1 - X_0 - u_t(X_t)\|^2] \\ &= \operatorname{argmin}_{u \in L^2(\mathbb{R}^d, \mu_t \times \mathcal{L}_{(0,1)})} \mathbb{E}_{(t,x,y) \sim \mathcal{L}_{(0,1)} \times P_{X_0, X_1}}[\|y - x - u_t(e_t(x, y))\|^2] \end{aligned}$$

and we are back at Proposition 7.3.

8 Numerical Examples for Flow Matching

8.1 Flow Matching Algorithms

Sampling from a product plan $\alpha = \mu_0 \times \mu_1$ can be reduced to sampling from the individual measures $z_i \sim \mu_0$, $x_i \sim \mu_1$ and simply building the product $(z_i, x_i) \sim \alpha$. This is the reason that training a flow matching model from a product plan is particularly easy, as can be seen in Algorithm 1.

Given two measures $\mu_0, \mu_1 \in \mathcal{P}_2(\mathbb{R}^d)$, sampling from an optimal transport plan $\alpha \in \Gamma_o(\mu_0, \mu_1)$ is usually not possible. Often both measures are not known analytically but only an approximation by samples, so that an optimal plan cannot be obtained. But even the plan for the approximation is often not computable since usually the number of samples is so high that solving the OT problem is computationally too expensive. In this case a popular method is minibatch OT flow matching [40]. The idea is to partition the samples $x_1, \dots, x_{N_t} \sim \mu_1$ into minibatches (smaller subsets), on which solving the OT problem is computational feasible. Details are described in Algorithm 2.

Once a flow vector field u^θ is learned, sampling is then done by sampling $z_i \sim \mu_0$ from the source distribution and using an ODE solver for $f'(t) = u_t^\theta(f(t))$, $f(0) = z_i$ to compute $f(1)$.

Algorithm 1 Learning u^θ from the plan $\alpha = \mu_0 \times \mu_1 \in \Gamma(\mu_0, \mu_1)$

N_b : batch size, N_e : number of epochs, N_t number of samples from the target distribution

x_1, \dots, x_{N_t} samples from the target distribution μ_1

Network $u^\theta : [0, 1] \times \mathbb{R}^d \rightarrow \mathbb{R}^d$ depending on a parameter $\theta \in \mathbb{R}^m$.

for $e = 1, \dots, N_e$ **do**

for $s = 1, \dots, \frac{N_t}{N_b}$ **do**

 Draw $(z_i) \sim \mu_0$ for $1 \leq i \leq N_b$

 Draw $t_i \sim \mathcal{L}_{(0,1)}$ for $1 \leq i \leq N_b$

 Compute $x_{t_i}^i = (1 - t_i)z_i + t_i x_{i+(s-1)N_b}$

 Compute $\mathcal{L}(\theta) = \frac{1}{N_b} \sum_{i=1}^{N_b} \left\| u^\theta(t_i, x_{t_i}^i) - (x_{i+(s-1)N_b} - z_i) \right\|^2$ and $\nabla_\theta \mathcal{L}(\theta)$

 Update θ using $\nabla_\theta \mathcal{L}(\theta)$

end for

end for

Return: θ

Algorithm 2 Learning u^θ from minibatch OT flow matching for μ_0 the source distribution and μ_1 the target distribution.

N_b : batch size, N_{bOT} OT batch size, N_e : number of epochs, N_t number of samples from the target distribution

x_1, \dots, x_{N_t} samples from the target distribution μ_1

Network $u^\theta : [0, 1] \times \mathbb{R}^d \rightarrow \mathbb{R}^d$ depending on a parameter $\theta \in \mathbb{R}^m$.

for $e = 1, \dots, N_e$ **do**

for $o = 1, \dots, \frac{N_t}{N_{bOT}}$ **do**

 Draw $z_i \sim \mu_0$ for $1 \leq i \leq N_{bOT}$

 Compute optimal transport map for

$$W_2 \left(\frac{1}{N_{bOT}} \sum_{i=1}^{N_{bOT}} \delta_{z_i}, \frac{1}{N_{bOT}} \sum_{i=1}^{N_{bOT}} \delta_{x_{i+(o-1)N_{bOT}}} \right)$$

 described by a function $T_o : \{1, \dots, N_{bOT}\} \rightarrow \{1 + (o-1)N_{bOT}, \dots, oN_{bOT}\}$

for $s = 1, \dots, \frac{N_{bOT}}{N_b}$ **do**

 Draw $t_i \sim \mathcal{L}_{(0,1)}$ for $1 \leq i \leq N_b$

 Compute $x_{t_i}^i = (1 - t_i)z_i + t_i x_{T_o(i)}$

 Compute $\mathcal{L}(\theta) = \frac{1}{N_b} \sum_{i=1}^{N_b} \left\| u^\theta(t_i, x_{t_i}^i) - (x_{T_o(i)} - z_i) \right\|^2$ and $\nabla_\theta \mathcal{L}(\theta)$

 Update θ using $\nabla_\theta \mathcal{L}(\theta)$

end for

end for

end for

Return: θ

8.2 Numerical Examples

For our first example we chose standard $2d$ Gaussian distribution as source distribution and a Gaussian mixture model with eight equality weighted modes as target distribution, see 7. In the middle, we can see the trajectories created by a vector field learned with minibatch OT flow matching, using a simple Euler method for solving the flow ODE. Here the trajectories are mostly straight, making sampling easier since the sampling quality does not depend as much on time discretization or the ODE solving method. On the left, the trajectories for a vector field learned via flow matching for a product plan is displayed, where again an Euler method was used to solve the flow ODE. Here the trajectories are much less straight and sample quality depends very much on the ODE solving quality. On the right we see the result for Neural ODEs, described in Section 10, which has trajectories differing from both of the flow matching approaches.

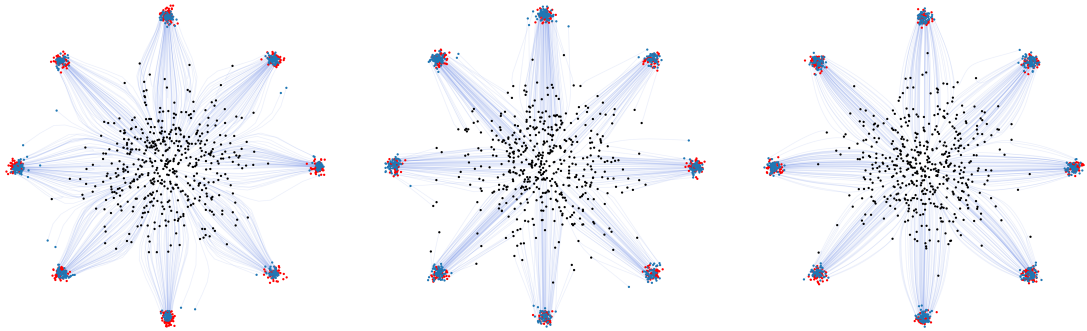


Figure 7: Trajectories of points from a vector field u^θ obtained via flow matching from a coupling $\alpha \in \Gamma(\mu_0, \mu_1)$. We chose $\mu_0 = \mathcal{N}(0, 1)$ and as target distribution μ_1 a Gaussian mixture model with 8 modes. Black: points $\{z_i\}_{i=1}^{300}$ drawn from the source distribution $\mu_0 = \mathcal{N}(0, 1)$. Blue: points sampled via the vector field from $\{z_i\}_{i=1}^{300}$. Red: points sampled from the target distribution. Blue lines: trajectories of the vector field. The left image shows the results for u^θ trained using the independent coupling and the middle image shows the result when trained with minibatch OT flow matching. The right image shows the result from training a continuous normalizing flow as in Section 10.

Finally, we show a high dimensional application of flow matching in Figure 8. Here we used the flow vector field from [30], which was already trained via minibatch OT flow matching on images of cat faces. For a comparison of the performance for the flow matching with different plans see [40, Table 2].



Figure 8: Single trajectory for a flow matching model trained on cat images. For the trained model, see [30]. Note that for the standard Gaussian distribution we can sample in each direction separately, so that the left starting sample contains the one-dimensional coordinates in each of the $d = 256^2$ directions for the red-green-blue channels.

9 Flow Matching in Bayesian Inverse Problems

In this section, we are interested in Bayesian inverse problems

$$W = F(X) + \Xi$$

for random variables $W : \Omega \rightarrow \mathbb{R}^m$, $X : \Omega \rightarrow \mathbb{R}^d$, a forward operator $F : \mathbb{R}^d \rightarrow \mathbb{R}^m$ and a random variable $\Xi : \Omega \rightarrow \mathbb{R}^m$ which is responsible for noisy outputs. The aim is to approximate the posterior distribution $P_{X|W=w}$. We propose to learn a map

$$g : \mathbb{R}^m \times \mathbb{R}^d \rightarrow \mathbb{R}^m \times \mathbb{R}^d, \quad (w, x) \mapsto (w, g_w(x))$$

such that

$$g_{\#}(P_W \times \mathcal{N}(0, 1)) = P_{W,X}.$$

This implies $g_{w,\#}\mathcal{N}(0, 1) = P_{X|W=w}$, since we have for any $f \in C_b(\mathbb{R}^m \times \mathbb{R}^d)$ that

$$\int_{\mathbb{R}^m \times \mathbb{R}^d} f dP_{W,X} = \int_{\mathbb{R}^m \times \mathbb{R}^d} f dg_{\#}(P_W \times \mathcal{N}(0, 1)) = \int_{\mathbb{R}^m} \int_{\mathbb{R}^d} f(w, x) d(g_{w,\#}\mathcal{N}(0, 1)) dP_W.$$

In particular, we can sample from $P_{X|W=w}$ by sampling from $\mathcal{N}(0, 1)$ and applying g_w . Again, we want to describe the generator g via a curve in a space of probability measures. However, now we need a curve, where the W -marginal does not change, i.e., a curve in the space

$$\mathcal{P}_{P_W} := \{\mu \in \mathcal{P}_2(\mathbb{R}^m \times \mathbb{R}^d) : \pi_{\#}^1 \mu = P_W\}.$$

In the next subsection, we will equip the space \mathcal{P}_{P_W} with a metric turning it into a complete metric space and determine couplings such that the corresponding curve stays in \mathcal{P}_{P_W} . Then we will use these curves for flow matching in order to learn conditional generating networks that approximate the posterior distribution $P_{X|W=w}$ for w sampled from P_W . This section is based on our paper [7], see also [23].

9.1 Conditional Wasserstein Distance

The notion of conditional Wasserstein distances appeared already in [25, Section 2.4] as well as in the PhD thesis of Gigli [14, Chapter 4], who studied a metric on the so-called "geometric tangent space" of the Wasserstein-2 space. Recently, conditional Wasserstein distances were studied in the realm of machine learning in [4] as well as in functional optimal transport in [21]. We will focus on its application in Bayesian flow matching as presented in our paper [7], where also the proofs of the following theorems and propositions are provided.

To fix the notation, let $\mathbf{u} = (w, x) \in \mathbb{R}^m \times \mathbb{R}^d$ and denote the projections by

$$\pi^1(\mathbf{u}) := w, \quad \pi^2(\mathbf{u}) := x.$$

For an arbitrary, fixed reference measure $\eta \in \mathcal{P}_2(\mathbb{R}^m)$, we consider the space

$$\mathcal{P}_\eta(\mathbb{R}^m \times \mathbb{R}^d) := \{\mu \in \mathcal{P}_2(\mathbb{R}^m \times \mathbb{R}^d) : \pi_\#^1 \mu = \eta\}.$$

In order to define a conditional Wasserstein distance on \mathcal{P}_η , we introduce, for $\mu, \nu \in \mathcal{P}_\eta(\mathbb{R}^m \times \mathbb{R}^d)$, the set of 4-plans

$$\Gamma_\eta = \Gamma_\eta(\mu, \nu) := \left\{ \alpha \in \Gamma(\mu, \nu) : \pi_\#^{1,1} \alpha = \Delta_\# \eta \right\},$$

where

$$\pi^{1,1}(\mathbf{u}_1, \mathbf{u}_2) := (\pi^1(\mathbf{u}_1), \pi^1(\mathbf{u}_2)) = \left(\pi^1((w_1, x_1)), \pi^1((w_2, x_2)) \right) = (w_1, w_2)$$

and $\Delta : \mathbb{R}^m \rightarrow \mathbb{R}^m \times \mathbb{R}^m$, $w \mapsto (w, w)$ is the diagonal map. Note that

$$\Delta^{-1}(w_1, w_2) = \emptyset \text{ if } w_1 \neq w_2 \quad \text{and} \quad \Delta^{-1}(w_1, w_2) = w \text{ if } w_1 = w_2 = w.$$

Now we define the *conditional Wasserstein(-2) distance* by

$$W_{2,\eta}(\mu, \nu) := \left(\min_{\alpha \in \Gamma_\eta(\mu, \nu)} \int_{(\mathbb{R}^m \times \mathbb{R}^d)^2} \|\mathbf{u}_1 - \mathbf{u}_2\|^2 d\alpha \right)^{\frac{1}{2}}.$$

Indeed, the above minimum is obtained and the set of optimal couplings is denoted by $\Gamma_{\eta,o}$. The following theorem collects important properties of the conditional Wasserstein distance.

Theorem 9.1. *The conditional Wasserstein space $(\mathcal{P}_\eta(\mathbb{R}^m \times \mathbb{R}^d), W_{2,\eta})$ is a complete metric space. The conditional Wasserstein distance has the following properties:*

i) *For $\mu, \nu \in \mathcal{P}_\eta(\mathbb{R}^m \times \mathbb{R}^d)$, it holds*

$$W_{2,\eta}^2(\mu, \nu) = \mathbb{E}_{w \sim \eta} [W_2^2(\mu^w, \nu^w)],$$

where μ^w, ν^w denote the disintegrations of μ, ν with respect to η , respectively.

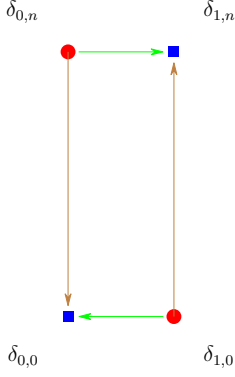


Figure 9: Consider $\eta = \frac{1}{2}\delta_0 + \frac{1}{2}\delta_1$, $\mu_n = \frac{1}{2}\delta_{0,n} + \frac{1}{2}\delta_{1,0}$ and $\nu_n = \frac{1}{2}\delta_{0,0} + \frac{1}{2}\delta_{1,n}$. Then $W_2(\mu_n, \nu_n) = 1$ is the length of $\xrightarrow{\text{green}}$ and $\xrightarrow{\text{green}}$ indicates the optimal transport map. Furthermore $W_{2,\eta}(\mu_n, \nu_n) = n$ is the length of $\xrightarrow{\text{red}}$ and $\xrightarrow{\text{red}}$ indicates the optimal transport for $W_{2,\eta}$.

ii) There exist optimal plans $\alpha_w \in \Gamma_o(\mu^w, \nu^w)$, $w \in \mathbb{R}^m$ such that

$$\alpha := \underbrace{(\delta_w \times \alpha_w)}_{\in \mathcal{P}_2(\mathbb{R}^m \times \mathbb{R}^d \times \mathbb{R}^d)} \times_w \eta \in \Gamma_{\eta,o}(\mu, \nu).$$

Note that ii) means, for any $f \in C_b(\mathbb{R}^d)$, that

$$\begin{aligned} \int_{(\mathbb{R}^m \times \mathbb{R}^d)^2} f \, d\alpha &= \int_{\mathbb{R}^m} \int_{\mathbb{R}^m \times \mathbb{R}^d \times \mathbb{R}^d} f(w_1, x_1, w_2, x_2) \, d\delta_{w_1}(w_2) d\alpha_{w_1}(x_1, x_2) d\eta(w_1) \\ &= \int_{\mathbb{R}^m} \int_{\mathbb{R}^d \times \mathbb{R}^d} f(w, x_1, w, x_2) \, d\alpha_w(x_1, x_2) d\eta(w). \end{aligned}$$

Remark 9.2. Proposition 9.1ii) indicates another use of the conditional Wasserstein distance. Namely if we have two measures $\mu_0, \mu_1 \in \mathcal{P}_\eta$ and we have that $W_2(\mu_0, \mu_1)$ is small that does not necessarily mean that the posteriors are close. We can see in Figure 9 that there exist $\eta \in \mathcal{P}_2(\mathbb{R})$, $\mu_n, \nu_n \in \mathcal{P}_\eta(\mathbb{R} \times \mathbb{R})$ such that $W_2(\mu_n, \nu_n) = 1$ and $\mathbb{E}_{w \sim \eta}[W_2^2(\mu_{0,w}, \mu_{1,w})] = W_{2,\eta}(\mu_n, \nu_n) = n$. This means that W_2 is not a good measure in order to access if a generator g is approximating the posteriors well. In contrast if we use $W_{2,\eta}$ we know that the posteriors are, at least in expectation, well approximated.

As shown in [23, Theorem 3.4] and [4], there is a counterpart of Theorem 3.3 for the conditional Wasserstein distance.

Theorem 9.3. Let $\mu_t : I \rightarrow \mathcal{P}_\eta(\mathbb{R}^m \times \mathbb{R}^d)$ be a narrowly continuous curve. Then μ_t is absolutely continuous in with respect to $W_{2,\eta}$ in the sense of (4), if and only if there exists a measurable vector field $v : I \times \mathbb{R}^m \times \mathbb{R}^d \rightarrow \mathbb{R}^m \times \mathbb{R}^d$ such that the following three conditions are fulfilled:

i) $(v_t)_j = 0$ as element in $L^2(\mathbb{R}, \mu_t)$ for a.e. $t \in [0, 1]$ and for all $j \leq m$,

- ii) $\|v_t\|_{L^2(\mathbb{R}^m \times \mathbb{R}^d, \mu_t)} \in L^1(I)$,
- iii) (μ_t, v_t) fulfills (CE).

In this case, the metric derivative $|\mu'_t|$ exists and we have $|\mu'_t| \leq \|v_t\|_{L^2(\mu_t, \mathbb{R}^m \times \mathbb{R}^d)}$ for a.e. $t \in I$.

The following theorem ensures that the curve μ_t associated to a plan $\alpha \in \Gamma_\eta(\mu_0, \mu_1)$ fulfills $\mu_t \in \mathcal{P}_\eta(\mathbb{R}^m \times \mathbb{R}^d)$ for all $t \in [0, 1]$ and the corresponding vector field does not move mass in the w component.

Theorem 9.4. *Let $\mu_0, \mu_1 \in \mathcal{P}_\eta(\mathbb{R}^m \times \mathbb{R}^d)$ and let $\alpha \in \Gamma_\eta(\mu_0, \mu_1)$. Let (μ_t, v_t) be the curve and measurable velocity field induced by α , i.e.*

$$\mu_t = e_{t,\#}\alpha, \quad \text{and} \quad v_t \mu_t = e_{t,\#}[(\mathbf{u}_2 - \mathbf{u}_1)\alpha] \quad \text{for a.e. } t \in [0, 1].$$

Then the following holds true:

- i) $\mu_t \in \mathcal{P}_\eta(\mathbb{R}^m \times \mathbb{R}^d)$ for all $t \in [0, 1]$,
- ii) $(v_t)_j = 0$ as element in $L^2(\mathbb{R}, \mu_t)$ for a.e. $t \in [0, 1]$ and for all $j \leq m$,
- iii) (μ_t, v_t) satisfy the continuity equation (CE) and

$$\|v_t\|_{L^2(\mathbb{R}^m \times \mathbb{R}^d, \mu_t)} \leq \|y - x\|_{L^2((\mathbb{R}^m \times \mathbb{R}^d)^2, \alpha)} \quad \text{for a.e. } t \in [0, 1].$$

In particular, we have $\|v_t\|_{L^2(\mathbb{R}^m \times \mathbb{R}^d, \mu_t)} \in L^1(I)$ and μ_t is an absolutely continuous curve with respect to $W_{2,\eta}$.

Proof. To proof i) and ii) follow from [7, Lemma 5, Proposition 6]. The first statements of iii) follow from Proposition 4.6 and finally the absolute continuity with respect to $W_{2,\eta}$ is implied by Theorem 9.3. \square

Remark 9.5. Note that for an absolutely curve $\mu_t \in \mathcal{P}_\eta$ and a vector field $v_t \in L^2(\mu_t, \mathbb{R}^m \times \mathbb{R}^d)$ it is not necessarily true that $v_j = 0$ for every $j \leq m$ since these components could encode η preserving maps. However, Proposition 9.4 ensures that for a curve associated to a plan $\alpha \in \Gamma_\eta(\mu_0, \mu_1)$ this is the case and in particular for a map ϕ which is a solution of the ODE $\partial_t \phi_t = v_t(\phi_t)$; $\phi_0 = \text{Id}$ we can conclude that $\pi^1(\phi_t(\mathbf{u})) = \pi^1(\mathbf{u})$.

The counterpart of Proposition 4.4 reads as follows, see [7, Lemma 5]).

Proposition 9.6. *Let $\mu_0, \mu_1 \in \mathcal{P}_\eta(\mathbb{R}^m \times \mathbb{R}^d)$ and let $\alpha \in \Gamma_{\eta,o}(\mu_0, \mu_1)$. Then the curve $\mu_t := (e_t)_\# \alpha$ is a geodesic in $(\mathcal{P}_\eta(\mathbb{R}^m \times \mathbb{R}^d), W_{2,\eta})$. In particular, $(\mathcal{P}_\eta(\mathbb{R}^m \times \mathbb{R}^d), W_{2,\eta})$ is a geodesic space.*

An illustration of the difference between geodesics with respect to W_2 and geodesics with respect to $W_{2,\eta}$ is given in Figure 10.

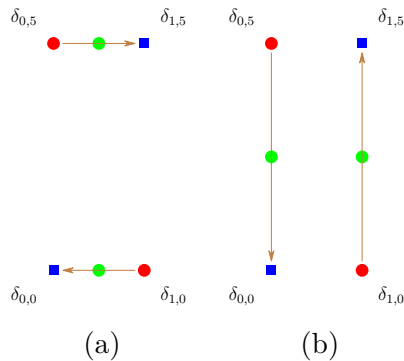


Figure 10: Consider $\eta = \frac{1}{2}\delta_0 + \frac{1}{2}\delta_1$, $\mu_0 = \frac{1}{2}\delta_{0,5} + \frac{1}{2}\delta_{1,0}$ and $\mu_1 = \frac{1}{2}\delta_{0,0} + \frac{1}{2}\delta_{1,5}$. (a) Geodesic with respect to W_2 , green: $\mu_{\frac{1}{2}}$. (b) Geodesic with respect to $W_{2,\eta}$, green: $\mu_{\frac{1}{2}}$.

9.2 Almost Conditional Couplings

One drawback of the space $\mathcal{P}_\eta(\mathbb{R}^m \times \mathbb{R}^d)$ is that we can in general not approximate $\mu \in \mathcal{P}_\eta(\mathbb{R}^m \times \mathbb{R}^d)$ by an empirical measure, if η is not empirical. In other words, an empirical approximation $\mu_n = \frac{1}{n} \sum_{i=1}^n \delta_{(w_i, x_i)}$ of $\mu \in \mathcal{P}_\eta(\mathbb{R}^m \times \mathbb{R}^d)$ with respect to W_2 is usually not an element of $\mathcal{P}_\eta(\mathbb{R}^m \times \mathbb{R}^d)$. Even if we approximate two measures $\mu, \nu \in \mathcal{P}_\eta(\mathbb{R}^m \times \mathbb{R}^d)$ with respect to W_2 by empirical measures μ_n, ν_n with $\pi_{\#}^1 \mu_n = \pi_{\#}^1 \nu_n$, it is not necessarily true that there is a sequence $\alpha_n \in \Gamma_{\pi_{\#}^1 \mu_n, \nu_n}$ such that α_n converges to an $\alpha \in \Gamma_{\eta, o}(\mu, \nu)$ as [7, Example 9] shows.

One way to overcome the above drawback is to relax the hard constraint $\pi^{1,1} \alpha = \Delta_{\#} \eta$ in the definition of the conditional Wasserstein distance. To this end, we define

$$d_\beta(\mathbf{u}_1, \mathbf{u}_2) := \|x_1 - x_2\|^2 + \beta \|w_1 - w_2\|^2, \quad \beta > 0.$$

Then

$$W_\beta(\mu, \nu) := \min_{\alpha \in \Gamma(\mu, \nu)} \left(\int_{(\mathbb{R}^m \times \mathbb{R}^d)^2} d_\beta(\mathbf{u}_1, \mathbf{u}_2) d\alpha \right)^{\frac{1}{2}}$$

defines a metric on $\mathcal{P}_2(\mathbb{R}^m \times \mathbb{R}^d)$. It turns out that for $0 \ll \beta$ the optimal couplings α in this metric are "close" to fulfilling $\pi^{1,1} \alpha = \Delta_\eta$ in the following sense, see [7, Proposition 10].

Proposition 9.7. *Let $\mu_0, \mu_1 \in \mathcal{P}_\eta(\mathbb{R}^m \times \mathbb{R}^d)$ and let $(\alpha_\beta)_\beta$ be a sequence of optimal transport plans from μ_0 to μ_1 with respect to W_β . Then we have*

$$\int_{\mathbb{R}^m \times \mathbb{R}^m} \|w_1 - w_2\|^2 d\pi^{1,1}_{\#} \alpha_\beta = \int_{(\mathbb{R}^m \times \mathbb{R}^d)^2} \|w_1 - w_2\|^2 d\alpha_\beta \rightarrow 0 \quad \text{as } \beta \rightarrow \infty.$$

The distance W_β successfully addresses the issue of approximating measures by empirical measures as the following proposition from [7, Proposition 12] shows.

Proposition 9.8. *Let $\mu, \nu \in P_\eta(\mathbb{R}^m \times \mathbb{R}^d)$ and let μ_n, ν_n be empirical measures which converge narrowly to μ, ν . Then, for a sequence $\beta_k \rightarrow \infty$, there exists an increasing subsequence n_k and optimal plans $\alpha_{n_k} \in \Gamma(\mu_{n_k}, \nu_{n_k})$ for $W_{\beta_k}(\mu_{n_k}, \nu_{n_k})$ such that α_{n_k} converges narrowly to an optimal plan $\alpha \in \Gamma_{\eta,o}(\mu, \nu)$.*

Remark 9.9. For $\beta > 0$ let $a_\beta : \mathbb{R}^m \times \mathbb{R}^d \rightarrow \mathbb{R}^m \times \mathbb{R}^d$ be defined by $a_\beta(w, x) = (\sqrt{\beta}w, x)$. Then an easy calculation shows that $W_\beta(\mu, \nu) = W_2(a_{\beta,\#}\mu, a_{\beta,\#}\nu)$ and there is a one-to-one correspondence between optimal plans for $W_\beta(\mu, \nu)$ and $W_2(a_{\beta,\#}\mu, a_{\beta,\#}\nu)$ given by $\alpha \mapsto (a_\beta, a_\beta)_\# \alpha$. Thus W_β and optimal plans can be computed by standard W_2 solvers. \diamond

9.3 Bayesian Flow Matching

Since $\Gamma_\eta(\mu_0, \mu_1) \subseteq \Gamma(\mu_0, \mu_1)$ we can learn the vector field v_t corresponding to $\alpha \in \Gamma_\eta(\mu_0, \mu_1)$ with the extended flow matching objective (27), i.e.,

$$\text{CFM}(\theta) := \mathbb{E}_{t \sim \mathcal{L}[0,1], (w, x_0, w, x_1) \sim \alpha} \left[\|v^\theta(t, e_t((w, x_0, w, x_1)) - (0, x_1 - x_0))\|^2 \right].$$

Since $\pi_\#^{1,1} \alpha = \Delta_\# \eta$, we only have to consider samples (w, x_0, w, x_1) from α . Further, since $v_j = 0$ for $j \leq m$, we can parametrize v_t^θ as function with values in \mathbb{R}^d instead of $\mathbb{R}^m \times \mathbb{R}^d$. In this way, we have for a solution of

$$\partial_t \phi_t(x) = v_t(\phi_t(x)), \quad \phi_0(x) = x$$

automatically that $\pi_\#^1(\phi_{t,\#}\mu_0) = \eta$.

Remark 9.10. In order to get absolutely continuous curves from plans, we have used i) direct product of measures or ii) optimal transport plans in the previous sections. Let us see how similar settings look in the Bayesian case.

i) Unfortunately, for $\mu_0, \mu_1 \in \mathcal{P}_\eta(\mathbb{R}^m \times \mathbb{R}^d)$ it does not hold that $\mu_0 \times \mu_1 \in \Gamma_\eta(\mu_0, \mu_1)$. A remedy is to use $\mu_0 = \eta \times \nu \in \mathcal{P}_2(\mathbb{R}^m \times \mathbb{R}^d)$ with some $\nu \in \mathcal{P}_d(\mathbb{R}^d)$ and the plan

$$\alpha := \tilde{\Delta}_\#(\nu \times \mu_1) \in \Gamma_\eta(\mu_0, \mu_1),$$

where

$$\tilde{\Delta} : \mathbb{R}^d \times \mathbb{R}^m \times \mathbb{R}^d \rightarrow (\mathbb{R}^m \times \mathbb{R}^d)^2, \quad \tilde{\Delta}(x_0, w_1, x_1) := (w_1, x_0, w_1, x_1).$$

In order to sample from α we only need to be able to sample from ν and μ_1 .

ii) We can use Proposition 9.1 ii) and solve the optimal transport problem for fixed samples w from η , to obtain an optimal coupling $\alpha \in \Gamma_{\eta,o}(\mu_0, \mu_1)$. In order to ensure that the $\alpha_w \in \Gamma_o(\mu_0^w, \mu_1^w)$ can be used to build $\alpha \in \Gamma_{\eta,o}(\mu_0, \mu_1)$, some measurability conditions must be ensured. For examples where these conditions are fulfilled, see e.g. [15, Corollary 1.2] and [7, Proposition 8].

Of course we can also choose $\beta \gg 0$ and compute an optimal transport plan α for $W_\beta(\mu_0, \mu_1)$. We then use the loss

$$\text{CFM}(\theta) := \mathbb{E}_{t \sim \mathcal{L}[0,1], (w_0, x_0, w_1, x_1) \sim \alpha} \left[\|v^\theta(t, e_t((w_0, x_0, w_1, x_1))) - (0, x_1 - x_0)\|^2 \right].$$

Although this is not exactly the loss for the plan α and we only have approximately $w_0 \cong w_1$, in practice this leads to good results, see also next section. Furthermore, we use minibatch OT described in Algorithm 2 to approximately minimize CFM. We will call this strategy minibatch OT Bayesian flow matching with respect to W_β .

9.4 Numerical Examples of Bayesian Flow Matching

In order to show the feasibility of Bayesian flow matching, we provide two examples.

1. Conditional image generation. We used the dataset Cifar10 [26], which consists of 10 classes of color images of size $32 \times 32 \times 3$. Here $\eta = \mathcal{P}_2(\mathbb{R}^{10})$ is defined by $\eta = \frac{1}{10} \sum_{i=1}^{10} \delta_{e_i}$, where e_i is the standard basis of \mathbb{R}^{10} . Then samples from μ_1 are of the form $(e_{l(x_i)}, x_i)$, where $l(x_i)$ is the class of x_i . The source measure is $\mu_0 := \eta \times \mathcal{N}(0, 1)$. For conditional image generation, we used trained flow matching models from [7]. For training with respect to $W_{2,\beta}$ the minibatch OT training algorithm 2 was used for Figure 11[(a),(b)]. For the plan $\alpha \in \Gamma_\eta(\mu_0, \mu_1)$ in Figure 11[(c)], we applied the coupling from Remark 9.10 and for training Algorithm 1.

Figure 11 shows generated images, where in row i the samples are generated from (e_i, z) where 10 different samples $z \sim \mathcal{N}(0, 1)$ are drawn. For $\beta = 1$, Figure 11[(a)] illustrates that the generation is not class conditional, i.e. in every row there are images of multiple classes. For $\beta = 100$ and for the conditional plan from Remark 9.10, we can see in Figure 11 that the generation is class conditional, meaning that every row only contains samples from one class.

Simple Bayesian inverse problem. The following example can be found in [7, Section 8.2]. Let $X \in \mathbb{R}^5$ be a random variable for which the law P_X is a Gaussian mixture model with 10 modes with means uniformly chosen in $[-1, 1]^5$ and standard derivations 0.1. We consider the Bayesian inverse problem

$$Y = AX + \Xi \quad \text{with} \quad A := \left(\frac{0.1}{i} \delta_{i,j} \right)_{i,j=1}^5.$$

The noise variable Ξ , which is independent from X , is distributed as $\mathcal{N}(0, 0.1)$. Then by [18, Lemma 11] the posterior distribution $P_{X|Y=y}$ is a Gaussian mixture model which can be analytically computed. This allows us to sample from $P_{X|Y=y}$.

Training Bayesian flow matching with α from Remark 9.10. Here we sample from

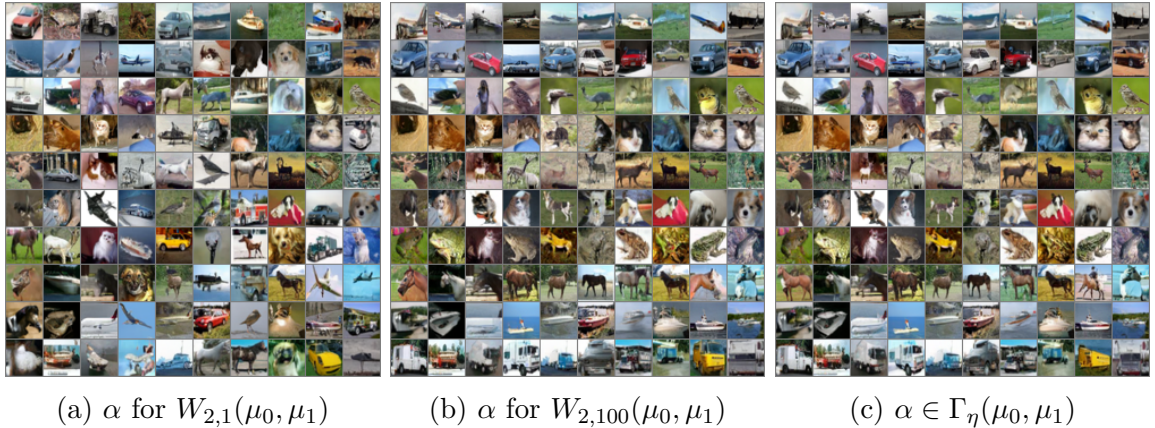


Figure 11: (Bayesian) Flow matching on Cifar10.

$\alpha \in \Gamma(P_Y \times \mathcal{N}(0, I_5), P_{Y,X})$ by sampling $x_i \sim P_X$, computing $y_i := f(x_i) + \xi_i \sim P_Y$ for $\xi_i \sim \mathcal{N}(0, 0.1 \text{ Id})$ and $z_i \sim \mathcal{N}(0, \text{Id})$. We then use (y_i, z_i, y_i, x_i) in order to approximate α and to compute $\text{CFM}(\theta)$. Batching in i and t is done as in Algorithm 1.

Training minibatch OT Bayesian flow matching with respect to $W_{2,100}$. Here we use Algorithm 2 for $\mu_0 = P_Y \times \mathcal{N}(0, \text{Id})$ and $\mu_1 = P_{Y,X}$. In order to be able to sample from μ_0 for a minibatch $(y_i, x_i)_{i=1}^{N_{bOT}} \sim P_{Y,X}$, where N_{bOT} is the minibatch size, we sample $z_i \sim \mathcal{N}(0, \text{Id})$ and use $(y_i, z_i)_{i=1}^{N_{bOT}} \sim \mu_0$.

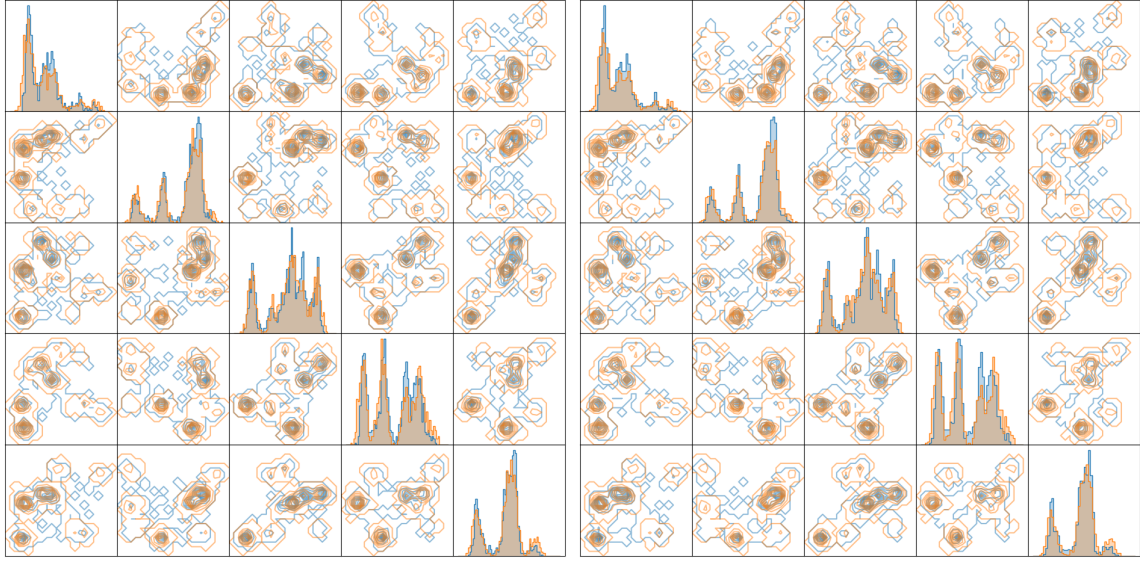
The results are depicted in Figure 12. To create this figure, we draw $x \sim P_X$ and computed an observation $y = Ax + \xi \sim P_Y$. Then we draw samples $x^{y,n}$, $1 \leq n \leq 1000$ from $P_{X|Y=y}$. The orange colored histograms on the diagonal are the one dimensional histograms of the projection onto the i -th component $\langle e_i, x^{y,n} \rangle$. For $i \neq j$ the orange colored two dimensional histograms of $(\langle e_i, x^{y,n} \rangle, \langle e_j, x^{y,n} \rangle)$ are shown in position (i, j) . The blue histograms are the output obtained by the flow matching procedures, i.e. instead of $x^{y,n}$, we use $\phi_1(y, z^n)$ for $z^n \sim \mathcal{N}(0, I_5)$, $1 \leq n \leq 1000$, where ϕ_t solves $\partial_t \phi_t = u_t^\theta(\phi_t)$, $\phi_0(y, z) = (y, z)$.

10 Continuous Normalizing Flows

Flow matching is related to continuous normalizing flows, which historically were introduced earlier, but appears to be more complicated when learned with a likelihood loss. To provide a more circumvent view, we add this section. A remark on (noncontinuous) normalizing flows is given in Appendix C.

Continuous normalizing flows aim to find a vector field v_t such that the solution $\psi : [0, 1] \times \mathbb{R}^d \rightarrow \mathbb{R}^d$ of

$$\partial_t \psi(t, x) = v_t(\psi(t, x)), \quad \psi(0, x) = x, \quad (28)$$



(a) minibatch OT flow matching for $W_{2,100}$

(b) α from Remark 9.10

Figure 12: Bayesian flow matching for an inverse problem.

satisfies $\psi(1, \cdot)_{\#}\mu_0 = \mu_1$. More precisely, for every $t \in [0, 1]$, the solution $\psi(t, \cdot) : \mathbb{R}^d \rightarrow \mathbb{R}^d$ has to be a diffeomorphism. In contrast to flow matching, continuous normalizing flow techniques work without previously determining the curve via plans, Markov kernels or a stochastic process, but approximate the vector field by a neural network using an appropriate loss function, namely the log-likelihood one.

Therefore, we first derive general properties of vector fields and associated curves to make the process invertible in the next Subsection 10.1. In other words, we will take care about the time reverse ODE. This will facilitate the finding of an appropriate loss function in Subsection 10.2. In Subsection 10.3, we deal with the minimization of the loss by computing gradients with the adjoint method.

In this section, we will exclusively work with absolutely continuous measures and switch from the notation of measures to those of densities. In particular, we will write $p_t := \psi(t, \cdot)_{\#}\rho_0$ for the density p_t of $\psi(t, \cdot)_{\#}\mu_0$, if it exists.

10.1 Curves of Probability Measures from ODEs

We start with classical results from the theory of ODEs, for existence and regularity see, e.g., [39, Corollary 2.6, Theorem 2.10].

Theorem 10.1. *Assume that $v_t \in C^l([0, 1] \times \mathbb{R}^d, \mathbb{R}^d)$, $l \geq 1$ fulfills a global Lipschitz*

condition in the second variable, i.e., there exists $K > 0$ such that

$$\|v_t(x) - v_t(y)\| \leq K\|x - y\| \quad \text{for all } x, y \in \mathbb{R}^d, t \in [0, 1].$$

Then, for any fixed $t_0 \in [0, 1]$ and $x_0 \in \mathbb{R}^d$, the initial value problem $f(t_0) = x_0$ and

$$f'(t) = v_t(f(t)), \tag{29}$$

admits a unique global solution $f : [0, 1] \rightarrow \mathbb{R}^d$. Furthermore, if we define $\psi(t, s, x) := f(t)$ for the solution f of (29) with initial condition $f(s) = x$, then it holds $\psi \in C^l([0, 1] \times [0, 1] \times \mathbb{R}^d, \mathbb{R}^d)$.

Concerning the reverse ODE, we obtain the following corollary.

Corollary 10.2. *In the setting of Theorem 10.1, we have that $\psi(t, s, \psi(s, t, x)) = x$. In particular, for $(t, s) \in [0, 1] \times [0, 1]$, the function $\psi^{t,s} : \mathbb{R}^d \rightarrow \mathbb{R}^d$ defined by $\psi^{t,s}(x) := \psi(t, s, x)$ is a $C^l(\mathbb{R}^d, \mathbb{R}^d)$ diffeomorphism with inverse $\psi^{s,t}$.*

Proof. Let f and g be a solution of (29) with initializations $f(t) = x$, and $g(s) = f(s) = \psi(s, t, x)$, respectively. By Theorem 10.1, we know that $f = g$ on $[0, 1]$ and therefore

$$g(t) = \psi(t, s, \psi(s, t, x)) = f(t) = x.$$

□

The next proposition shows that under the above smoothness assumptions $\psi(t, \cdot) : \mathbb{R}^d \rightarrow \mathbb{R}^d$ is indeed a C^2 diffeomorphism.

Proposition 10.3. *Assume that $v_t \in C^l([0, 1] \times \mathbb{R}^d, \mathbb{R}^d)$, $l \geq 2$ globally Lipschitz in the second variable. Then (28) admits a unique global solution and $\psi \in C^l([0, 1] \times \mathbb{R}^d, \mathbb{R}^d)$. If $\mu_0 = p_0 \mathcal{L}$ with $p_0 \in C^{l-1}(\mathbb{R}^d)$, then the curve $\mu_t := \psi(t, \cdot)_\# \mu_0$ admits a density $p_t \in C^{l-1}([0, 1] \times \mathbb{R}^d)$. Furthermore, if there exists $t_0 \in [0, 1]$ such that $p_{t_0}(x) > 0$ for all $x \in \mathbb{R}^d$, then $p_t(x) > 0$ for all $x \in \mathbb{R}^d$ and all $t \in [0, 1]$.*

Proof. The existence and uniqueness follow directly from Theorem 10.1. Since $\psi(t, \cdot)$ is a $C^l(\mathbb{R}^d, \mathbb{R}^d)$ diffeomorphism by Corollary 10.2 we know that $\det(\nabla_x \psi(t, \cdot)(x)) \neq 0$. Furthermore using (1) we conclude that μ_t is absolutely continuous with density

$$p_t(x) = \frac{p_0 \circ \psi(t, \cdot)^{-1}(x)}{\det(\nabla_x \psi(t, \cdot)(x))}.$$

The latter equation implies the remaining claims. □

Corollary 10.4. *Let $v_t \in C^2([0, 1] \times \mathbb{R}^d, \mathbb{R}^d)$ be globally Lipschitz and $\mu_0 = p_0 \mathcal{L}$ with $p_0 \in C^1(\mathbb{R}^d)$. Let $\psi \in C^l([0, 1] \times \mathbb{R}^d, \mathbb{R}^d)$ be the solution of (28) and $p_t := \psi(t, \cdot)_\# p_0$. Then (p_t, v_t) fulfills the continuity equation in a strong sense*

$$\partial_t p_t + \operatorname{div}(p_t v_t) = 0, \quad x \in \mathbb{R}^d, t \in [0, 1].$$

Proof. By Remark 3.6, we know that (28) implies for all $\varphi \in C_c^\infty((0, 1) \times \mathbb{R}^d)$ that

$$0 = \int_0^1 \int_{\mathbb{R}^d} \langle \nabla_x \varphi, v_t \rangle + \partial_t \varphi \, d[\psi(t, \cdot)_\# \mu_0] \, dt = \int_0^1 \int_{\mathbb{R}^d} (\operatorname{div}(v_t p_t) + \partial_t p_t) \varphi \, dx \, dt.$$

By Theorem 10.3, we know that $p_t \in C^1(\mathbb{R}^d)$, so that the function in the inner brackets is continuous, which yields the assertion. \square

10.2 Likelihood Loss for Continuous Normalizing Flow

Opposite to flow matching, we assume that the initial density of the ODE is the target density, and the final one approximates the latent density, i.e.,

$$p_0 \approx p_{\text{data}}, \quad p_1 = p_{\text{latent}}.$$

We assume that the vector field and thus, also the corresponding ODE solution depend on a parameter vector $\theta \in \mathbb{R}^n$, i.e.,

$$\partial_t \psi^\theta(t, x) = v_t^\theta(\psi(t, x)), \quad \psi^\theta(0, x) = x.$$

By the previous subsection, we know for $v_t^\theta \in C^2([0, 1] \times \mathbb{R}^d, \mathbb{R}^d)$ with Lipschitz continuous second component for all $t \in [0, 1]$, that $S^\theta := \psi^\theta(1, \cdot)$ is a C^2 diffeomorphism and $T^\theta := (S^\theta)^{-1}$ fulfills $p_0 := T_\#^\theta p_1$. Moreover, we have for $p_t := \psi^\theta(t, \cdot)_\# p_0$ that

$$p_1 = S_\#^\theta p_0 = S_\#^\theta T_\#^\theta p_1 = p_1 \quad \text{and} \quad T_\#^\theta p_1 = T_\#^\theta S_\#^\theta p_0 = p_0.$$

As *loss function*, the log-likelihood function appears to be a reasonable choice

$$\mathcal{L}(\theta) = \mathbb{E}_{x \sim p_X} [-\log T_\#^\theta p_1] = \mathbb{E}_{x \sim p_X} [-\log p_0].$$

Alternatively, this may be reformulated using the Kullback-Leibler divergence between p_X and $T_\#^\theta p_1$, see Remark 2.3. In order to minimize the loss function using backpropagation, we must compute the gradient of $\log(T_\#^\theta p_1) = \log p_0(x)$ with respect to θ . To this end, we introduce the function $\ell : [0, 1] \times \mathbb{R}^d \rightarrow \mathbb{R}^d$ by

$$\ell(t, x) := \log(p_t(\psi(t, x))) - \log(p_0(x)), \tag{30}$$

so that the loss function can be rewritten setting $t = 1$ as

$$\mathbb{E}_{x \sim p_X} [-\log p_0(x)] = \mathbb{E}_{x \sim p_X} [\ell(1, x) - \log p_1(\psi(1, x))]. \tag{31}$$

Interestingly, ℓ is the solution of an ODE which includes the velocity field v_t .

Proposition 10.5. *Let $v \in C^2([0, 1] \times \mathbb{R}^d, \mathbb{R}^d)$ be Lipschitz continuous in the second component for all $t \in [0, 1]$ and let $p_0 \in C^1(\mathbb{R}^d)$ be a strictly positive density. For the solution $\psi \in C^1([0, 1] \times \mathbb{R}^d, \mathbb{R}^d)$ of (28), let $p_t := \psi(t, \cdot)_{\#} p_0$. Then $\ell : [0, 1] \times \mathbb{R}^d \rightarrow \mathbb{R}^d$ in (30) is the solution of the ODE*

$$\partial_t \ell(t, x) = -(\nabla \cdot v_t)(\psi(t, x)), \quad \ell(x, 0) = 0$$

Proof. By the chain rule, we obtain

$$\begin{aligned} \partial_t \ell(t, x) &= \frac{d}{dt} \log(p_t(\psi(t, x))) = \frac{1}{p_t(\psi(t, x))} \frac{d}{dt} p_t(\psi(t, x)) \\ &= \frac{1}{p_t(\psi(t, x))} \left(\langle \nabla_x p_t(\psi(t, x)), \partial_t \psi(t, x) \rangle + \partial_t p_t(\psi(t, x)) \right). \end{aligned}$$

and further by applying the definition of ψ for the first term and the continuity equation from Corollary 10.4 for the second one,

$$\begin{aligned} \partial_t \ell(t, x) &= \frac{1}{p_t(\psi(t, x))} \left(\langle \nabla_x p_t(\psi(t, x)), v_t(\psi(t, x)) \rangle - \operatorname{div} \left(p_t(\psi(t, x)) v_t(\psi(t, x)) \right) \right) \\ &= \frac{1}{p_t(\psi(t, x))} \left(\langle \nabla_x p_t(\psi(t, x)), v_t(\psi(t, x)) \rangle \right. \\ &\quad \left. - \langle \nabla_x p_t(\psi(t, x)), v_t(\psi(t, x)) \rangle - p_t(\psi(t, x)) (\operatorname{div} v_t)(\psi(t, x)) \right) \\ &= -\operatorname{div}(v_t(\psi(t, x))). \end{aligned}$$

□

Now we can combine the ODEs for ψ and ℓ into the ODE system

$$\begin{pmatrix} \partial_t \Psi_1(t, x, y, \theta) \\ \partial_t \Psi_2(t, x, y, \theta) \\ \partial_t \Psi_3(t, x, y, \theta) \end{pmatrix} = \begin{pmatrix} v_t(\Psi_1(t, x, y, \theta), \theta) \\ -(\operatorname{div}_x v_t)(\Psi_1(t, x, y, \theta), \theta) \\ 0 \end{pmatrix}, \quad \begin{pmatrix} \Psi_1(0, x, y, \theta) \\ \Psi_2(0, x, y, \theta) \\ \Psi_3(0, x, y, \theta) \end{pmatrix} = \begin{pmatrix} x \\ 0 \\ \theta \end{pmatrix}$$

where $x \in \mathbb{R}^d, y \in \mathbb{R}$. Note that Ψ_2 corresponds to ℓ from (30) and Ψ_3 remains θ . Making the velocity field dependent on a parameter $\theta \in \mathbb{R}^n$, we can rewrite the loss function (31) as

$$\mathcal{L}(\theta) = \mathbb{E}_{x \sim p_X} \left[\Psi_2(1, x, 0, \theta) - \log p_1(\Psi_1(1, x, 0, \theta)) \right].$$

Now the main challenge is to find $\nabla_{\theta} \mathcal{L}(\theta)$. To this end, consider

$$F(x, y, \theta) := y - \log p_1(x).$$

Then

$$F \circ (\Psi(1, \cdot, \cdot, \cdot))(x, y, \theta) = \Psi_2(1, x, 0, \theta) - \log p_1(\Psi_1(1, x, 0, \theta))$$

and we can compute by the Leibniz rule for measure spaces

$$\nabla_{\theta} \mathcal{L}(\theta) = \mathbb{E}_{x \sim p_X} [\nabla_{\theta} (F \circ (\Psi(1, \cdot, \cdot, \cdot)))(x, y, \theta)]. \quad (32)$$

In the next subsection, we show how to compute $\nabla_{\theta} (F \circ \Psi(1, \cdot, \cdot, \cdot))(x, y, \theta)$ by solving a system of ODEs.

10.3 Computing Gradients with the Adjoint Method

This section is based on the original paper [10] as well as the blog [35].

To start from an arbitrary time $s \in [0, 1]$, we use the following notation. For $v_t \in C^2([0, 1] \times \mathbb{R}^d, \mathbb{R}^d)$, let $\boldsymbol{\psi} : [0, 1] \times [0, 1] \times \mathbb{R}^d \rightarrow \mathbb{R}^d$ be the solution of

$$\partial_t \boldsymbol{\psi}(t, s, x) = v_t(\boldsymbol{\psi}(t, s, x)), \quad \boldsymbol{\psi}(s, s, x) = x. \quad (33)$$

For fixed $s = 0$, we have $\psi(t, x) = \boldsymbol{\psi}(t, 0, x)$. For an arbitrary $F \in C^2(\mathbb{R}^d)$, we define a function $a : [0, 1] \times \mathbb{R}^d \rightarrow \mathbb{R}^d$ by

$$a_t(x) := \nabla_x (F \circ \boldsymbol{\psi}(1, t, \cdot))(\boldsymbol{\psi}(t, x)).$$

Note that $a_t(x)$ is a row vector here.

Proposition 10.6. *Let $v_t \in C^2([0, 1] \times \mathbb{R}^d, \mathbb{R}^d)$ be Lipschitz continuous in the second variable, and let $\boldsymbol{\psi} : [0, 1] \times \mathbb{R}^d \rightarrow \mathbb{R}^d$ be the solution of (28). Then it holds*

$$\partial_t a_t(x) = -a_t(x) (\nabla_x v_t)(\boldsymbol{\psi}(t, x)). \quad (34)$$

Proof. Since $v_t \in C^2([0, 1] \times \mathbb{R}^d, \mathbb{R}^d)$, we have by Theorem 10.1 that $\boldsymbol{\psi} \in C^2([0, 1] \times [0, 1] \times \mathbb{R}^d, \mathbb{R}^d)$. Noting that

$$\boldsymbol{\psi}(1, 0, x) = \boldsymbol{\psi}(1, t, \cdot) \circ \boldsymbol{\psi}(t, 0, x) = \boldsymbol{\psi}(1, t, \cdot) (\boldsymbol{\psi}(t, x)),$$

we obtain

$$\begin{aligned} a_0(x) &= \nabla_x (F \circ \boldsymbol{\psi}(1, 0, \cdot))(\boldsymbol{\psi}(0, x)) \\ &= \nabla_x (F \circ (\boldsymbol{\psi}(1, t, \cdot) \circ \boldsymbol{\psi}(t, 0, \cdot))) (\boldsymbol{\psi}(0, x)) \\ &= \nabla_x ((F \circ \boldsymbol{\psi}(1, t, \cdot)) \circ \boldsymbol{\psi}(t, \cdot))(x) = a_t(x) \nabla_x \boldsymbol{\psi}(t, x). \end{aligned}$$

Since the left hand side does not depend on t , we obtain after differentiation with respect to t that

$$0 = \partial_t (a_t(x)) \nabla_x \boldsymbol{\psi}(t, x) + a_t(x) \partial_t (\nabla_x \boldsymbol{\psi}(t, x)). \quad (35)$$

Next, we compute

$$\partial_t(\nabla_x \psi(t, x)) = \nabla_x(\partial_t \psi(t, x)) = \nabla_x(v_t(\psi(t, x))) = (\nabla_x v_t)(\psi(t, x)) \nabla_x \psi(t, x).$$

Then we get in (35) that

$$0 = \partial_t(a_t(x)) \nabla_x \psi(t, x) + a_t(x) (\nabla_x v_t)(\psi(t, x)) \nabla_x \psi(t, x).$$

By Corollary 10.2, we know that $\psi(t, x)$ invertible with differentiable inverse, so that the matrix $\nabla_x \psi(t, x)$ is invertible and we obtain the assertion (34). \square

To compute gradients of v_t^θ with respect $\theta \in \mathbb{R}^n$, we extend the ODE (33) for $\boldsymbol{\psi} : [0, 1] \times [0, 1] \times \mathbb{R}^d \times \mathbb{R}^n \rightarrow \mathbb{R}^d \times \mathbb{R}^n$ and $v : \times [0, 1] \times \mathbb{R}^d \times \mathbb{R}^n \rightarrow \mathbb{R}^d$ as

$$\partial_t \boldsymbol{\psi}(t, s, x, \theta) = \begin{pmatrix} v_t(\boldsymbol{\psi}(t, s, x, \theta)) \\ 0 \end{pmatrix}, \quad \boldsymbol{\psi}(s, s, x, \theta) = (x, \theta)$$

where we use the same symbols $\boldsymbol{\psi}$ and v_t for convenience. Again, we write ψ for $\boldsymbol{\psi}(\cdot, 0, \cdot, \cdot)$. Now let $F \in C^2(\mathbb{R}^d \times \mathbb{R}^n)$ be a function *which does not depend on the second component* and define $a : [0, 1] \times \mathbb{R}^d \times \mathbb{R}^n \rightarrow \mathbb{R}^d \times \mathbb{R}^n$ by

$$a_t(x, \theta) := \nabla_{x, \theta}(F \circ \boldsymbol{\psi}(1, t, \cdot, \cdot))(\psi(t, x, \theta)) = (a_t^x, a_t^\theta).$$

Note that in the loss function (32) we need

$$a_0^\theta = \nabla_\theta(F \circ \boldsymbol{\psi}(1, \cdot, \cdot))(x, \theta). \quad (36)$$

Then (34) modifies to

$$\partial_t a_t(x) = -a_t(x) \nabla_{x, \theta} \begin{pmatrix} v_t \\ 0 \end{pmatrix} (\psi(t, x, \theta)).$$

Since

$$\nabla_{x, \theta} \begin{pmatrix} v_t \\ 0 \end{pmatrix} = \begin{pmatrix} \nabla_x v_t & \nabla_\theta v_t \\ 0 & 0 \end{pmatrix},$$

we obtain finally

$$\begin{pmatrix} \partial_t \psi(t, x, \theta) \\ \partial_t a_t^x(x, \theta) \\ \partial_t a_t^\theta(x, \theta) \end{pmatrix} = \begin{pmatrix} v_t(\psi(t, x, \theta), \theta) \\ a_t^x(x, \theta)(\nabla_x v_t)(\psi(t, x, \theta)) \\ a_t^x(x, \theta)(\nabla_\theta v_t)(\psi(t, x, \theta)) \end{pmatrix} \quad (37)$$

As noted above, we need to compute a_0^θ to get $\nabla_\theta \mathcal{L}(\theta)$ in (32). In (37) the initial conditions at $t = 0$ are implicitly already encoded, since we used for our calculations that $\psi(0, x, \theta) = (x, \theta)$. However, to get a_0^θ , we need to find the appropriate condition

for $t = 1$ such that the solution of (37) matches the initial condition at $t = 0$. Since F does not depend on θ and we know that $\psi(1, 1, x, \theta) = (x, \theta)$, we can conclude

$$a_1^\theta = \nabla_\theta(F \circ \psi(1, 1, \cdot, \cdot)) = \nabla_\theta F = 0.$$

Furthermore, with $x^1 := \psi(1, x, \theta)$ we have that

$$a_1^x(x, \theta) = \nabla_x(F \circ \psi(1, 1, \cdot, \cdot))(x^1) = (\nabla_x F)(x^1).$$

Hence we can obtain $a_0^\theta = \nabla_\theta(F \circ \psi(1, \cdot, \cdot))(x, \theta)$ by solving (37) with initial conditions

$$\psi(1, x, \theta) = (x^1, \theta); \quad a_1^x(x, \theta) = (\nabla_x F)(x^1); \quad a_1^\theta(x, \theta) = 0.$$

For the special loss (32) the variable x consists of two parts, namely (x, y) and ψ corresponds to Ψ and thus we can evaluate the gradient of the loss function.

10.4 Numerical Examples of Continuous Normalizing Flows

By (32) and (36), training a continuous normalizing flow needs the computation of

$$\nabla_\theta \mathcal{L}(\theta) = \mathbb{E}_{x \sim p_X} [a_0^\theta(x)],$$

where we approximate the expectation by an empirical expectation. In order to compute a_0^θ we need to solve (37). The only ingredients for solving this equation are the vector field $v_t(x, y, \theta)$, the gradients thereof, and the initial conditions. The velocity field v_t and its gradients are available since we parametrize it by a neural network. For the first initial condition we need $\psi(1, x, 0, \theta)$ which we can obtain by solving $\partial_t f(t) = v_t(f(t), \theta), f(0) = (x, 0)$. For the second initial condition we need $\nabla_{x,y} F$ for $F(x, y) = y - \log p_1(x)$. Thus we need to be given a density where the gradient $\nabla_x \log p_1$ is tractable, which is the case, e.g., for the standard Gaussian distribution. In total we need samples from p_X and a density p_1 for which $\nabla_x \log p_1$ is tractable. The computation of $a_0^\theta(x)$ can then be done by solving (37), for which we used the library [11]. Figure 13 shows the trajectories for a vector field obtained via continuous normalizing flow training with three different target distributions. For Figure 13a we chose a GMM with 8 equally weighted modes. The trajectories differ from the ones obtained by flow matching in Figure 7. For Figure 13b resp. Figure 13c we chose the moons resp. spirals data set from [33].

11 A Glimpse at Score-Based Diffusion

Diffusion models go back to [36] and [38]. They can be transformed into CNFs, thus allowing tractable likelihood computation with numerical ODE solvers [37]. However, diffusion models are based on stochastic differential equations (SDEs). Roughly

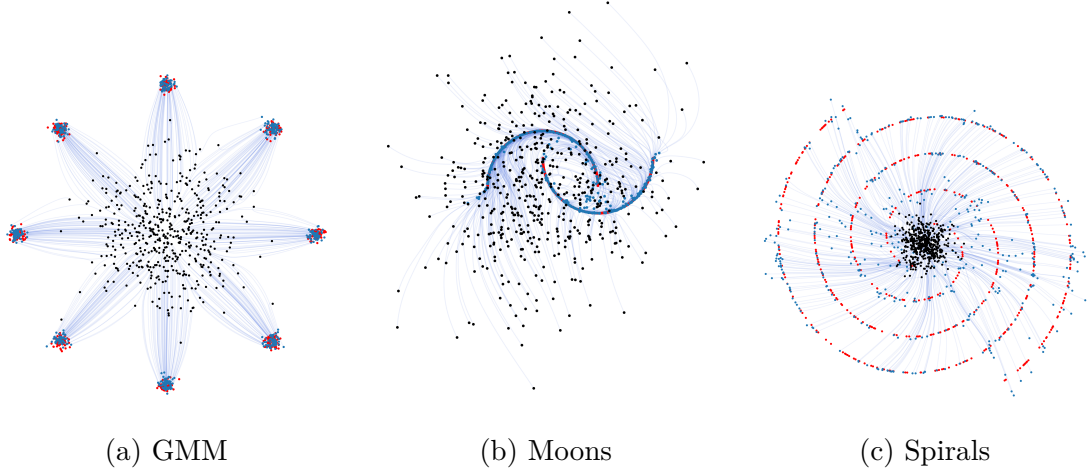


Figure 13: Trajectories of points from a vector field v_t^θ obtained via a vector field obtained by training a CNF. We chose $\mu_0 = \mathcal{N}(0, 1)$. Black: points $\{z_i\}_{i=1}^{300}$ drawn from the source distribution $\mu_0 = \mathcal{N}(0, 1)$. Blue: points sampled via the vector field from $\{z_i\}_{i=1}^{300}$. Red: points sampled from the target distribution. Blue lines: trajectories of the vector field.

speaking, the forward SDE computes $(X_t)_{t \in [0, T]}$ starting with the target distribution by

$$dX_t = f(t, X_t) dt + g(t) dW_t, \quad X_0 \sim P_{\text{data}}, \quad (38)$$

where W_t is a standard Brownian motion. A usual choice is

$$f(t, X_t) := -\frac{1}{2}\beta_t X_t \quad \text{and} \quad g(t) := \sqrt{\beta_t}$$

with a positive, increasing so-called "time schedule" β , e.g., $\beta_t = \beta_{\min} + t(\beta_{\max} - \beta_{\min})$ for some $0 < \beta_{\min} \ll \beta_{\max}$. Then the SDE becomes a linear one

$$dX_t = -\frac{1}{2}\beta_t X_t dt + \sqrt{\beta_t} dW_t, \quad X_0 \sim P_{\text{data}},$$

which has the closed form solution

$$X_t = \sqrt{1 - e^{-h(t)}} Z + e^{-\frac{h(t)}{2}} X_0, \quad h(t) := \int_0^t \beta_s ds, \quad (39)$$

where $Z \sim \mathcal{N}(0, I_d)$. Hence, X_t in (39) reaches Z for $t \rightarrow \infty$. Then $X_t \sim P_{X_t}$, $t > 0$ has a density p_{X_t} , and under certain assumptions, a reverse process becomes

$$dY_t = \left(-f(T-t, Y_t) + g(T-t)^2 \nabla \log p_{X_{T-t}}(Y_t) \right) dt + g(T-t) dW_t, \quad Y_0 \sim X_T. \quad (40)$$

However, the reverse SDE depends on the so-called *score* $\nabla \log p_{X_t}$. Score-based models intend to approximate the score by a neural network s^θ by minimizing, for

$T > 0$ large enough

$$\mathcal{L}(\theta) := \min_{\theta} \mathbb{E}_{t \sim \mathcal{L}_{[0,T]}} \mathbb{E}_{x \sim P_{X_t}} \left[\|s_t^\theta(x) - \nabla \log p_{X_t}(x)\|^2 \right].$$

Usually, we do not have access to $\nabla \log p_t$. Fortunately, by [41, Appendix], the loss function can be rewritten, up to a constant, as

$$\mathcal{L}(\theta) = \mathbb{E}_{x_0 \sim P_{\text{data}}, t \sim \mathcal{L}_{[0,T]}} \mathbb{E}_{x \sim P_{X_t|X_0=x_0}} \left[\|s_t^\theta(x) - \nabla \log p_{X_t|X_0=x_0}(x)\|^2 \right],$$

which does not involve the score itself, but instead the conditional distribution. For (39), this is simply a Gaussian

$$P_{X_t|X_0=x_0} = \mathcal{N}(b_t x_0, (1 - b_t^2) I_d) \quad \text{with} \quad b_t = e^{-\frac{h(t)}{2}}$$

since X_0 and Z are independent. This implies

$$\nabla \log p_{X_t|X_0=x_0}(x) = \nabla \left(-\frac{1}{2(1-b_t^2)} \|x - b_t x_0\|^2 \right) = -\frac{x - b_t x_0}{1 - b_t^2}.$$

Plugging this into the loss function, we get

$$\mathcal{L}(\theta) = \mathbb{E}_{t \sim \mathcal{L}_{[0,T]}} \mathbb{E}_{x_0 \sim P_{\text{data}}} \mathbb{E}_{x \sim P_{X_t|X_0=x_0}} \left[\left\| s_t^\theta(x) + \frac{x - b_t x_0}{1 - b_t^2} \right\|^2 \right].$$

Once the score is computed, we can use it in the reverse SDE (40), starting with the $Z \sim \mathcal{N}(0, I_d)$ which approximates X_T for T large enough.

For the forward PDE (38), the corresponding densities $p_t = p_{X_t}$ fulfill the *Fokker-Planck equation*

$$\begin{aligned} \partial_t p_t(x) &= -\nabla \cdot (f(t, x) p_t(x)) + g(t)^2 \Delta p_t(x) \\ &= -\nabla \cdot \underbrace{\left(f(t, x) - g(t)^2 \nabla_x \log p_t(x) \right)}_{v_t} p_t(x) \end{aligned} \quad (41)$$

which is the continuity equation for P_{X_t} . This gives the relation to the previous sections. In particular, given the score, we can also use the flow ODE (7) for sampling. Moreover, we could compute the log density via Proposition 10.5.

For $f(t, x) = -\frac{1}{2}\beta_t x$ as above, we obtain $v_t(x) = -\frac{1}{2}\beta_t x - g(t)^2 \nabla \log p_t(x)$. This is closely related to the vector field associated to the independent coupling which was computed to be $v_t(x) = \frac{x}{t} + \frac{1-t}{t} \nabla \log p_t(x)$ in Proposition 4.11 and Remark 6.5.

Finally, we like to mention that the above (Fokker-Planck) continuity equation (41) arises from a so-called Wasserstein gradient flow of the KL divergence $KL(p, p_{\text{data}})$, i.e., the velocity field v_t is in the subdifferential of the above KL function at p_t , see e.g. [2, Chapter 10.4].

References

- [1] L. Ambrosio, E. Brué, and D. Semola. *Lectures on Optimal Transport*. UNITEXT. Springer International Publishing, 2021.
- [2] L. Ambrosio, N. Gigli, and G. Savaré. *Gradient flows: in metric spaces and in the space of probability measures*. Springer Science & Business Media, 2005.
- [3] L. Ardizzone, J. Kruse, C. Rother, and U. Köthe. Analyzing inverse problems with invertible neural networks. In *7th International Conference on Learning Representations, ICLR 2019, New Orleans, LA, USA, May 6-9, 2019*, 2019.
- [4] R. Barboni, G. Peyré, and F.-X. Vialard. Understanding the training of infinitely deep and wide resnets with conditional optimal transport. *arXiv preprint arXiv:2403.12887*, 2024.
- [5] Q. Bertrand, R. Emonet, A. Gagneux, S. Martin, and M. Massias. A visual dive into conditional flow matching. <https://dl.heeere.com/conditional-flow-matching/blog/conditional-flow-matching/>.
- [6] V. I. Bogachev and M. A. S. Ruas. *Measure Theory*, volume 1. Springer, 2007.
- [7] J. Chemseddine, P. Hagemann, C. Wald, and G. Steidl. Conditional Wasserstein distances with applications in Bayesian OT flow matching. *arXiv preprint arXiv:2403.18705*, 2024.
- [8] R. Chen, J. Behrmann, D. K. Duvenaud, and J.-H. Jacobsen. Residual flows for invertible generative modeling. In *Advances in Neural Information Processing Systems*, volume 32. Curran Associates, Inc., 2019.
- [9] R. Chen, Y. Rubanova, J. Bettencourt, and D. Duvenaud. Neural ordinary differential equations. *Advances in Neural Information Processing Systems*, 31, 2018.
- [10] R. T. Chen, Y. Rubanova, J. Bettencourt, and D. K. Duvenaud. Neural ordinary differential equations. *Advances in Neural Information Processing Systems*, 31, 2018.
- [11] R. T. Q. Chen. torchdiffeq, 2018.
- [12] G. Daras, A. G. Dimakis, and C. Daskalakis. Consistent diffusion meets tweedie: Training exact ambient diffusion models with noisy data. *arXiv preprint arXiv:2404.10177*, 2024.
- [13] L. Dinh, J. Sohl-Dickstein, and S. Bengio. Density estimation using real NVP. In *5th International Conference on Learning Representations, ICLR 2017, Toulon, France, April 24-26, 2017, Conference Track Proceedings*, 2017.

- [14] N. Gigli. On the geometry of the space of probability measures endowed with the quadratic Optimal Transport distance. *PhD Thesis*, 2008. cvgmt preprint.
- [15] A. González-Sanz and S. Sheng. Linearization of monge-amp\ere equations and data science applications. *arXiv preprint arXiv:2408.06534*, 2024.
- [16] I. J. Goodfellow, J. Pouget-Abadie, M. Mirza, B. Xu, D. Warde-Farley, S. Ozair, A. Courville, and Y. Bengio. Generative adversarial nets. *Advances in Neural Information Processing Systems*, pages 2672–2680, 2014.
- [17] P. Hagemann, J. Hertrich, and G. Steidl. Generalized normalizing flows via Markov chains. In *Non-local Data Interactions: Foundations and Applications*. Cambridge University Press, 2022.
- [18] P. Hagemann, J. Hertrich, and G. Steidl. Stochastic normalizing flows for inverse problems: A Markov chains viewpoint. *SIAM/ASA Journal on Uncertainty Quantification*, 10(3):1162–1190, 2022.
- [19] P. Hagemann and S. Neumayer. Stabilizing invertible neural networks using mixture models. *Inverse Problems*, 37(8), 2021.
- [20] K. He, X. Zhang, S. Ren, and J. Sun. Deep residual learning for image recognition. In *Proceedings of the IEEE Conference on Computer Vision and Pattern Recognition*, pages 770–778, 2016.
- [21] B. Hosseini, A. W. Hsu, and A. Taghvaei. Conditional optimal transport on function spaces. *arXiv preprint arXiv:2311.05672*, 2024.
- [22] O. Kallenberg and O. Kallenberg. *Foundations of Modern Probability*, volume 2. Springer, 1997.
- [23] G. Kerrigan, G. Migliorini, and P. Smyth. Dynamic conditional optimal transport through simulation-free flows. *arXiv preprint arXiv:2404.04240*, 2024.
- [24] D. P. Kingma and M. Welling. Auto-encoding variational bayes. *arXiv preprint arXiv:1312.6114*, 2013.
- [25] B. R. Kloeckner. Extensions with shrinking fibers. *Ergodic Theory and Dynamical Systems*, 41(6):1795–1834, 2021.
- [26] A. Krizhevsky, G. Hinton, et al. Learning multiple layers of features from tiny images. 2009.
- [27] Y. Lipman, R. T. Q. Chen, H. Ben-Hamu, M. Nickel, and M. Le. Flow matching for generative modeling. In *The Eleventh International Conference on Learning Representations*, 2023.

- [28] Q. Liu. Rectified flow: A marginal preserving approach to optimal transport. *arXiv preprint arXiv:2209.14577*, 2022.
- [29] X. Liu, C. Gong, and qiang liu. Flow straight and fast: Learning to generate and transfer data with rectified flow. In *The Eleventh International Conference on Learning Representations*, 2023.
- [30] S. Martin, A. Gagneux, P. Hagemann, and G. Steidl. PnP-flow: Plug-and-play image restoration with flow matching. *arXiv preprint arXiv:2410.02423*, 2024.
- [31] G. Peyré, M. Cuturi, et al. Computational optimal transport: With applications to data science. *Foundations and Trends® in Machine Learning*, 11(5-6):355–607, 2019.
- [32] G. Plonka, D. Potts, G. Steidl, and M. Tasche. *Numerical Fourier Analysis. Applied and Numerical Harmonic Analysis*. Birkhäuser, second edition, 2023.
- [33] M. Poli, S. Massaroli, A. Yamashita, H. Asama, J. Park, and S. Ermon. Torchdyn: Implicit models and neural numerical methods in pytorch.
- [34] F. Santambrogio. Optimal Transport for applied mathematicians. *Birkäuser*, 2015.
- [35] I. Schurov. Adjoint state method, backpropagation and neural odes. <https://ilya.schurov.com/post/adjoint-method/>.
- [36] J. Sohl-Dickstein, E. Weiss, N. Maheswaranathan, and S. Ganguli. Deep unsupervised learning using nonequilibrium thermodynamics. In F. Bach and D. Blei, editors, *Proceedings of the 32nd International Conference on Machine Learning*, volume 37 of *Proceedings of Machine Learning Research*, pages 2256–2265, Lille, France, 07–09 Jul 2015. PMLR.
- [37] Y. Song, C. Durkan, I. Murray, and S. Ermon. Maximum likelihood training of score-based diffusion models. In A. Beygelzimer, Y. Dauphin, P. Liang, and J. W. Vaughan, editors, *Advances in Neural Information Processing Systems*, 2021.
- [38] Y. Song and S. Ermon. Generative modeling by estimating gradients of the data distribution. *ArXiv 1907.05600*, 2019.
- [39] G. Teschl. *Ordinary Differential Equations and Dynamical Systems*, volume 140. American Mathematical Society, 2024.
- [40] A. Tong, N. Malkin, G. Huguet, Y. Zhang, J. Rector-Brooks, K. Fatras, G. Wolf, and Y. Bengio. Improving and generalizing flow-based generative models with minibatch optimal transport. In *ICML Workshop on New Frontiers in Learning, Control, and Dynamical Systems*, 2023.

- [41] P. Vincent. A connection between score matching and denoising autoencoders. *Neural computation*, 23(7):1661–1674, 2011.
- [42] H. Wu, J. Köhler, and F. Noé. Stochastic normalizing flows. In H. Larochelle, M. A. Ranzato, R. Hadsell, M. Balcan, and H. Lin, editors, *Advances in Neural Information Processing Systems 2020*, 2020.
- [43] Y. Zhang, P. Yu, Y. Zhu, Y. Chang, F. Gao, Y. N. Wu, and O. Leong. Flow priors for linear inverse problems via iterative corrupted trajectory matching. *arXiv preprint arXiv:2405.18816*, 2024.

A Proof of Theorem 3.1

Recall that a family \mathcal{A} of subsets of a set X is called *monotone class*, if

- $\bigcup_{i=1}^{\infty} A_i \in \mathcal{A}$ for every increasing sequence $A_i \in \mathcal{A}$, and
- $\bigcap_{i=1}^{\infty} A_i \in \mathcal{A}$ for every decreasing sequence $A_i \in \mathcal{A}$.

For a family of subsets B of X , we call the smallest monotone class containing B the *monotone class generated by B* . The following theorem can be found, e.g., in [6, Theorem 1.9.3)].

Theorem A.1 (Monotone class theorem). *Let \mathcal{A} be an algebra of sets, i.e., a collection of sets such that $A \in \mathcal{A}$ implies $X \setminus A \in \mathcal{A}$, and $A, B \in \mathcal{A}$ implies $A \cup B \in \mathcal{A}$. Then the σ -algebra generated by \mathcal{A} coincides with the monotone class generated by \mathcal{A} . In particular, any monotone class containing \mathcal{A} also contains the σ -algebra generated by \mathcal{A} .*

Theorem 3.1 Let $\mu_t : I \rightarrow \mathcal{P}_2(\mathbb{R}^d)$ be a narrowly continuous curve. Then, for every Borel set $B \subseteq \mathbb{R}^d$, we have that $t \mapsto \mu_t(B)$ is measurable, i.e., $\mu_t : I \times \mathcal{B}(\mathbb{R}^d) \rightarrow \mathbb{R}$ is a Markov kernel.

Proof. Step 1: Let \mathcal{A} be the set of all measurable sets $B \subseteq \mathbb{R}^d$ such that there exists a series $f_n \in C_b(\mathbb{R}^d)$, $\|f\|_{\infty} \leq 1$ such that $\|f_n - 1_B\|_{L^1(\mu_t)} \rightarrow 0$ for all $t \in I$. Note that for such sequences with $\|f_n - 1_A\|_{L^1(\mu_t)} \rightarrow 0$, $\|g_n - 1_B\|_{L^1(\mu_t)} \rightarrow 0$, we have that $\|\min\{f_n, g_n\} - 1_{A \cap B}\|_{L^1(\mu_t)} \rightarrow 0$ and $\|(1 - f_n) - 1_{X \setminus A}\|_{L^1(\mu_t)} \rightarrow 0$. The former follows from $\min\{a, b\} = \frac{a+b}{2} - \frac{|a-b|}{2}$ and the fact that the L^1 -limit is linear and interchanges with the absolute value by the reverse triangle inequality. The latter uses $1 \in L^1(\mu_t)$, i.e. the finiteness of the measure μ_t . Since trivially, $\emptyset \in \mathcal{A}$, it follows that \mathcal{A} is an algebra of sets and we checked the first requirement of the monotone class theorem.

Step 2: We will show that for $A \in \mathcal{A}$, the map $t \mapsto \mu_t(A)$ is measurable. Let $f_n \in C_b(\mathbb{R}^d)$, $\|f_n\|_\infty \leq 1$ be such that $\|f_n - 1_A\|_{L^1(\mu_t)} \rightarrow 0$ for all t . For all t we have by dominated convergence and $\|f_n - 1_A\|_{L^1(\mu_t)} \rightarrow 0$ that

$$t \rightarrow \mu_t(A) = \int 1_A d\mu_t = \int \lim_{n \rightarrow \infty} f_n d\mu_t = \lim_{n \rightarrow \infty} \int f_n d\mu_t.$$

Consequently, since $t \rightarrow \int f_n d\mu_t$ is continuous, we can conclude that $t \mapsto \mu_t(A)$ is measurable as a pointwise limit of continuous functions.

Furthermore it is easy to show that any open measurable set is in \mathcal{A} since for an open set A we can approximate 1_A pointwise from below by a series of continuous bounded functions. Thus the σ -algebra generated by \mathcal{A} contains $\mathcal{B}(\mathbb{R}^d)$.

Step 3: We show that \mathcal{C} , which contains all $C \in \mathcal{B}(\mathbb{R}^d)$ such that $t \mapsto \mu_t(C)$ is measurable, is a monotone class. Thus we have to show that for an increasing sequence of measurable sets $C_i \in \mathcal{C}$ and $C = \cup_{i \in \mathcal{N}} C_i$, we have that $C \in \mathcal{C}$, i.e. $t \mapsto \mu_t(A)$ is measurable and the same for intersections. But this is true since $\mu_t(C) = \lim_{i \rightarrow \infty} \mu_t(C_i)$ and pointwise limits of measurable functions are measurable.

Finally, since by Step 2 it holds $\mathcal{A} \subseteq \mathcal{C}$, we can conclude that $\mathcal{B}(\mathbb{R}^d) \subseteq \mathcal{C}$ by the monotone class theorem and thus the claim. \square

B Measurability of v_t in Lemma 5.7

Proposition B.1. For $\mu_0, \mu_1 \in \mathcal{P}_2(\mathbb{R}^d)$, let $\alpha \in \Gamma(\mu_0, \mu_1)$ and $\mu_t := e_{t, \#} \alpha$. Let $\bar{\alpha} = a_{\#}(\mathcal{L}_{(0,1)} \times \alpha)$, where $a(t, x, y) = (t, e_t(x, y), y)$ and denote the disintegration with respect to $\pi^{t,1}(t, x, y) = (t, x)$ by $\bar{\alpha}^{t,x}$. Finally, define

$$v(t, x) := \int_{\mathbb{R}^d} \frac{y - x}{1 - t} d\bar{\alpha}^{t,x}(y)$$

for $(t, x) \in (0, 1) \times \mathbb{R}^n$. Then v is the velocity field induced by α . For $\alpha_t = (e_t, \pi^2)_{\#} \alpha$, $\alpha_t = \alpha_t^x \times_x \mu_t$ and $v_t(x) = \int_{\mathbb{R}^d} \frac{y-x}{1-t} d\alpha_t^x(y)$ we have that

$$v(t, \cdot) = v_t$$

for a.e. $t \in (0, 1)$.

Proof. Note that $\pi_{\#}^{t,1} \bar{\alpha} = (t, e_t)_{\#} (\mathcal{L}_{(0,1)} \times \alpha) = \mu_t \times_t \mathcal{L}_{(0,1)}$. Hence

$$\begin{aligned} \int f(t, x) \int \frac{y-x}{1-t} d\bar{\alpha}^{t,x}(y) d(\mu_t \times_t \mathcal{L}_{(0,1)}) &= \int f(t, x) \frac{y-x}{1-t} d\bar{\alpha}(t, x, y) \\ &= \int f(t, e_t(x, y))(y-x) d(\alpha \times \mathcal{L}_{(0,1)}) \\ &= \int f(t, x) de_{\#}((y-x)\alpha \times \mathcal{L}_{(0,1)}). \end{aligned}$$

Thus, v is the vector field induced by α since we verified (10). As in the proof of Lemma 4.5 it follows $v(t, \cdot) = v_t$ for almost all $t \in (0, 1)$. More precisely, by carefully checking the definition of disintegration we will show that $\bar{\alpha}^{t,x} = \alpha_t^x$ for a.e. $t \in [0, 1]$. Let $\{f_n\}_{n \in \mathbb{N}} \subset C_b(\mathbb{R}^d \times \mathbb{R}^d)$ be a dense subset. Then for every $h \in C_b([0, 1])$ we have that

$$\begin{aligned} \int_0^1 h(t) \int_{\mathbb{R}^d} \int_{\mathbb{R}^d} f_n(x, y) d\bar{\alpha}^{t,x}(y) d\mu_t(x) dt &= \int_0^1 h(t) \int_{\mathbb{R}^d \times \mathbb{R}^d} f_n(e_t(x, y), y) d\alpha dt \\ &= \int_0^1 h(t) \int_{\mathbb{R}^d \times \mathbb{R}^d} f_n(x, y) d\alpha_t dt \end{aligned}$$

and therefore

$$\int_{\mathbb{R}^d} \int_{\mathbb{R}^d} f_n(x, y) d\bar{\alpha}^{t,x}(y) d\mu_t(x) = \int_{\mathbb{R}^d \times \mathbb{R}^d} f_n(x, y) d\alpha_t \quad \text{for a.e. } t \in [0, 1].$$

Thus there exists a zero set N such that

$$\int_{\mathbb{R}^d} \int_{\mathbb{R}^d} f_n(x, y) d\bar{\alpha}^{t,x}(y) d\mu_t(x) = \int_{\mathbb{R}^d \times \mathbb{R}^d} f_n(x, y) d\alpha_t$$

for all $t \in [0, 1] \setminus N$ and all $n \in \mathbb{N}$. Using that $\{f_n\}_{n \in \mathbb{N}} \subset C_b(\mathbb{R}^d \times \mathbb{R}^d)$ is dense we can conclude that $\bar{\alpha}^{t,x} = \alpha_t^x$ as Markov kernels for a.e. $t \in [0, 1]$. Hence, $v(t, \cdot) = v_t$ for a.e. $t \in (0, 1)$. \square

C Remark on Normalizing Flows

Let us have a quick look at normalizing flows which are invertible neural networks. Other invertible neural networks are residual networks [8, 20], which we will not address in this paper.

A *normalizing flow* between two distributions $\mu_i \in \mathcal{P}(\mathbb{R}^d)$, $i = 0, 1$ is a C^1 diffeomorphism $T : \mathbb{R}^d \rightarrow \mathbb{R}^d$ such that

$$\mu_1 = T_{\#} \mu_0.$$

Normalizing flows were approximated by neural networks T^θ which have a special architecture in order to be invertible [3, 13]. To this end, a loss function is minimized, e.g. the KL divergence between the push-forward of the latent distribution $T_{\#}^\theta \mu_0$ and the data distribution μ_1 . Due to the special network architecture, normalizing flows are not suited for in high dimensional problems. Moreover, they suffer from a limited expressiveness, e.g., when trying to map a unimodal (Gaussian) distribution to a multimodal one, their Lipschitz constants explodes [19]. Stochastic normalizing flows [42] circumvent this problem by introducing stochastic layers. For the definition of stochastic normalizing flows via Markov kernels and an overview, we refer to [17, 18].

In contrast to normalizing flows, recent generative models like flow matching and continuous normalizing flows as well as score based diffusion models use, instead of learning a map $T : \mathbb{R}^d \rightarrow \mathbb{R}^d$, curves in the space of probability measures, which slowly transform the latent distribution into the data distribution. In this way, at every time step only a small change of probability measures has to be learned as opposed to learning everything in one step.